Bulk crystal growth from gas phase

by Michal Bockowski

Institute of High Pressure Physics Polish Academy of Sciences,
Sokolowska 29/37, 01-142 Warsaw, Poland

email: bocian@unipress.waw.pl

Outline

1. Why do we grow crystals?

2. How can we grow crystals and what does it depend on?

3. Driving force for crystal growth

4. Silicon, sapphire and gallium nitride - wafering procedures – the way to obtain substrates

5. Growth from gas phase

6. Epitaxy

7. Theory: bulk growth from gas phase (vapor phase)

8. II-VI and IV-VI crystals: Cadmium Telluride, Lead Selenide and their cousins by physical vapor transport

9. Silicon Carbide and Aluminum Nitride by physical vapor transport

10. Gallium Nitride by halide vapor phase epitaxy
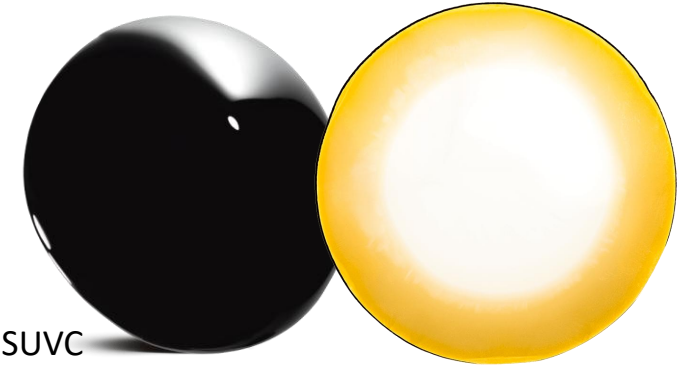
11. Summary

Why do we grow crystals?

Curiosity

Examples?
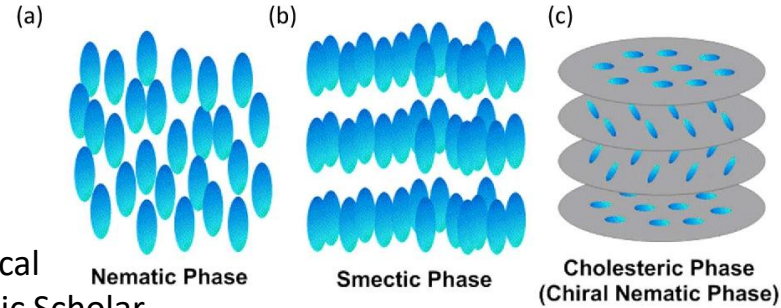
Elastic Interactions between Optical and Topological Solitons in Chiral Nematic Liquid Crystal | Semantic Scholar

(a) Nematic Phase

(b) Smectic Phase
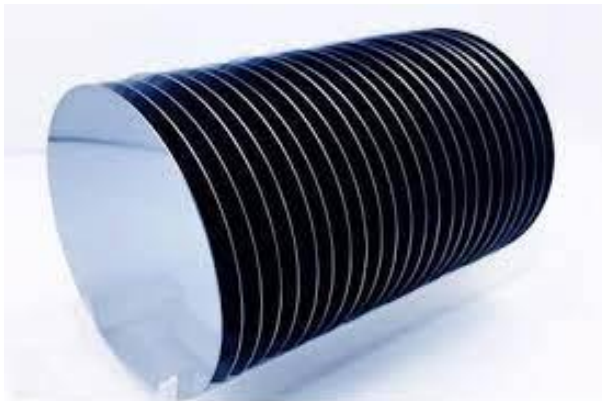
(c) Cholesteric Phase (Chiral Nematic Phase)

Aluminum Nitride (AlN) Technology Overview - Crystal IS - CISUVC

Applications

Examples?

Substrates and epi-structures fabrication for making devices

Epi-wafers - VIGO System - innovative infrared detectors MCT, InAs, InAsSb

Silicon Wafer | Si Wafer | Silicon Substrate | Si Substrate | Thin Si Slice - AEM Deposition

Why do we grow crystals?

Jewellery

Resin Necklace Silicon Carbide and Silver Flakes Carborundum | Etsy

Norstel SiC Gemstones | Ceramic Forum, Glass Manufacturing Technology and Wide-Gap Semiconductors
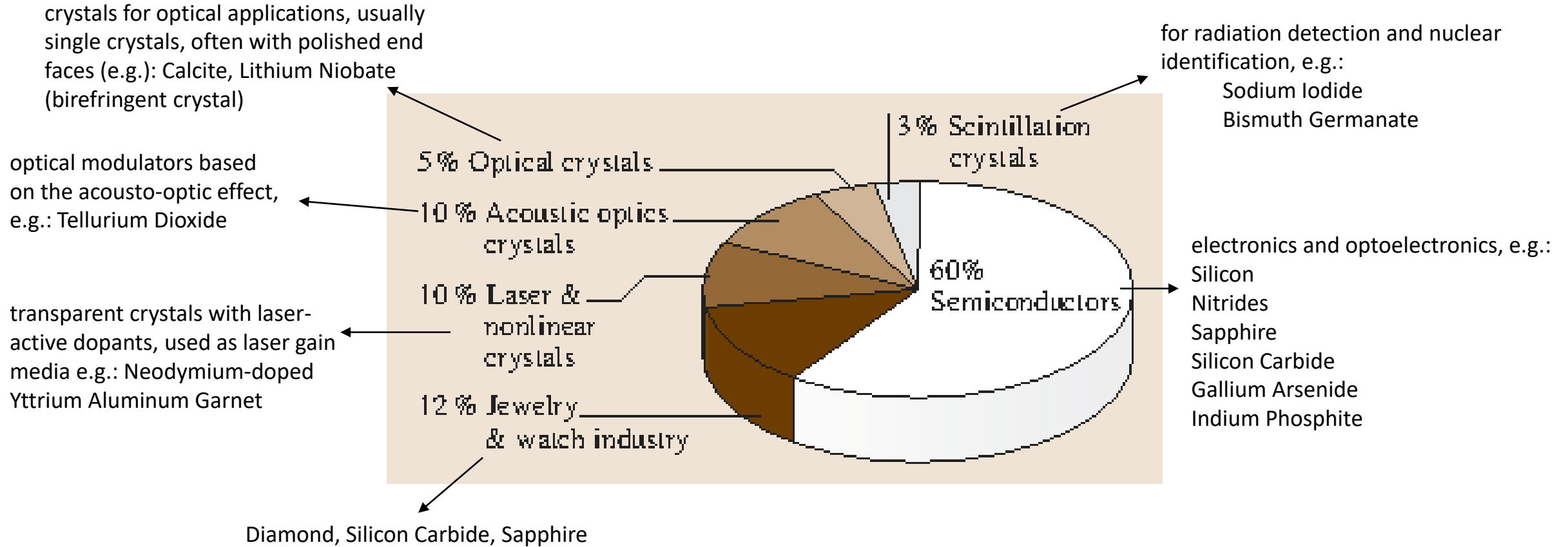
Why do we grow crystals?

Jewellery

"Some say that lab-grown diamonds might be okay for 'cheap' jewellery but ask: do they truly signify love and romance?"
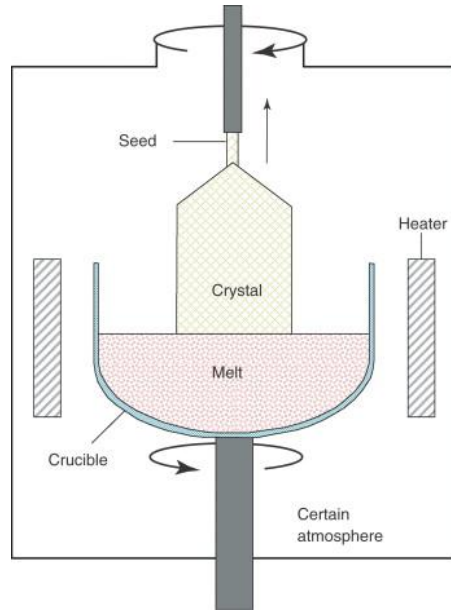
Would you propose with a synthetic diamond? - Jeweller Magazine: Jewellery News and Trends

Why do we grow crystals?

crystals for optical applications, usually single crystals, often with polished end faces (e.g.): Calcite, Lithium Niobate (birefringent crystal)

for radiation detection and nuclear identification, e.g.:
    Sodium Iodide
    Bismuth Germanate

optical modulators based on the acousto-optic effect, e.g.: Tellurium Dioxide

electronics and optoelectronics, e.g.:
Silicon
Nitrides
Sapphire
Silicon Carbide
Gallium Arsenide
Indium Phosphite

transparent crystals with laser-active dopants, used as laser gain media e.g.: Neodymium-doped Yttrium Aluminum Garnet

Diamond, Silicon Carbide, Sapphire

3% Scintillation crystals

5% Optical crystals

10% Acoustic optics crystals

10% Laser & nonlinear crystals

12% Jewelry & watch industry

60% Semiconductors

How can we grow crystals and what does it depend on?

Crystal Growth From Melt

G. Müller, J. Friedrich,
in Encyclopedia of Condensed Matter Physics, 2005

Crystal Growth From Solution
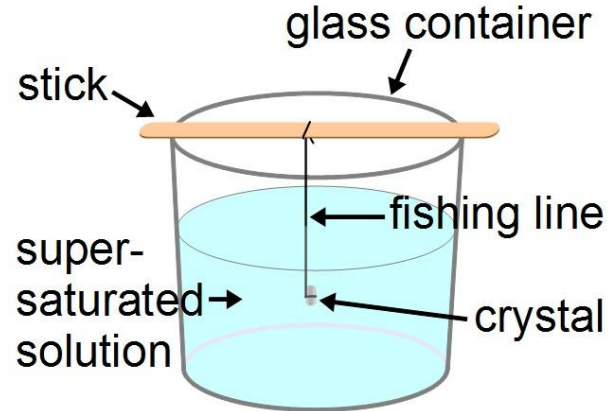
Make big Rochelle salt crystals from seeds (rimstar.org)

Crystal Growth From Gas Phase
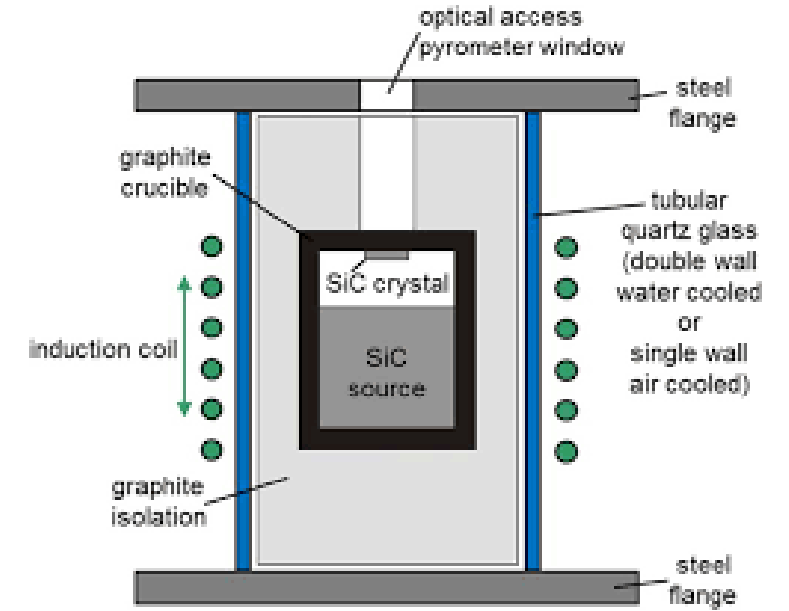
P. J Wellmann 2018
Semicond. Sci. Technol. **33** 103001

Remark: back to curiosity : SiC from liquid phase; sapphire from solution etc.

Driving force for crystal growth

Supersaturation - the difference of thermodynamic potentials at the interface between a crystal and its environment.

What Is Supersaturation?
Supersaturation is a non-equilibrium, physical state in which a solution contains more solute than the equilibrium solubility allows, at given conditions such as temperature and pressure of the system. Supersaturation is also used to describe the level at which the solute concentration exceeds its solubility at given conditions, expressed as:
ΔC (supersaturation) = C (actual concentration) – C* (solubility).

How Do You Control Supersaturation?
A typical way to generate supersaturation is to dissolve a substance in a solvent at elevated temperature and then cool the solution down. As the temperature is reduced, the system enters the metastable supersaturated state; as cooling continues, the metastable limit will be reached. At this point the nucleation process will occur, supersaturation will diminish or end and the liquid phase solute concentration will ultimately attain equilibrium at the solubility curve.
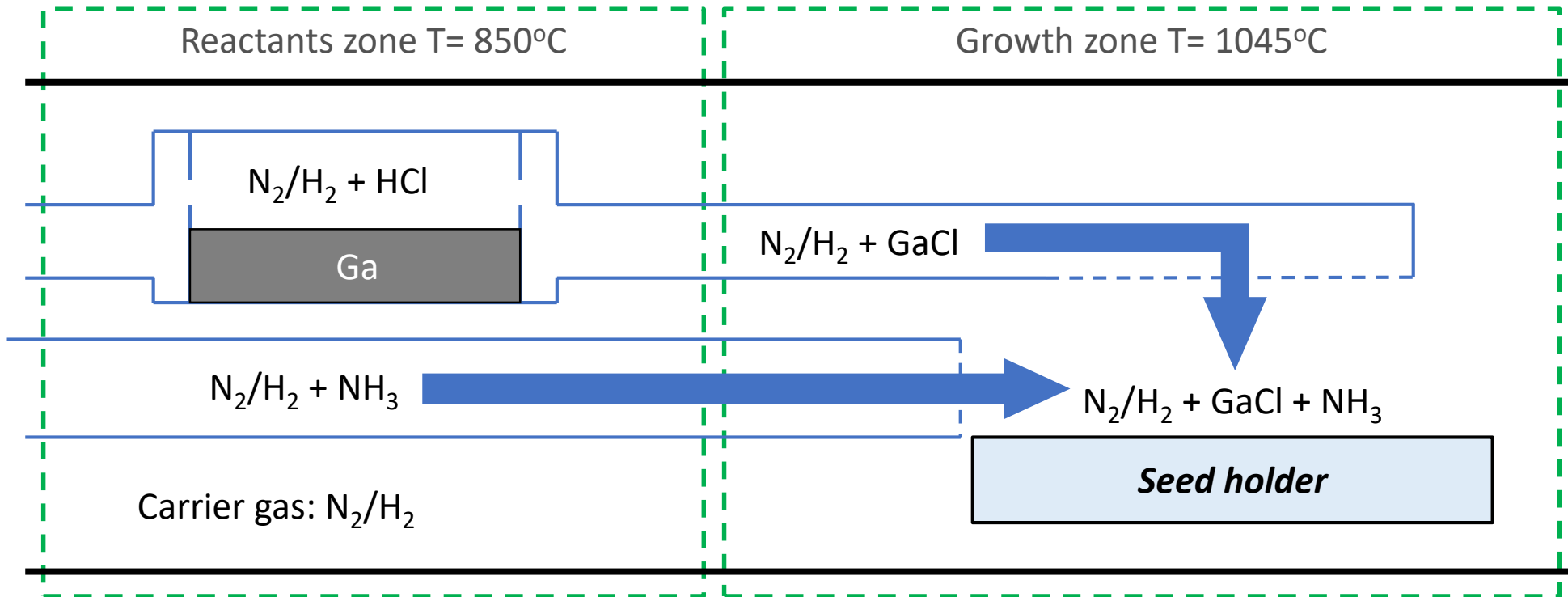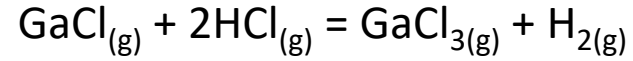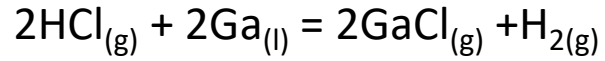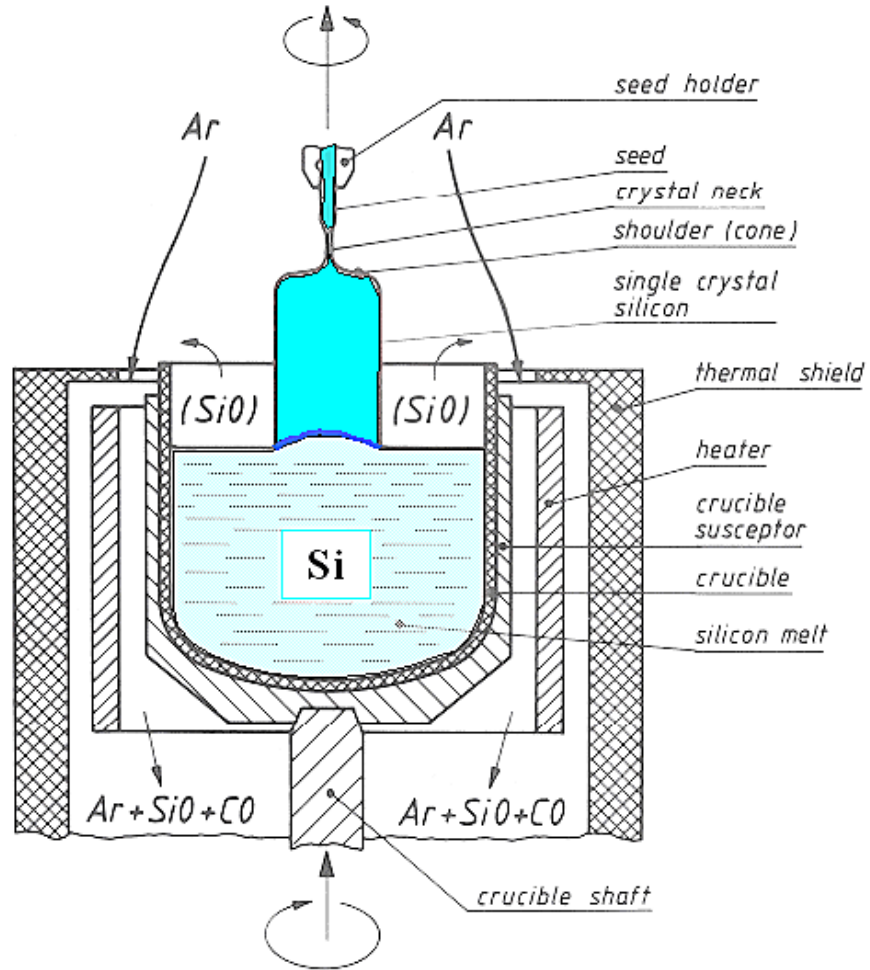
Driving force for crystal growth

crucible

N_2 molecules under pressure

Dissociative adsorption of N_2 on liquid metal surface

Dissolution and transport to the crystallization zone

Spontaneous crystallization

Ga

GaN

10 000 atm
1500°C

ΔT

T

$T=600\sim850°C$, $P_{N_2} < 100MPa$

$N \equiv N$ N_2 molecule with low thermal vibration

e-

$N \equiv N$

e) — $N^{*\,-}$ —————— $N^{*\,-}$ —

Ga   Na+   Na+   Ga
   Ga   Na
Na   e-

$(Ga_xN_y)\cdot(Na_z?)$

GaN crystal

Na-Ga melt

$\Delta T=0$

?

I. Grzegory et al. in Bulk Crystal Growth of Electronic, Optical and Optoelectronic Materials, ed. by P. Capper, Wiley&Sons, (2005), 173

Y. Mori, Osaka Univ.

9

Driving force for crystal growth

$$2HCl_{(g)} + 2Ga_{(l)} = 2GaCl_{(g)} + H_{2(g)}$$

$$GaCl_{(g)} + 2HCl_{(g)} = GaCl_{3(g)} + H_{2(g)}$$

$$GaCl_{(g)} + NH_{3(g)} = GaN_{(s)} + HCl_{(g)} + H_{2(g)}$$

Reactants zone T= 850°C   Growth zone T= 1045°C

N_2/H_2 + HCl

Ga

N_2/H_2 + GaCl

N_2/H_2 + NH$_3$

N_2/H_2 + GaCl + NH$_3$

Carrier gas: N_2/H_2

Seed holder

$$\Delta P_{GaCl} = [P^\circ_{GaCl} - (P_{GaCl_3} + P_{GaCl})]$$ at ammonia rich conditions

A. Koukitu, Y. Kumagai in Technology of Gallium Nitride Crystal Growth, Springer-Verlag, 2010, p. 31.

Silicon

Beginning of crystal growth

Labels: seed holder, seed, crystal neck, shoulder (cone), single crystal silicon, thermal shield, heater, crucible susceptor, crucible, silicon melt, crucible shaft

Ar, Ar, (SiO), (SiO), Si, Ar+SiO+CO, Ar+SiO+CO

Czochralski Crystal Growth Process (uni-kiel.de)

E. DornbergerWacker, Chemie AG · Polysilicon

Sapphire
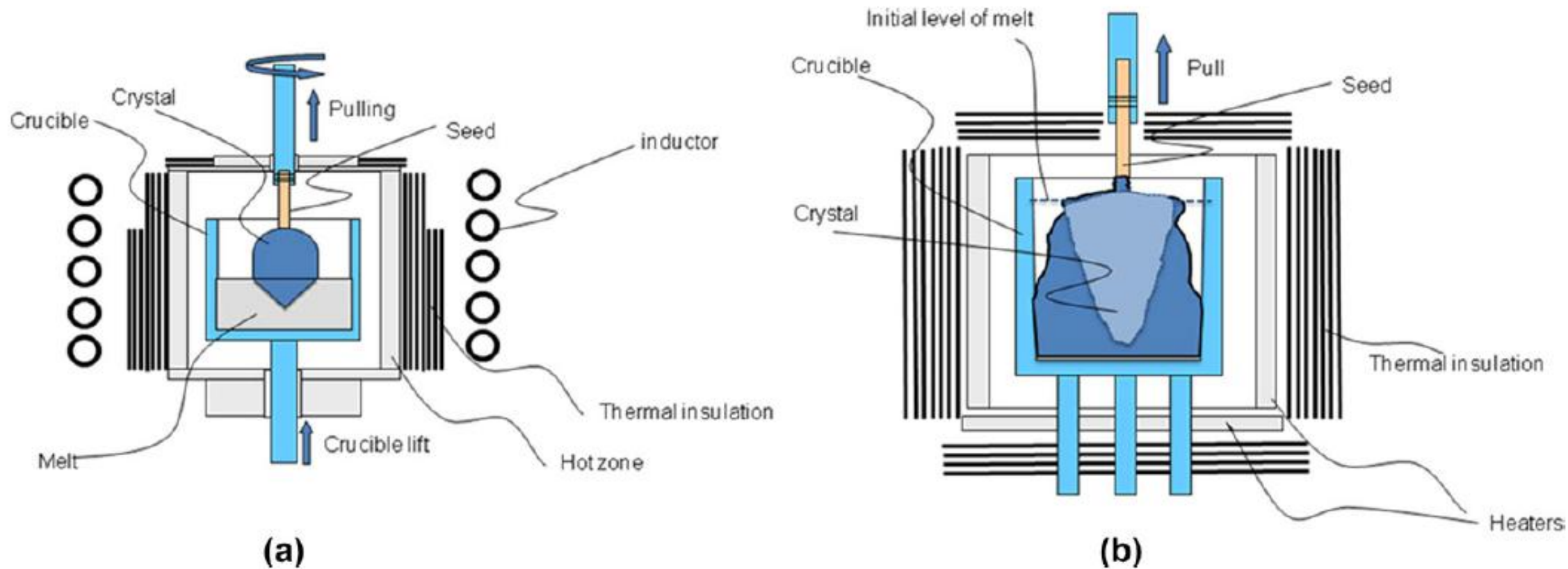
Fig. 4 Schematic representation of (a) the Czochralski method and (b) the Kyropoulos method.

Sapphire
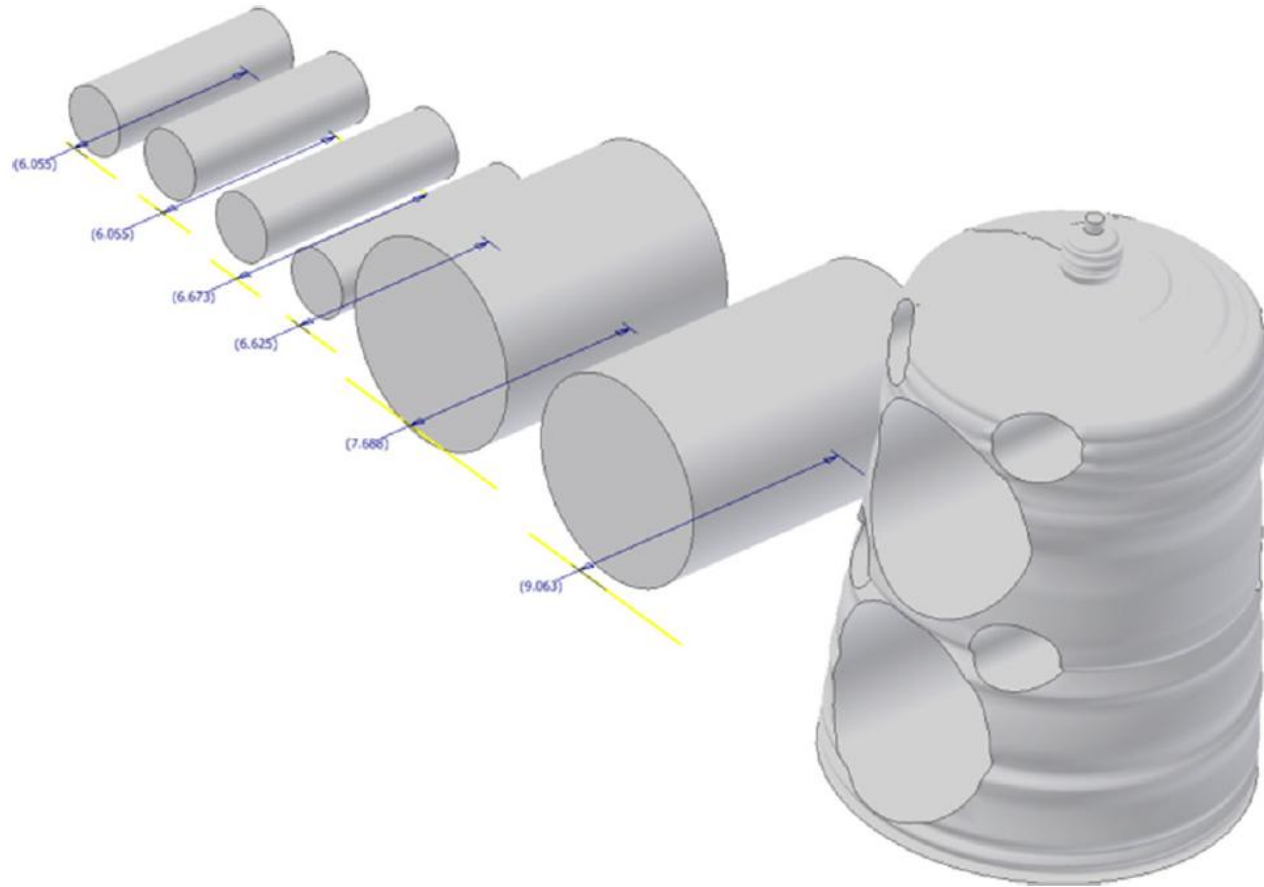
Fig. 2   Schematic representation of the core drilling of c-axis rods from an a-axis Kyropoulos-grown sapphire crystal.

Kyropoulos method - Wikipedia

Wafering procedures – the way to obtain substrates

Pulling Single Crystal Silicon Ingots

Single Crystal Silicon Ingots

Peripheral Grinding

An ingot with a notch
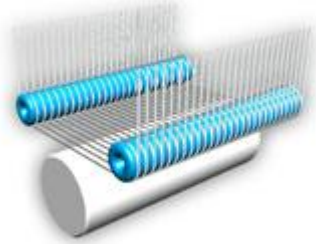
Slicing

Beveling (Peripheral Rounding)
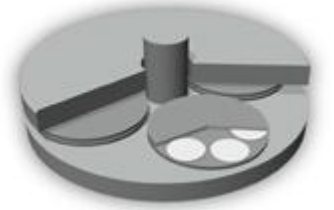
Lapping (Double Side Lapping)
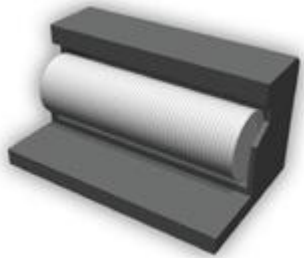
Etching (Chemical Polishing)

Heat Treatment to Remove Unstable Donors

Polishing (Single Side Mirror Polishing)

Cleaning

Inspections

Packaging

Shipping

Silicon Wafer Production Process | GlobalWafers Japan (sas-globalwafers.co.jp)

Production of Ammonothermal GaN Substrates

As-grown crystals

Crystallization

Machining process

Seeds
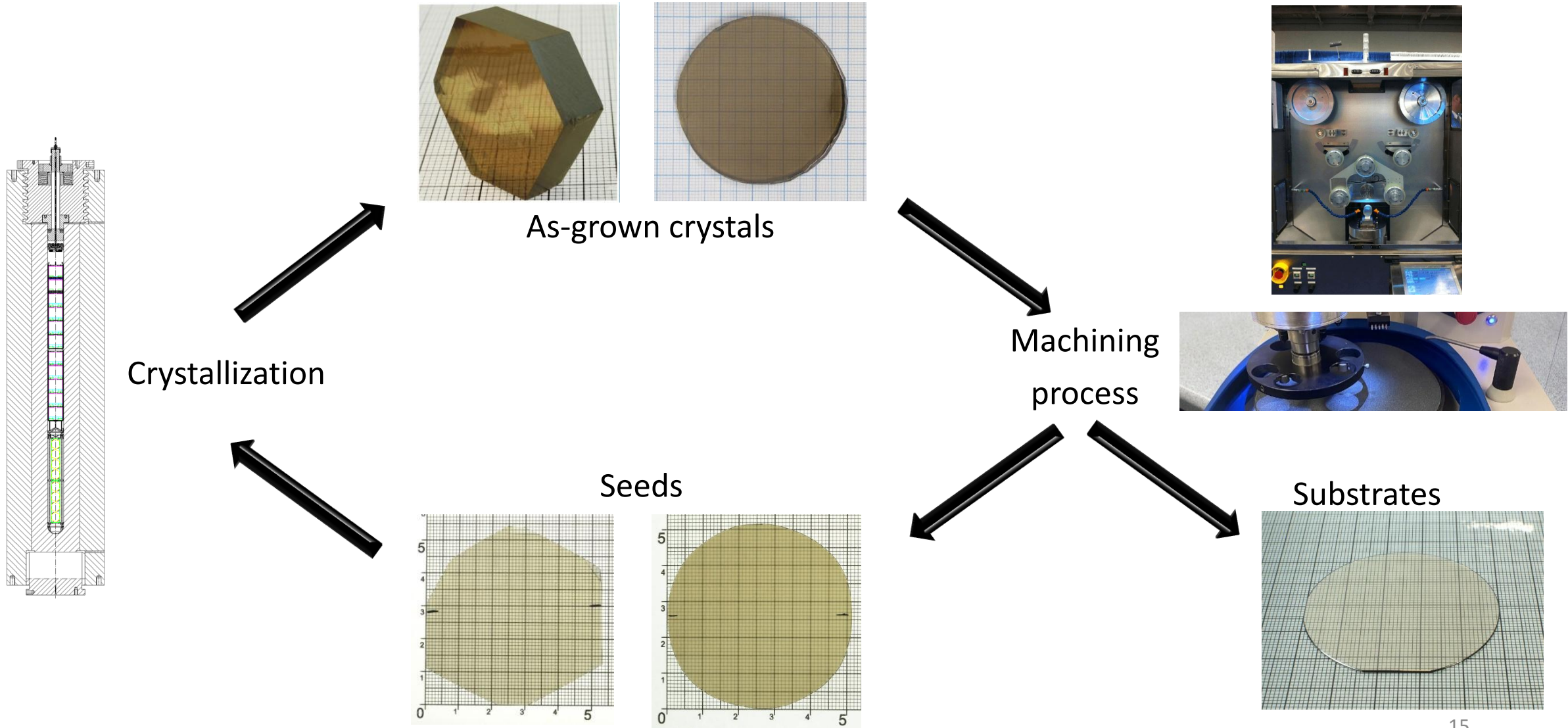
Substrates

Wafering procedures – the way to obtain substrates

1. The new-grown crystal is sliced off from its seed (a wire saw is used)
2. The (10-10) facet is found (a measuring device (gauge) and a goniometer are used)

a)

b)

3. The (0001) facet is found (a goniometer and a CNC machine are used)

Goniometer:
an instrument for the precise measurement of angles, especially one used to measure the angles between the faces of crystals.


CNC

R. Kucharski, J. Skladanowski

Wafering procedures – the way to obtain substrates

Wafering procedures – the way to obtain substrates

General specification

DESCRIPTION	UNIT	VALUE
Orientation		(0001) C plane
Thickness	μm	500 (±50)
Dimension(s)	mm	Ø50,4 (±0,6)
Primary Flat (PF)	mm	16 (±1)
Secondary Flat (SF)	mm	8 (±1)
Bow	μm	0 (±20)
Total Thickness Variation (TTV)	μm	≤ 60
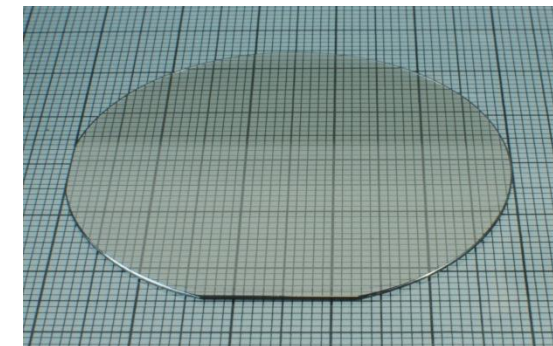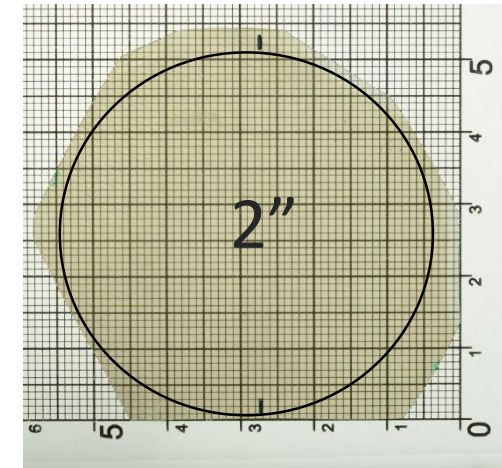
Wafering procedures – the way to obtain substrates
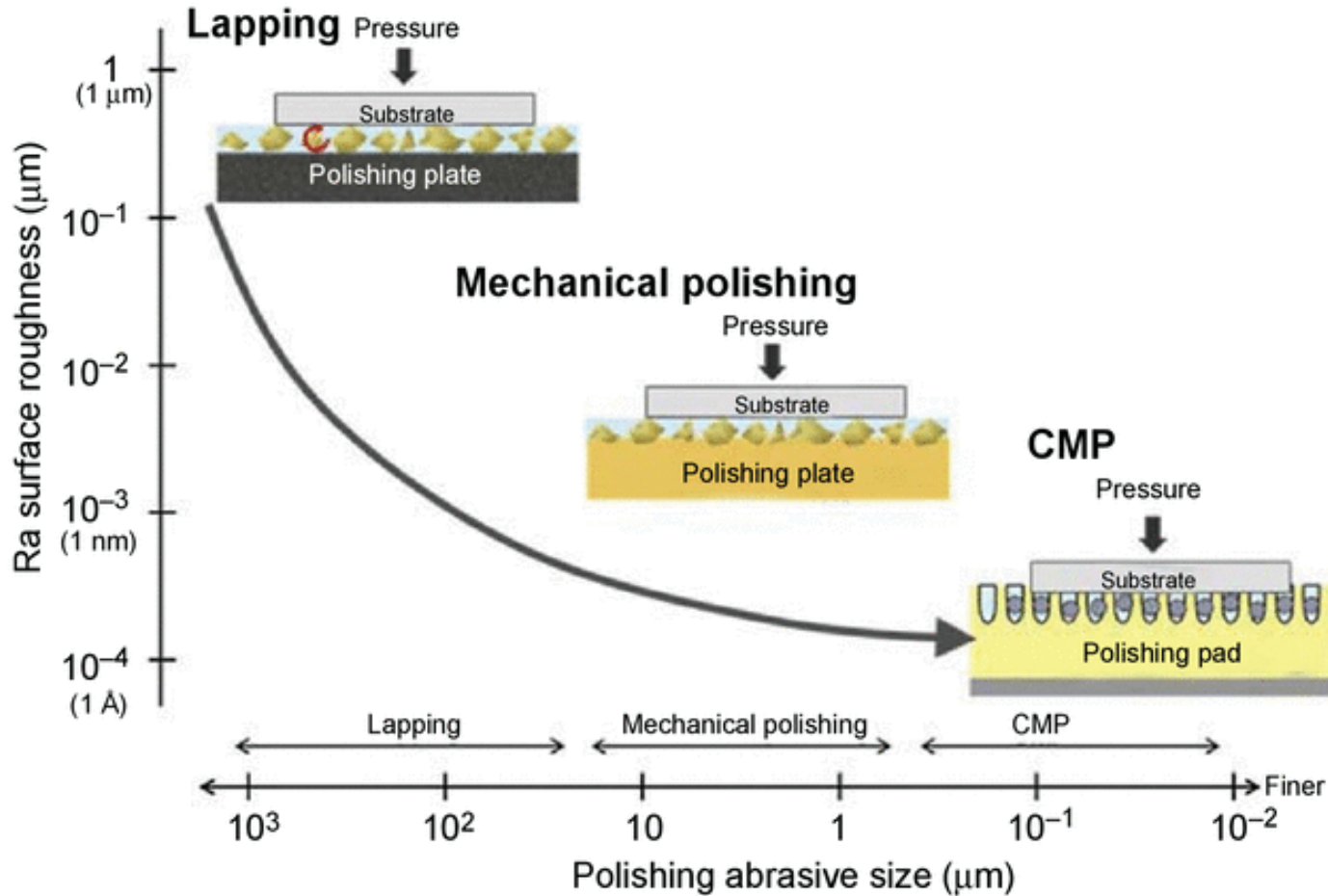
Steps:
1. Grinding (and edge grinding)
2. Lapping
3. Mechanical polishing
4. Chemo-mechanical polishing

Wafering procedures – the way to obtain substrates

A

B

B
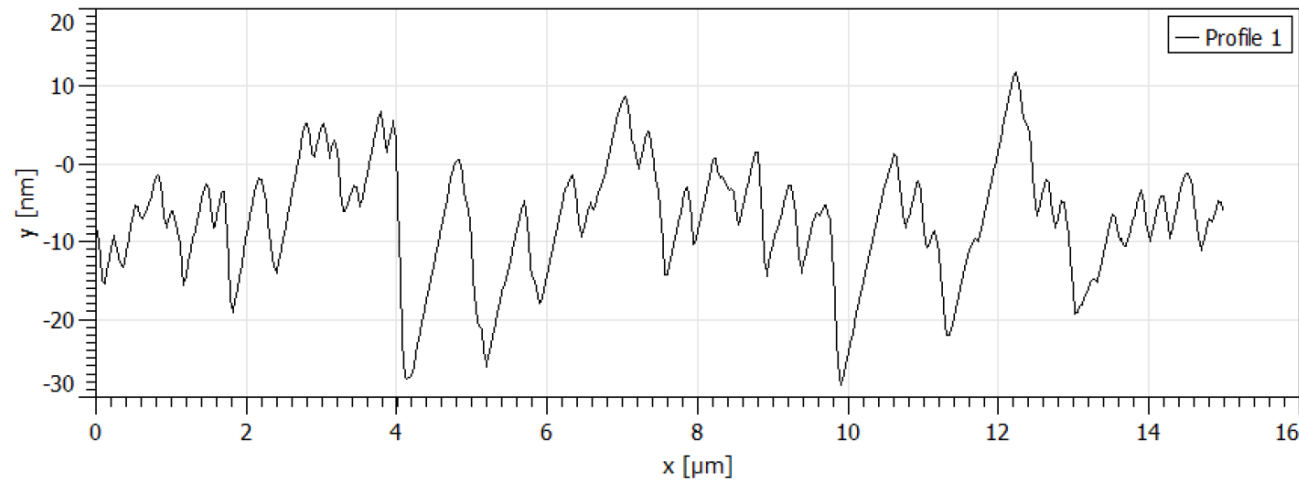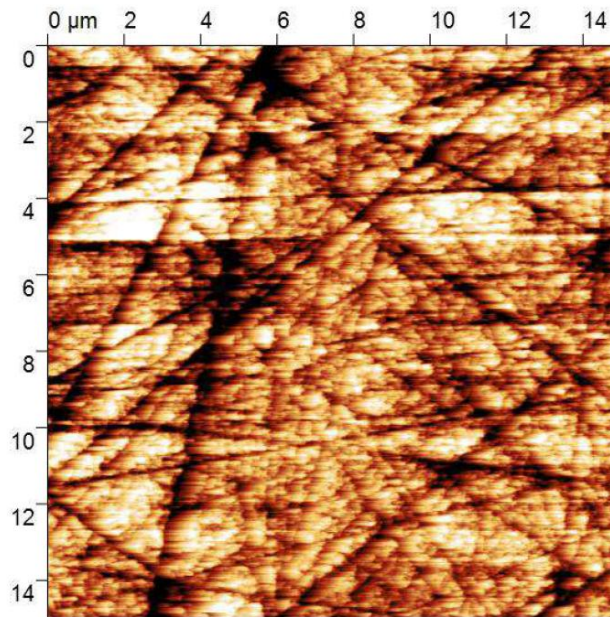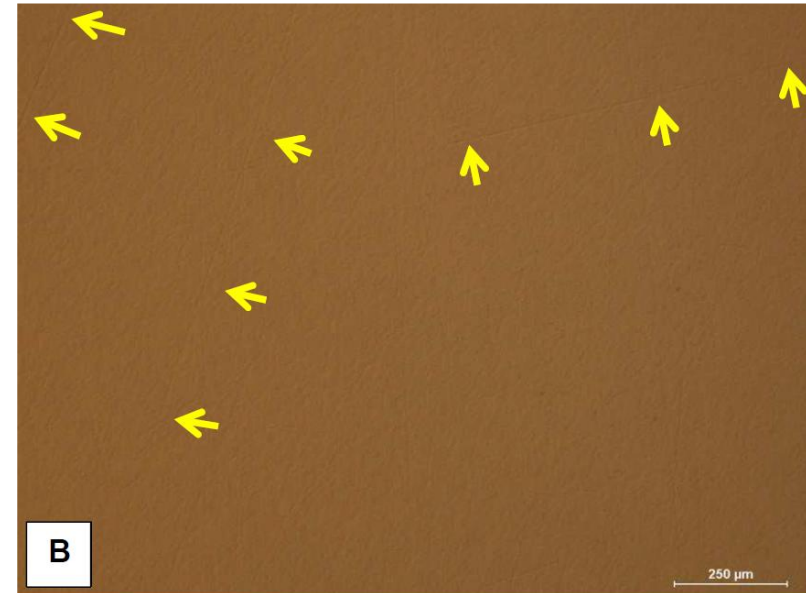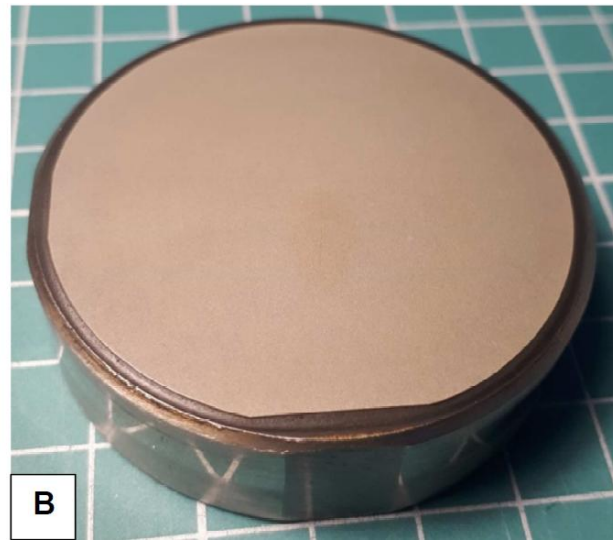
P. Nita

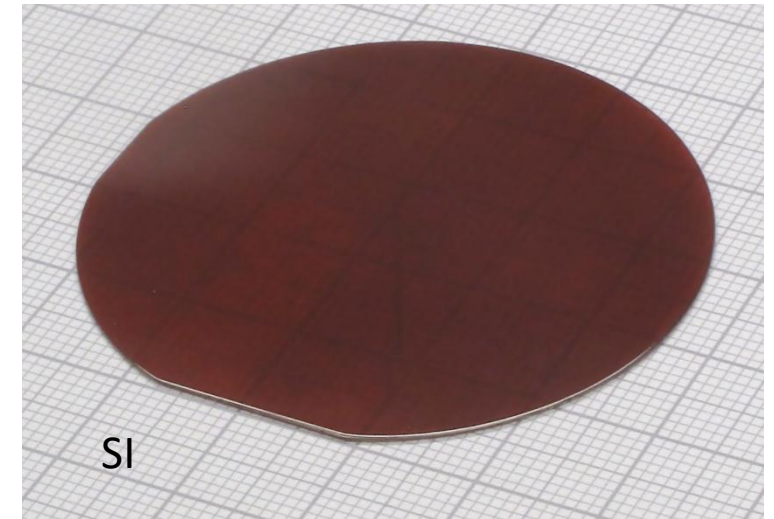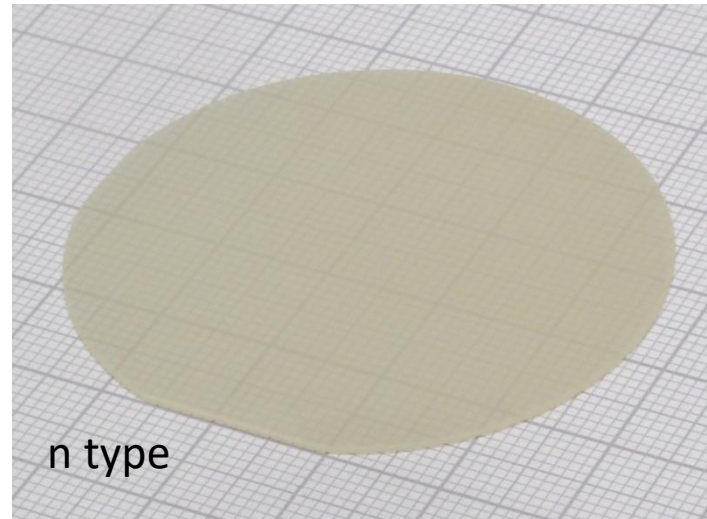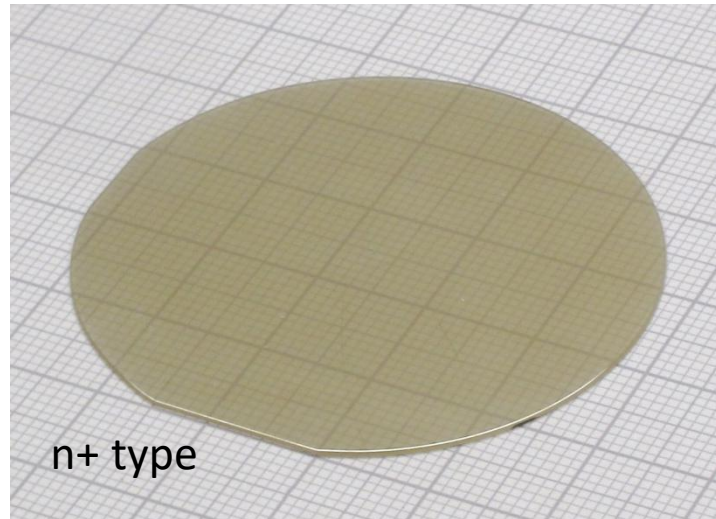# Wafering procedures – the way to obtain substrates

P. Nita

Wafering procedures – the way to obtain substrates

A. Sidor-Żak, M. Fijałkowski, A. Nowakowska-Szkudlarek
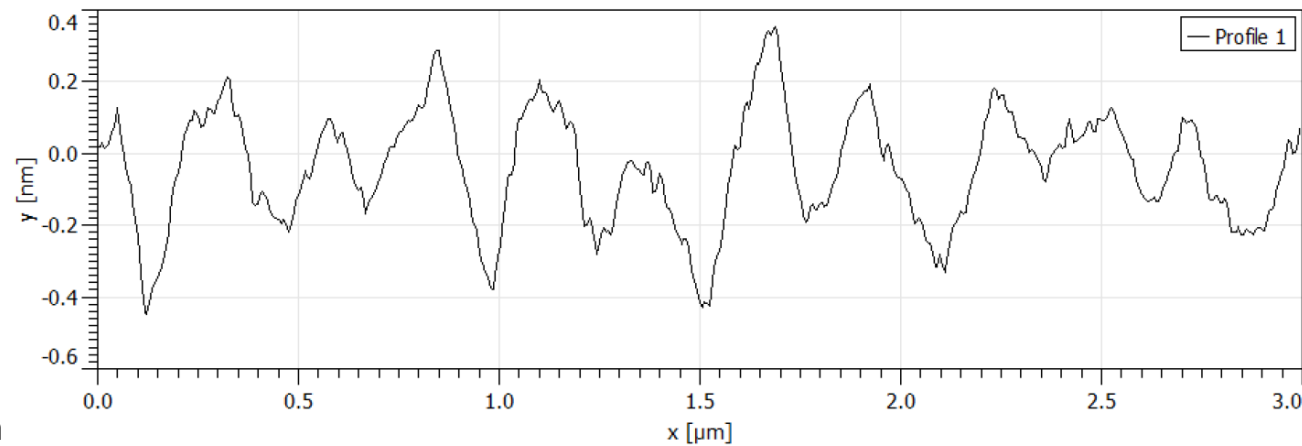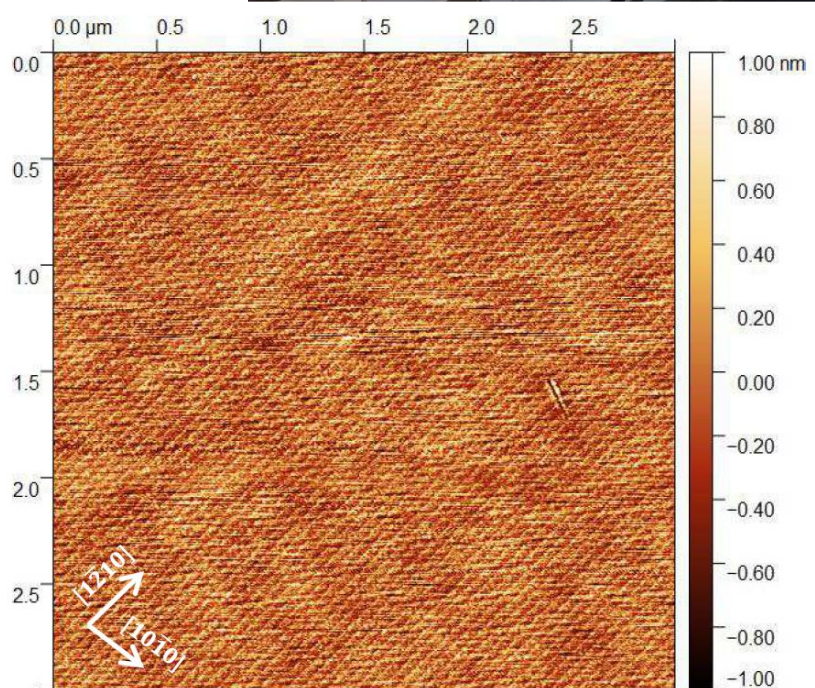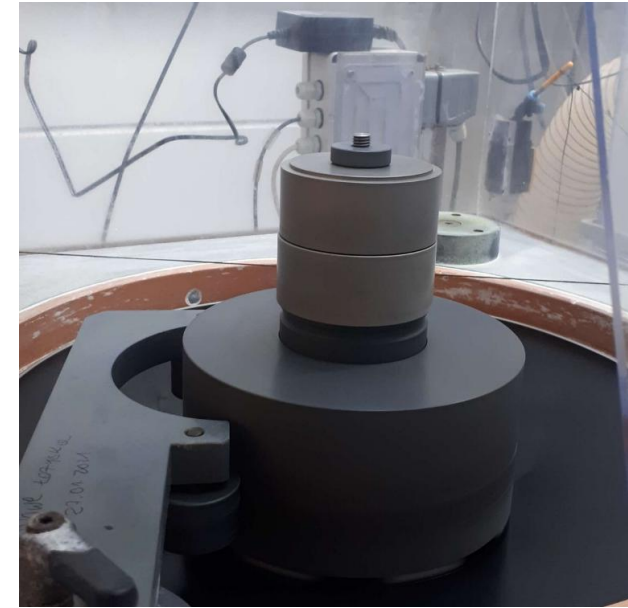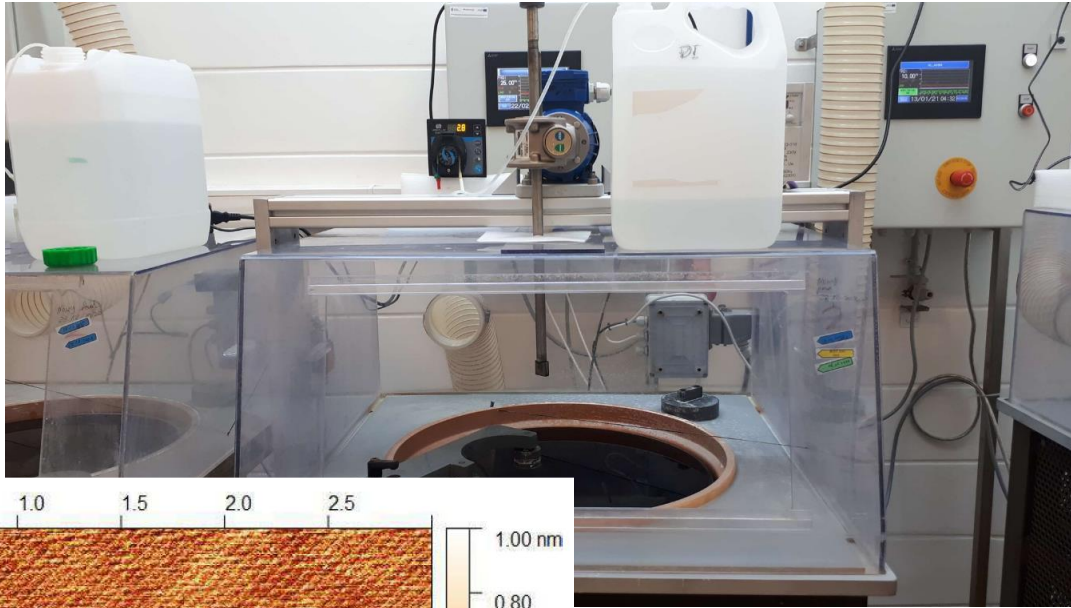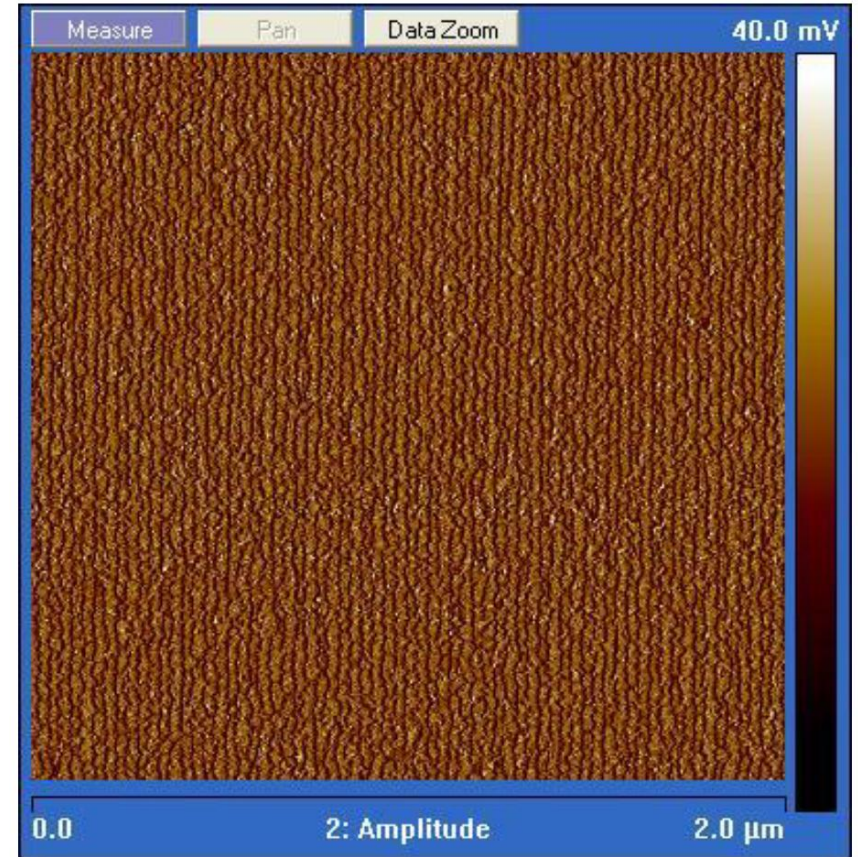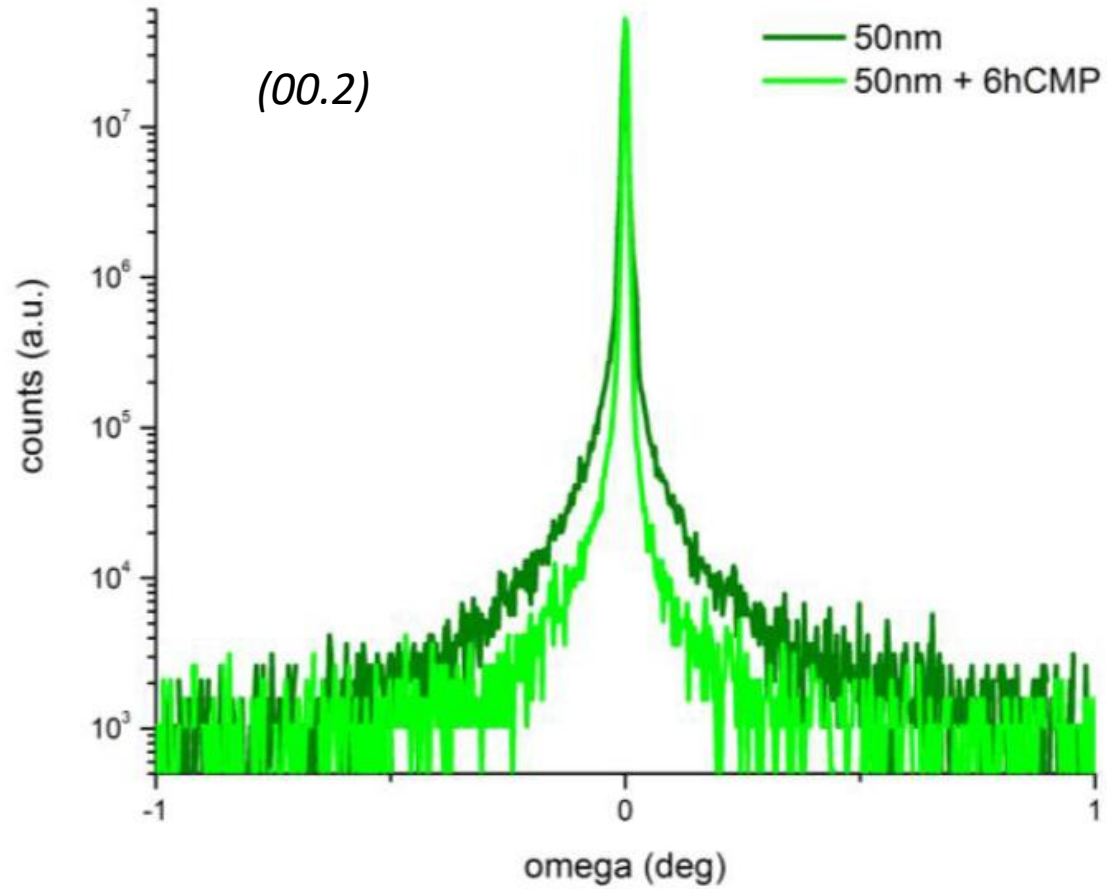
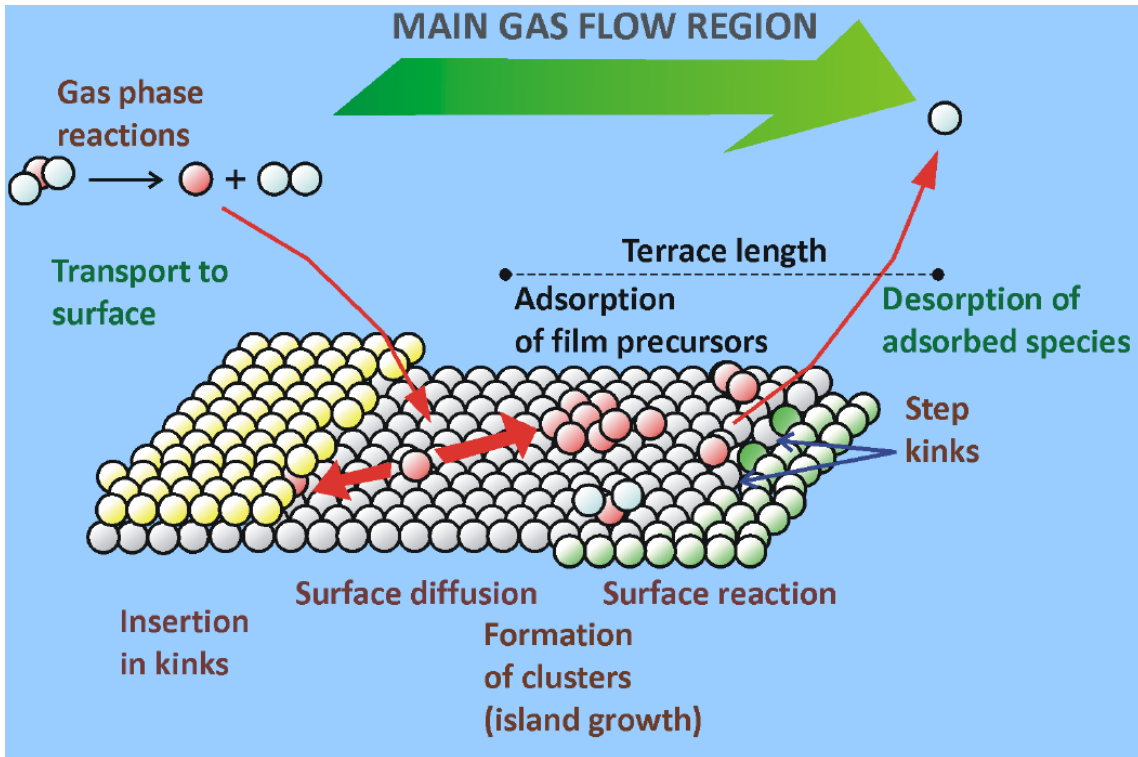# Ammonothermal GaN Substrates – Electrical Properties

n+ type

n type

SI

Material type	Conductivity type	Carrier concentration [cm^{-3}]	Carrier mobility [cm^2/Vs]	Resistivity [Ωcm]	Available size [inch]
High carrier concentration	n+ type	~10^{19}	~150	10^{-3}	2
Low carrier concentration	n type	~10^{18}	~250	10^{-2}	2
High resistivity (Mn-doped)	semi-insulating (SI)	-	-	≥10^8	2

23

Growth from gas phase

- Vapor crystal growth (VCG) processes, which involve the crystallization of a solid from the vapor phase, are of particular importance in modern device technology especially in the field of semiconductor-based heterostructures in which the techniques of film and epitaxial layer deposition have witnessed a very impressive development.

- However, also as regards bulk (or volume) crystals, VCG plays a role as an alternative to melt and solution growth when these techniques are not easily accessible.

- This is the case, for melt growth, when the melting point is too high or the melt decomposes, when destructive solid/solid transitions occur below the melting point and when undesired reactions take place between melt and container (crucible) walls.

- VCG is also an alternative to solution growth when no suitable solvent can be found and/or the incorporation of solvent traces has to be avoided.

Epitaxy

MAIN GAS FLOW REGION

Gas phase reactions

Transport to surface

Terrace length

Adsorption of film precursors

Desorption of adsorbed species

Step kinks

Insertion in kinks

Surface diffusion

Formation of clusters (island growth)
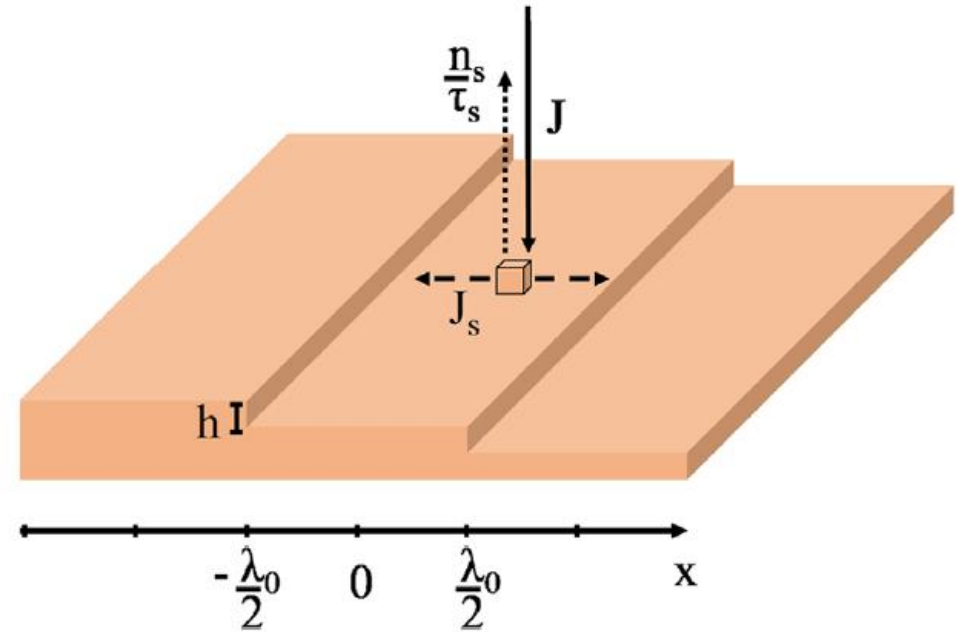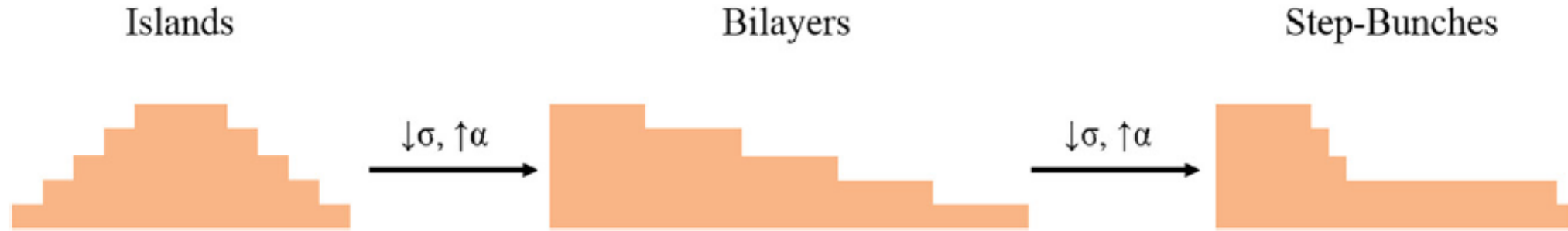
Surface reaction

Epitaxial growth (nptel.ac.in)

Fig. 2. Schematic of an ideal step and terrace morphology and the motion of species (adapted from Ref. [8]).

I. Bryan et al. / Journal of Crystal Growth 438 (2016) 81-89
[8] T. Shitara, T. Nishinaga, Jpn. J. Appl. Phys. 28 (1989) 1212.

Epitaxy

Islands   Bilayers   Step-Bunches

$\downarrow\sigma, \uparrow\alpha$ $\downarrow\sigma, \uparrow\alpha$

The same surface morphology could be achieved either by changing the misorientation angle, which controlled the terrace width, or vapor supersaturation, which controlled the surface diffusion length.
For a fixed vapor supersaturation, a critical misorientation angle existed for the transition between bilayer steps and step-bunches, however, this critical misorientation angle could be controlled by the vapor supersaturation to some degree.

1100°C

1 nm

0 nm

400 nm

I. Bryan et al. / Journal of Crystal Growth 438 (2016) 81-89
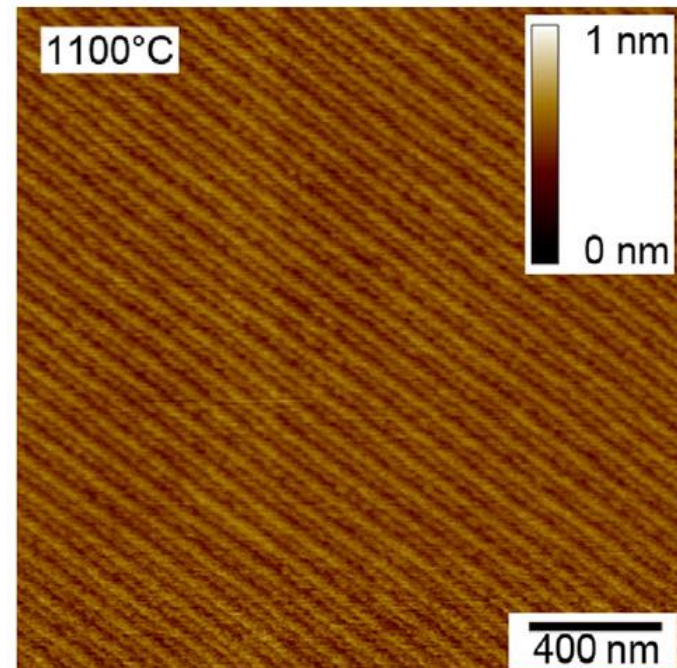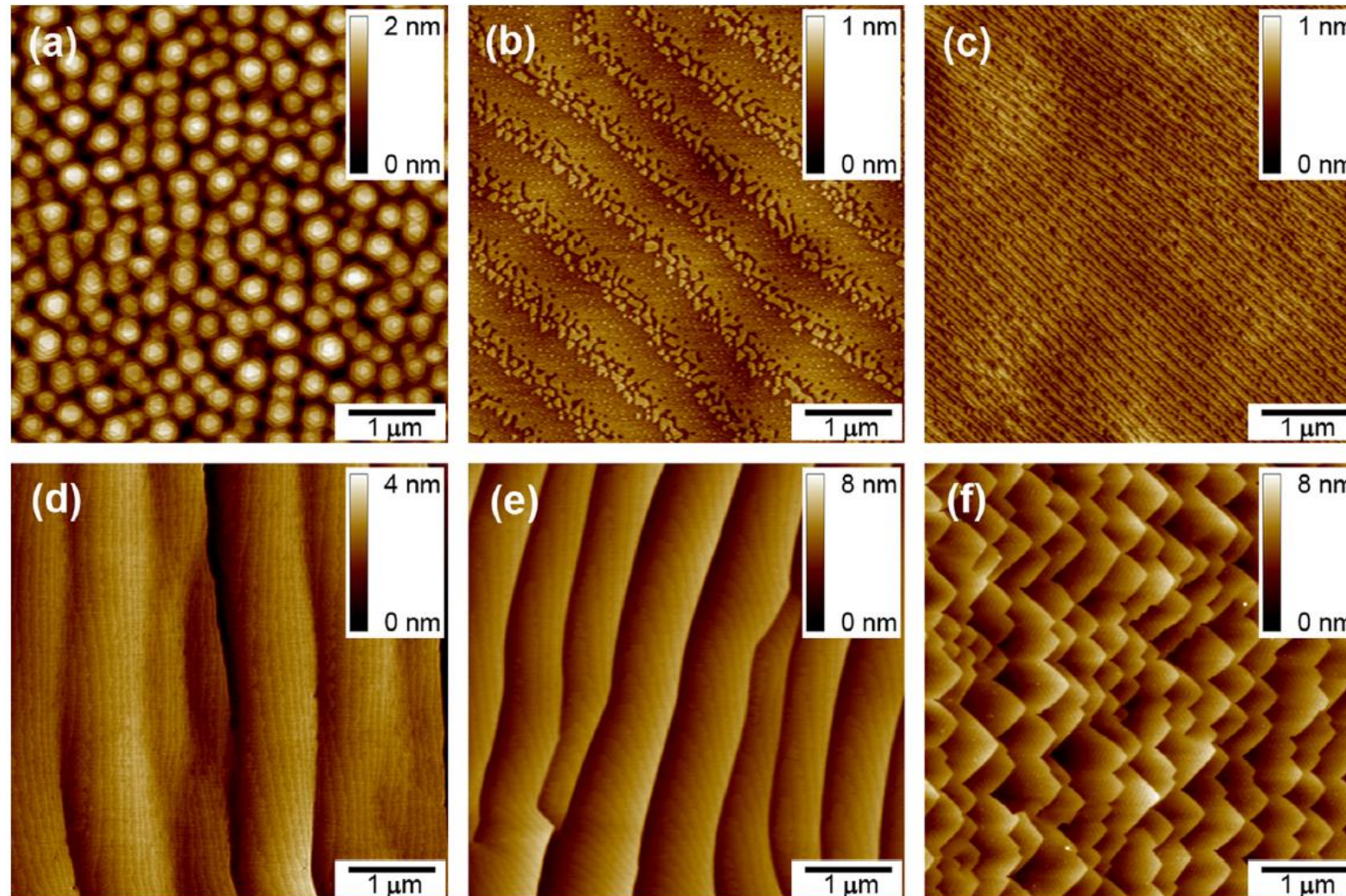
Epitaxy

Fig. 1. AFM images representing the 6 distinct types of surface morphologies attainable for AlN epitaxial layers grown with the absence of dislocations. The distinct features include 3D island formation (a), bilayer steps with (b) and without (c) 2D nuclei, and different types of step bunching (d)–(f).
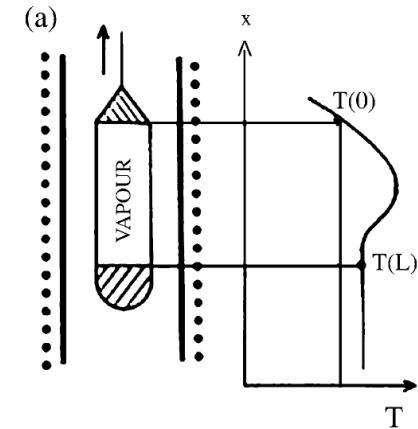
Theory: bulk growth from gas phase (vapor phase)

- Various VCG techniques have been described and classified. In all cases, a source region at a temperature T(L), which contains the starting material (usually a polycrystalline charge or a mixture of polycrystalline constituents of the final crystals) is distinguished from a deposition (crystallization) region kept at a distance L far apart at a temperature T(0) (with T(0) ≠ T(L)).

- Owing to the temperature gradient, the gaseous species within this volume undergo chemical potential gradients, and hence concentration gradients, thus driving a gaseous motion between source and crystallization region. As this motion is coupled to the SV- and VS-transitions at T(L) and T(0), respectively, an efficient mass transfer can develop under favorable thermodynamic conditions.

C. Paorici, G. Attolini / Progress in Crystal Growth and Characterization of Materials 48/49 (2004)
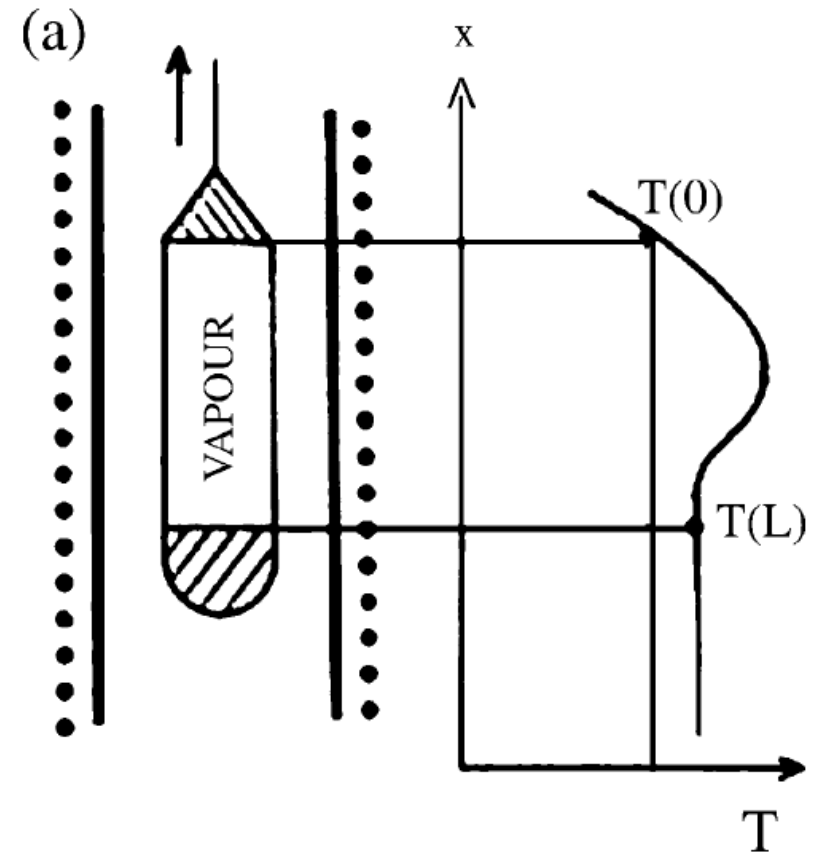
Theory: bulk growth from gas phase (vapor phase)

- The mass transfer, which can assume the form of a cyclic process in closed-tube (CT) (ampoule) configurations, is often referred to as ''gas flow crystallization'' in open-tube (OT) configurations, in which it takes place in the presence of an inert carrier gas.

- Variants between CT-PVT and OT-PVT are the so-called semiopen (SO), semiclosed (SC) and self-sealing (SS) methods, here indicated SOPVT, SCPVT and SSPVT.
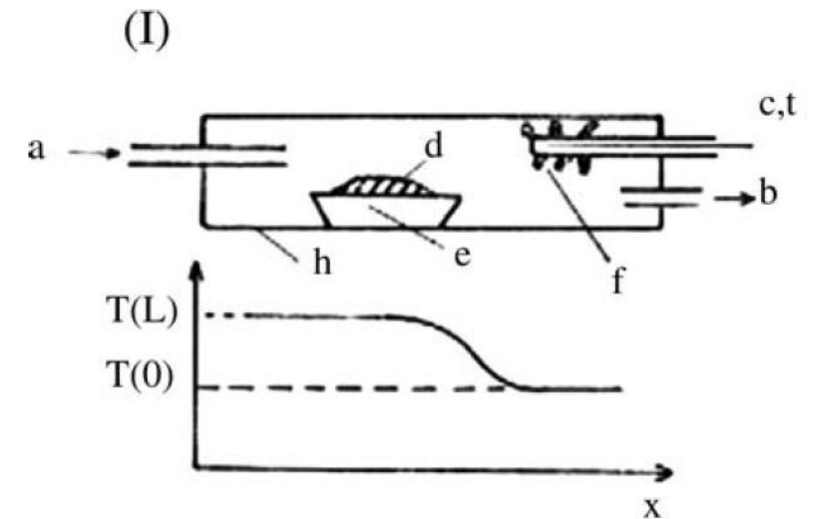
Theory: bulk growth from gas phase (vapor phase)
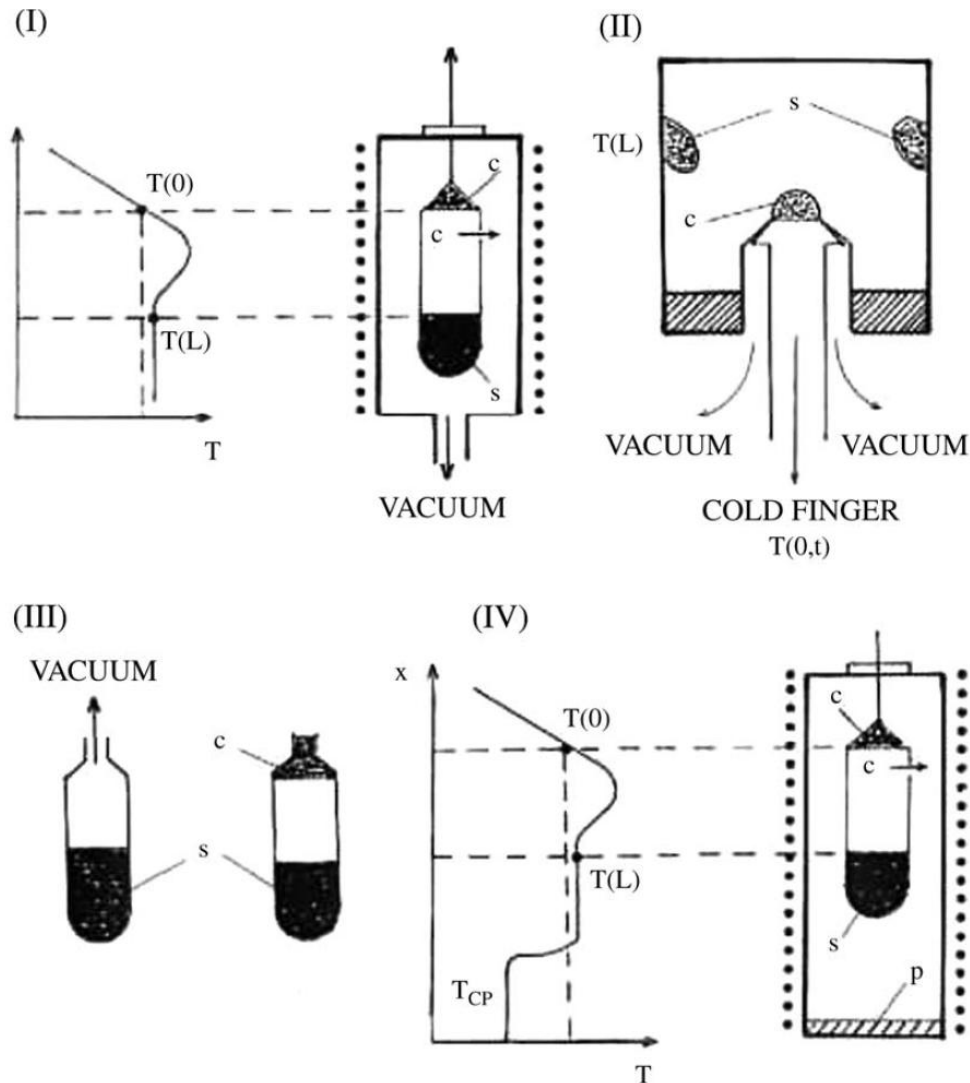
(I)   SOPVT set-up operating in the pulling mode;

(II)   SOPVT (cooling mode); the source material is let to stick on the inner wall of the container and the crystal grows on a pedestal where temperature $T(0,t)$ decreases with time;

(III) SSPVT: the growth starts in SOPVT mode (left) until the closure of the effusion hole (right) by the growing crystal;

(IV) SCPVT: vacuum is replaced by a cold point (TCP) where excess components condense. c: Crystal, s: source material, e: effusion hole (leak), p: material condensed in a cold point.

Theory: bulk growth from gas phase (vapor phase)

According to how the SV-transitions develop at the source region, the VCG processes can be distinguished as ''physical'' or ''chemical''.

Physical methods

- In these methods, which are referred to as based on ''physical vapor transport'' (PVT), the SV-transitions occur by sublimation while the crystallization is the reverse vapor/solid (VS) process.

- Both CT- and OT-configurations can be employed. CT- and OT-configurations are often referred to as PVT and PVD (physical vapor deposition).

- The physical methods can be used for growing bulk crystals provided the sublimation pressure is sufficiently high, otherwise the low vapor density involved does not allow a practically feasible growth rate of bulk crystals.

Theory: bulk growth from gas phase (vapor phase)

<u>Chemical methods</u>

- A possibility of circumventing the low-pressure limit of the physical methods is that available using the so-called chemical methods.

- For growing bulk crystals, the most commonly employed of these methods is ''chemical vapor transport'' (CVT) in CT-configurations (ampoule technique). Here the source material undergoes a progressive volatilization by means of suitable heterogeneous chemical reactions called ''chemical transport reactions''.

- The idea of shifting vapor-solid equilibria along a temperature gradient, in such a way as to achieve a CVT process suitable for growing bulk crystals, dates to 1956 [1] when Schafer et al. transported silicon in a closed ampoule by reacting it with chlorine. Soon after, Nitsche et al. were able to grow Zn and Cd sulphides and selenides by reacting them with iodine [2,3].

[1] H. Schafer, H. Jakob, K. Etzel, Z. Anorg. Allg. Chem. 286 (1956) 27.
[2] R. Nitsche, J. Phys. Chem. Solids 17 (1960) 163.
[3] R. Nitsche, H.U. Boelsterli, M. Lichtensteiger, J. Phys. Chem. Solids 21 (1961) 199.

Theory bulk growth from gas phase (vapor phase)

In CT-CVT, a small amount of a substance X, called ''transport agent'', in gaseous form at the operating temperature of the process, is reacted with the source material, A(s), giving rise to sufficiently high-pressure gaseous products. For practical applications, in the growth of bulk crystals the overall pressures usually range within 0.1-10 atm. Owing to the different concentration of each gaseous product in the source and crystallization region, these products flow to the crystallization region where the chemical reaction is reversed. By this reversion, A(s) is again formed and, should the solidification rate be small enough to meet the requirements of crystal growth stability, bulk crystals can be grown.

$$A(s) + X(g) \underset{T(0)}{\overset{T(L)}{\rightleftharpoons}} AX(g) \quad T(L) \neq T(0)$$
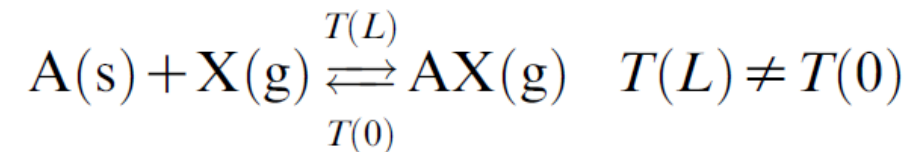
Theory: bulk growth from gas phase (vapor phase)

CVT can also be performed in OT-configurations provided that the transport agent is continuously supplied from an outside source, usually with the help of a flowing inert carrier gas. The first utilization of an OT-CVT procedure dates back to 1959, when Antell and Effer were able to grow InP and InAs using InI_3 as a transport agent.
[G.R. Antell, D. Effer, J. Electrochem. Soc. 106 (1959) 509]

When operating in OT-configurations, two more chemical processes have to be taken into consideration besides CVT, namely ''vapor decomposition'' (VD) and ''direct synthesis'' (DS). Here the solid charge is replaced by gaseous constituents (precursors) of the final crystal, as schematically represented by

$$AX(g) \xrightarrow{T(0),G} A(s, crystal) + X(g) \quad (VD)$$

$$A(g) + B(g) \xrightarrow{T(0),G} AB(s, crystal) \quad (DS)$$
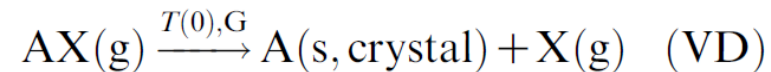
where G stands for an inert carrier gas.

$$A(g) + H_2S(g) \xrightarrow{T(0),H_2} AS(s) + H_2(g), \quad A = Cd, Zn$$
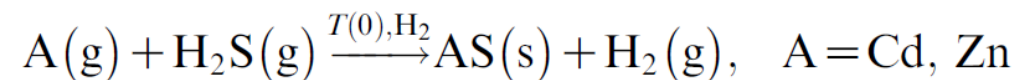
Theory: bulk growth from gas phase (vapor phase)

Common features of the VCG processes, and hence of PVT and CVT when used for growing bulk crystals, are the slow growth rates and the great difficulty to control the formation of a single nucleus owing to spurious (parasitic) nucleations.

The slow growth rates (typically 10^{-6} cm/s, to be compared to melt growth rates of $10^{-4} - 10^{-2}$ cm/s), not only depend on the latent heat of solidification, which is much greater for vapors than it is for melts (typically: 50-100 kcal/mol against 1-10 kcal/mol) but also on the kinetic barriers to the integration of growth units from the vapor, which increase when the crystallization temperature decreases and the growing interface displays a lower level of atomic roughness.

Parasitic nucleation, for which the growth of only one nucleus becomes very critical, depends on the width of the Ostwald-Miers region, which is very narrow when compared to melt growth
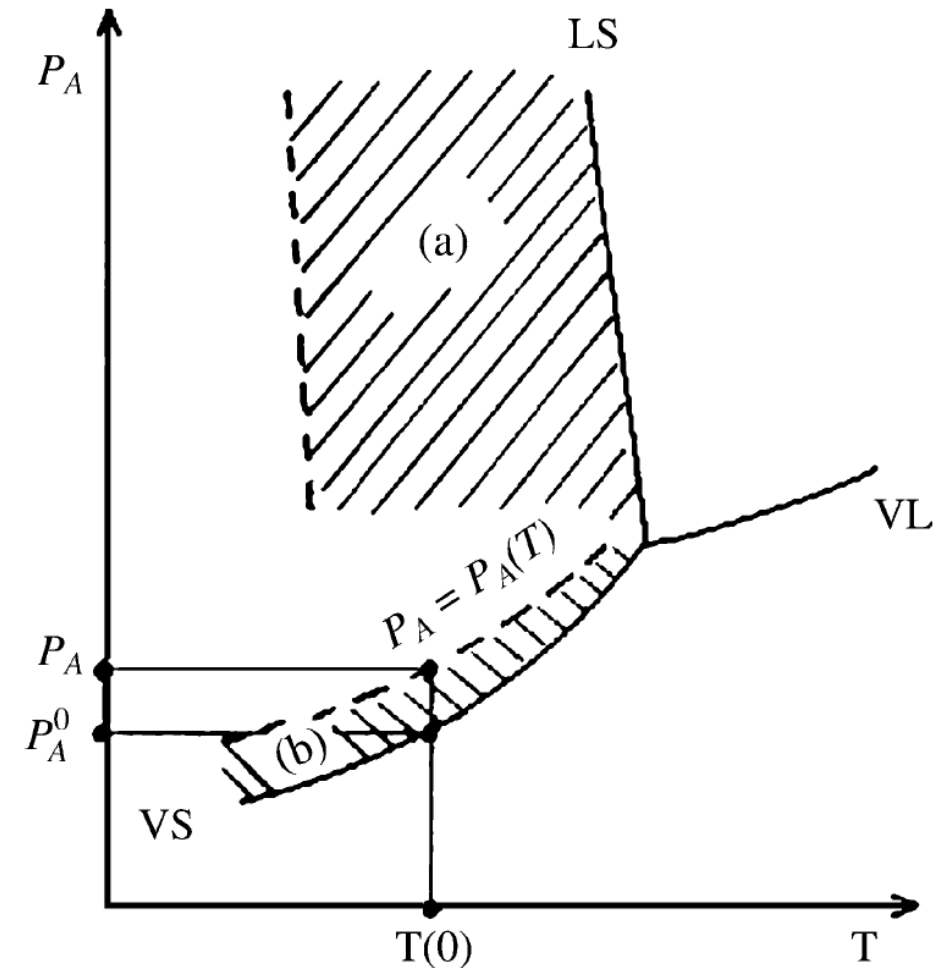
Theory: bulk growth from gas phase (vapor phase)

- It is the temperature range in which the melt can be kept in the supercooled state or the solution in the supersaturated state.

- Analogously, there is an Ostwald-Miers range not only in the transition from the liquid to the solid phase, but also in the transition from the gas phase to the liquid or solid phase.

- In the Czochralski process for the production of silicon monocrystals, the temperature of the liquid silicon is kept within the Ostwald-Miers range in order to ensure undisturbed and offset-free crystallization.

Ostwald-Miers area (Ostwald-Miers-Bereich) - wikipe.wiki (wikibook.wiki)
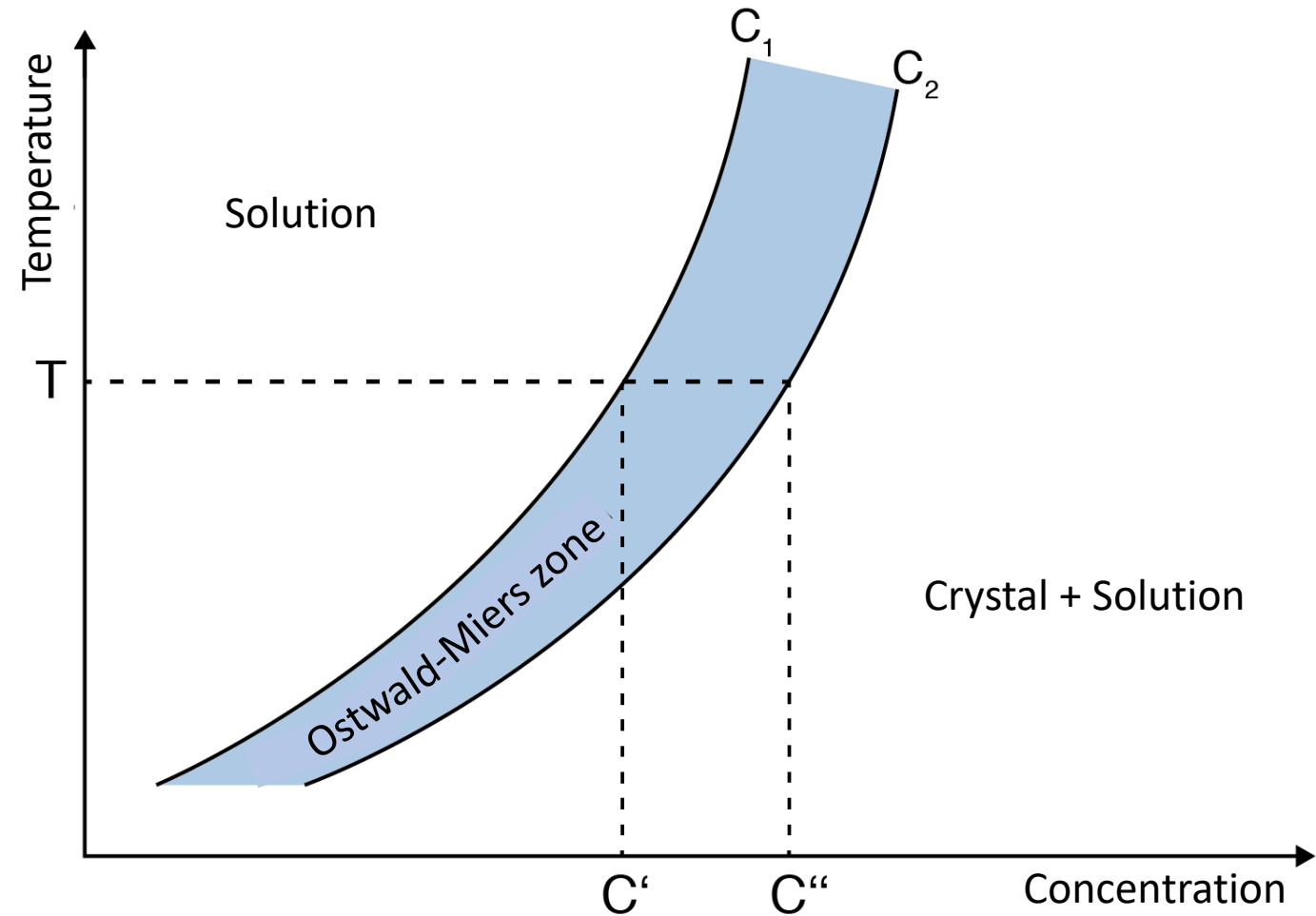
II-VI crystals

II-VI crystals are likely to shoot in prominence in the near future. Their direct band gap nature, their large range of transparency, and the availability of a wide choice of band gap offer interesting device possibilities.

Properties	CdS	CdTe	Cd$_{1-x}$Zn$_x$Te	ZnS	ZnTe	ZnSe
Growth Mehod	PVT	PVT	Bridgman	Bridgman	Bridgman	CVD
Structure	Hexagonal	Cubic	Cubic	Cubic	cubic	Cubic
Lattice Constant (A)	a=4.1367 c=6.7161	a = 6.483	a=6.486	5.420	6.103	a= 5.6685
Density (g/cm^3)	4.821	5.851	5.851	4.08	5.633	5.264
Melting Point (^{o}C)	1287	1047	1045	1830	1239	1517
Max. size (mm)	25x25x15	25 x 10 x 10	40 x 40 x 10	40d x40h	40d x40h	25x25x15

Bridgman method
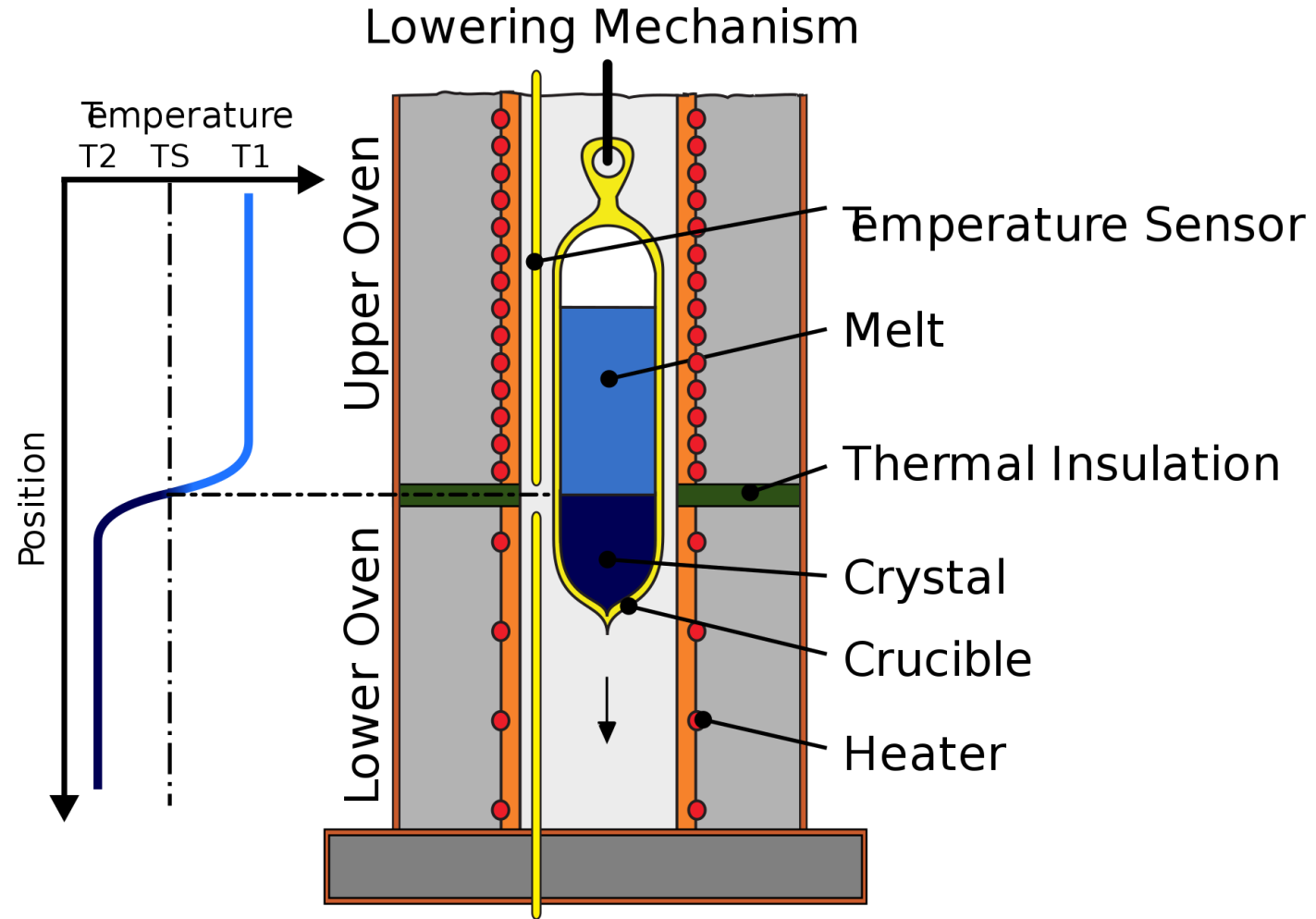
II-VI crystals: Cadmium Telluride (CdTe)
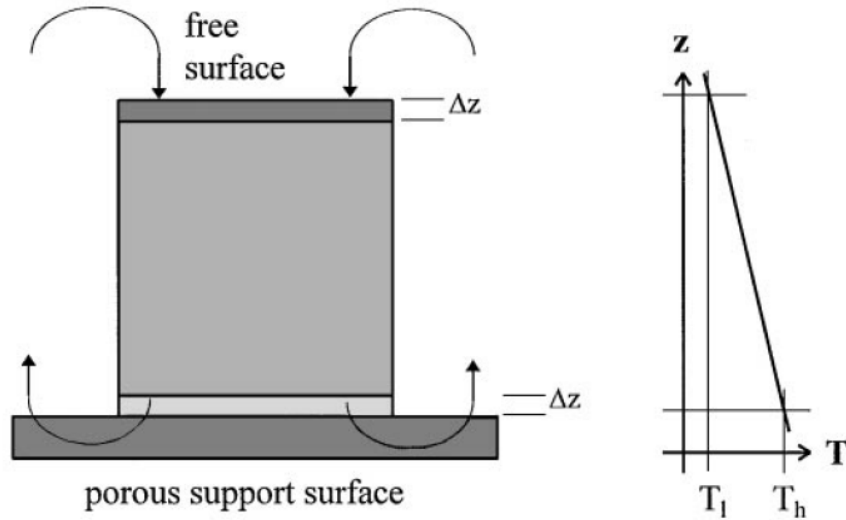
Fig. 1. Idealised schematic diagram showing the self-selecting vapour growth (SSVG) method under steady-state conditions. Sublimation occurs from the bottom of the boule through a porous support and the material lost is re-incorporated at the free surface. At the steady state in a time Δt the boule looses a thickness Δz and it "falls" by this amount to rest on the support. Ideally, a thickness Δz is re-incorporated on the top of the boule at the cooler free surface. The positions of the support and the free surface remain fixed and material is continuously re-cycled from the bottom to the top of the boule.
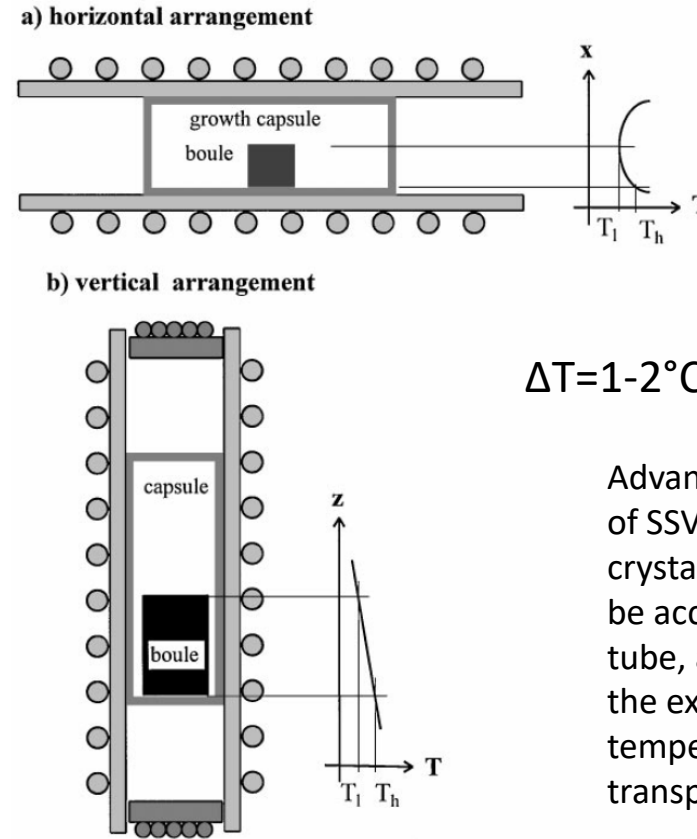
Fig. 2. Schematic diagrams of (a) the horizontal and (b) vertical arrangements of self-selecting vapour growth. In the horizontal arrangement the (radial) temperature gradient is controlled by thermal radiation from the ends of a tube furnace. For the vertical arrangement used in this work the temperature gradient is axial and is controlled by additional heaters installed on the ends of the furnace liner tube.

ΔT=1-2°C

Advantages of the vertical version of SSVG are that it allows larger crystals to be grown than might be accommodated in a horizontal tube, and further that it allows the experimenter to adjust the temperature gradient driving transport.

II-VI crystals: Cadmium Telluride (CdTe)

HF+H$_2$O+CH$_3$COOH to detect twinning, inclusions and dislocations
35 g FeCl$_3$ in 10 ml de-ionised water fo detect dislocation

100 µm
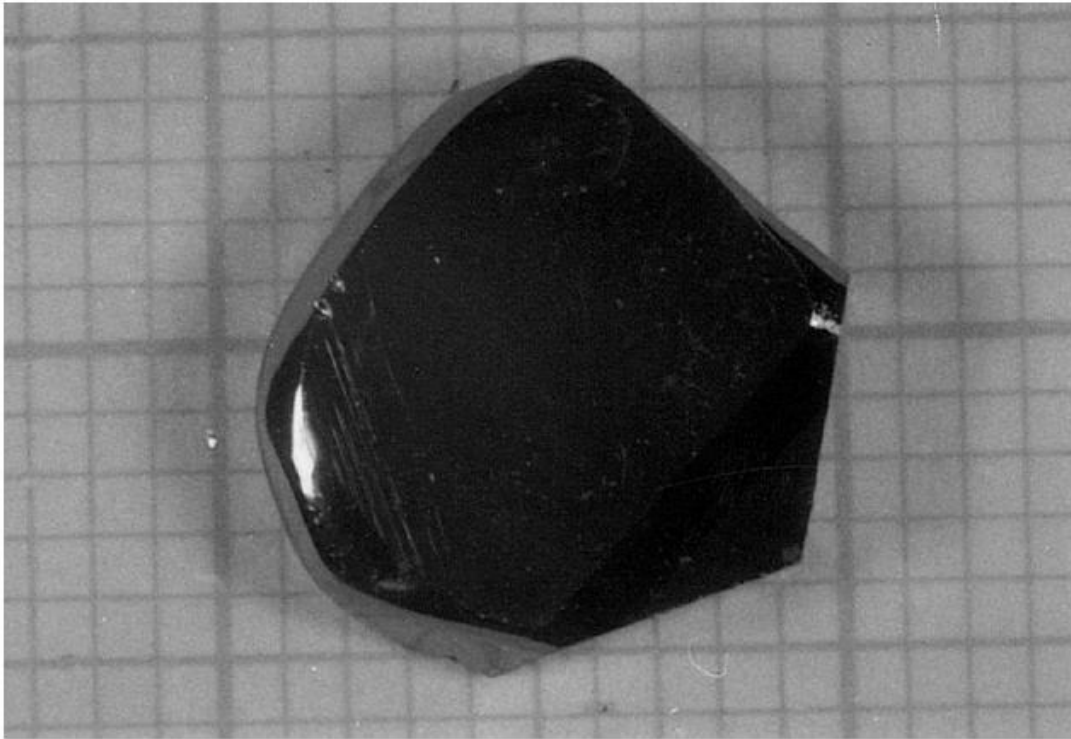
Fig. 3. Photograph of the growth surface of single crystal CdTe $(\bar{1}\,\bar{1}\,\bar{1})$B formed from polycrystalline source material by the SSVG process.
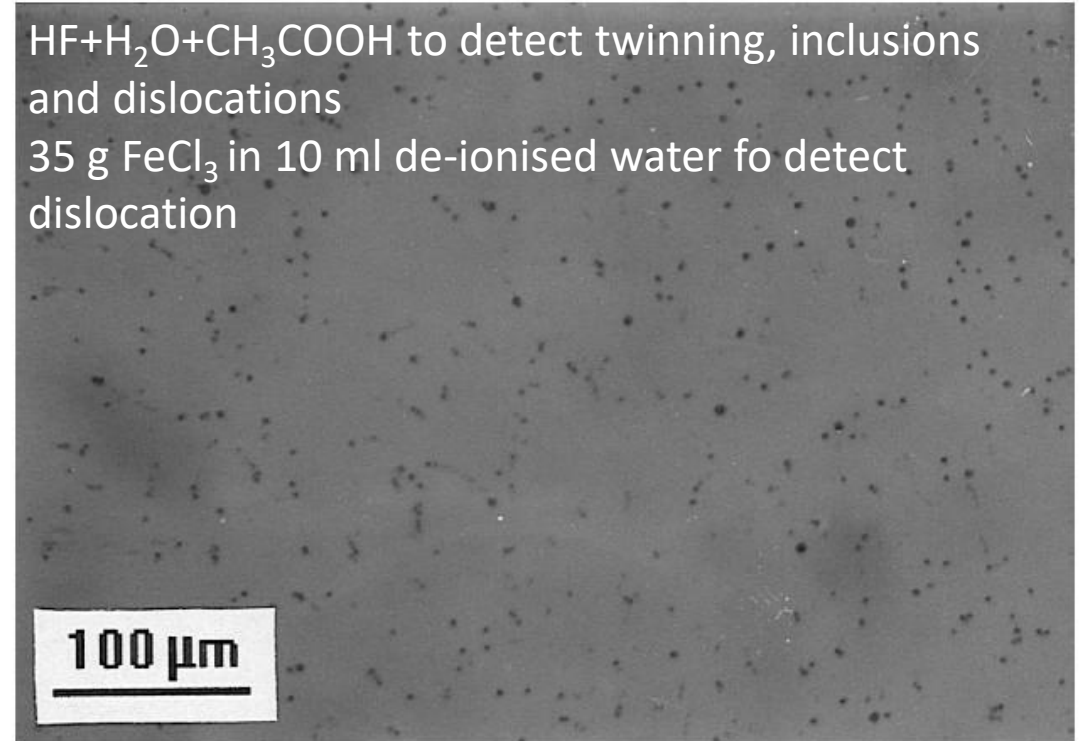
Fig. 4. An apparently random distribution of etch pits having a density of 3×10^5 cm^{-2} was found on a $(\bar{1}\,\bar{1}\,\bar{1})$B oriented slice of CdTe cut at 1.0 cm above the source material in the growth direction.

A. Szczerbakow et al. / Journal of Crystal Growth 191 (1998) 673–678

IV-VI crystals: Lead Selenide and its cousines (Pb(Se,S); (PbSn)Se; (PbSn)Te etc.)
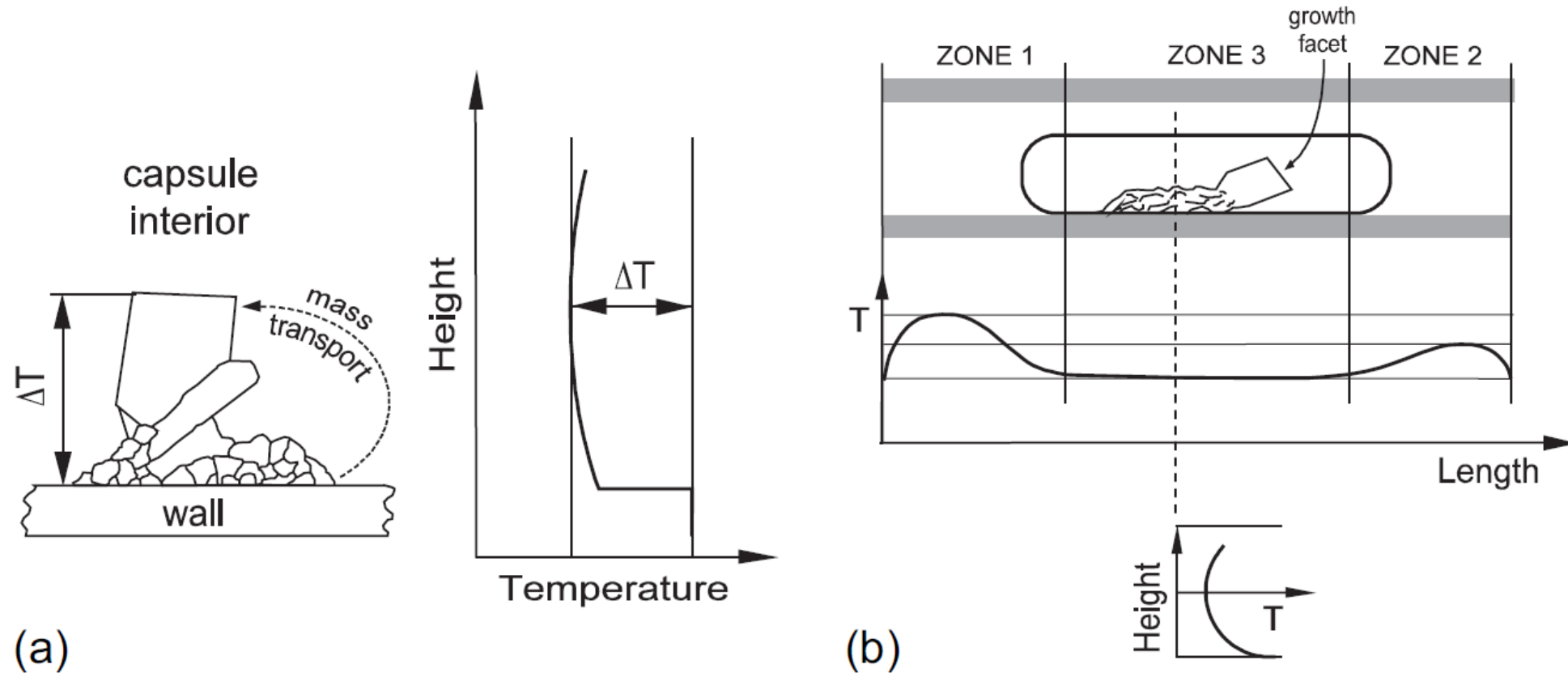
Fig. 1. Schematic diagrams and temperature profiles of idealised (a) and practical (b) SSVG systems.

IV-VI crystals: Lead Selenide and its cousines (Pb(Se,S); (PbSn)Se; (PbSn)Te etc.)
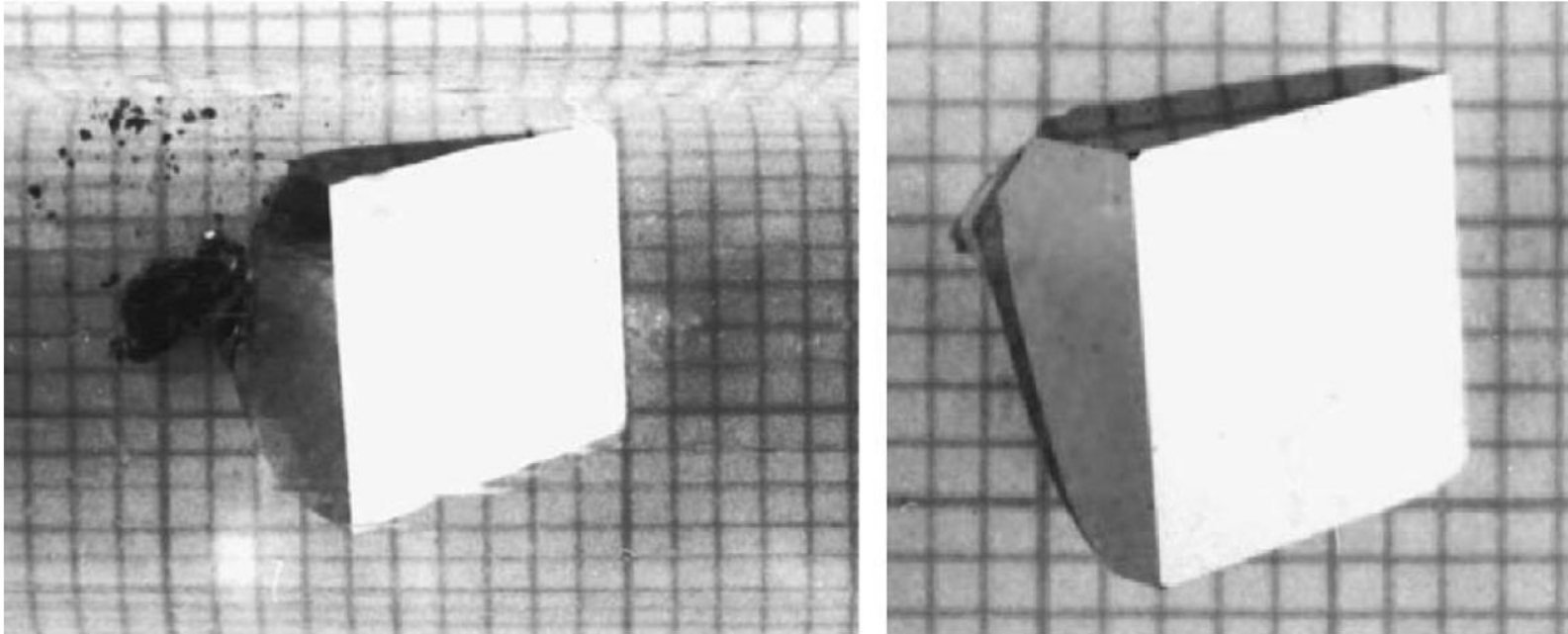
Fig. 2. $PbSe_{0.92}S_{0.08}$ is grown in a practical SSVG system like that in Fig. 1b. The grown crystal has a very distinct crystal habit and there has been almost full conversion of the polycrystalline charge to a single crystal [1]. The crystal is viewed inside the quartz capsule (left hand image) and after removal from it (right hand image). Scale: 1 mm squares.

IV-VI crystals: Lead Selenide and its cousines (Pb(Se,S); (PbSn)Se; (PbSn)Te etc.)
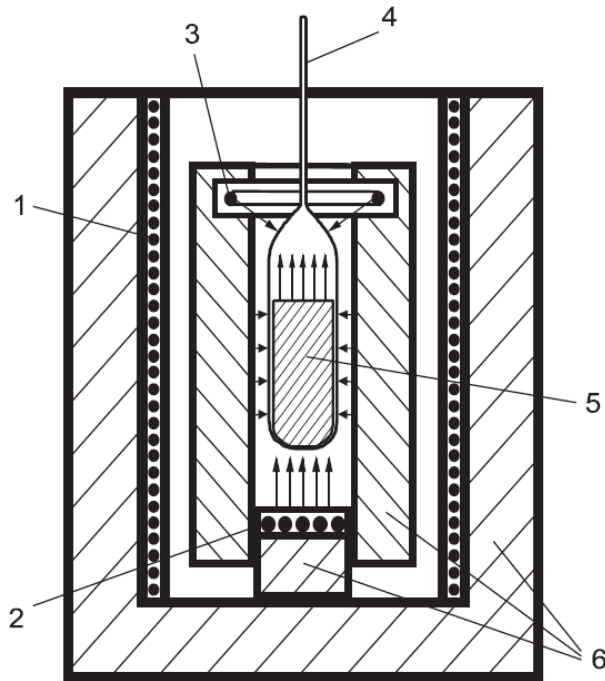
Fig. 10. Schematic diagram of a vertical SSVG system — 1, main heater ensuring the plateau near the growth temperature; 2, heater generating the process-driving temperature difference; 3, heater protecting against condensation in the ampoule top; 4, capillary for condensing traces of an excess element; 5, crystal; 6, thermal insulation. The arrows indicate the main currents of thermal radiation [23].

PbSe crystal

IV-VI crystals: Lead Selenide and its cousines (Pb(Se,S); (PbSn)Se; (PbSn)Te etc.)

ZnTe

$Cd_{1-x}Zn_xTe$

x=0.033

$Cd_{0.8}Zn_{0.2}Te$

4 cm

A. Szczerbakow, K. Durose / Progress in Crystal Growth and Characterization of Materials 51 (2005)
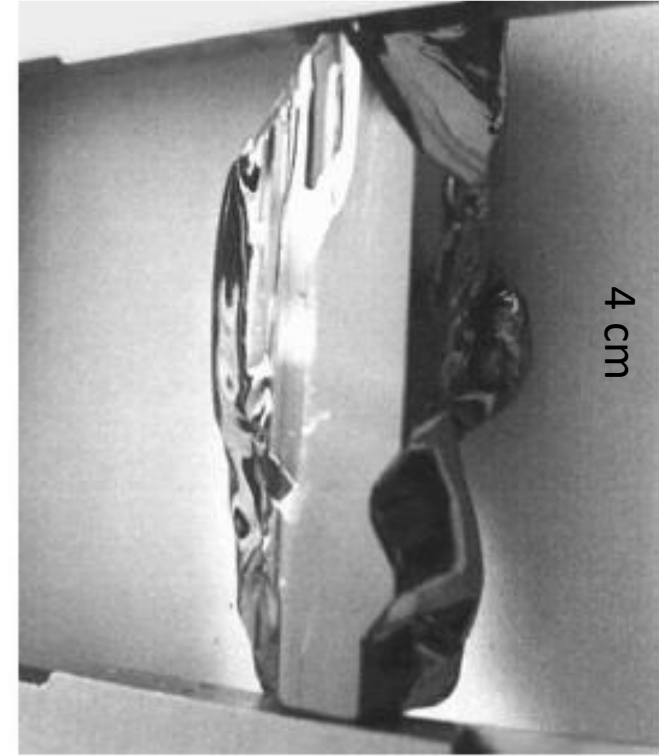
Topological crystalline insulator states in $Pb_{1-x}Sn_xSe$
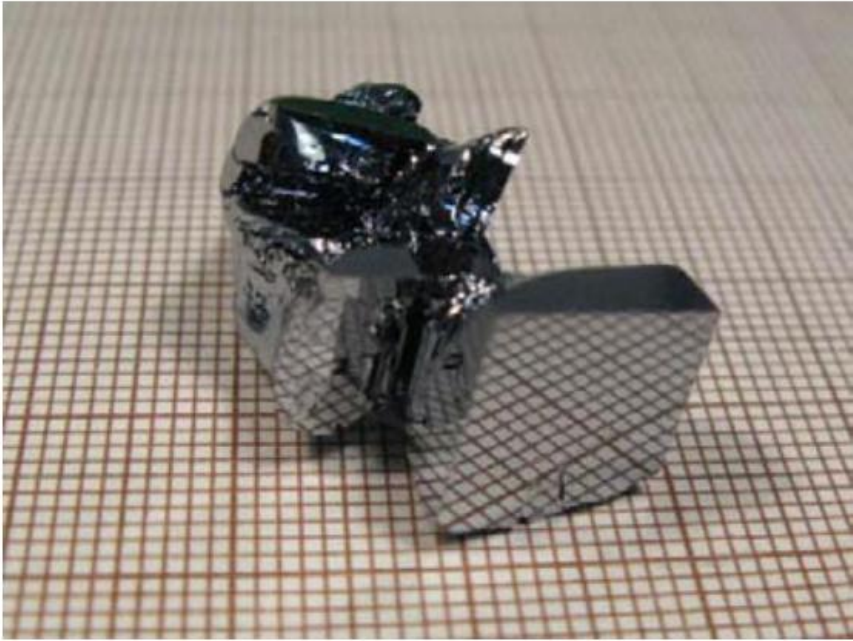
Supplementary Figure 1.
As-grown $Pb_{0.77}Sn_{0.23}Se$ bulk monocrystal. The mirror-like planes at the front part of the crystal are natural (001) facets of a rock-salt-type crystal.
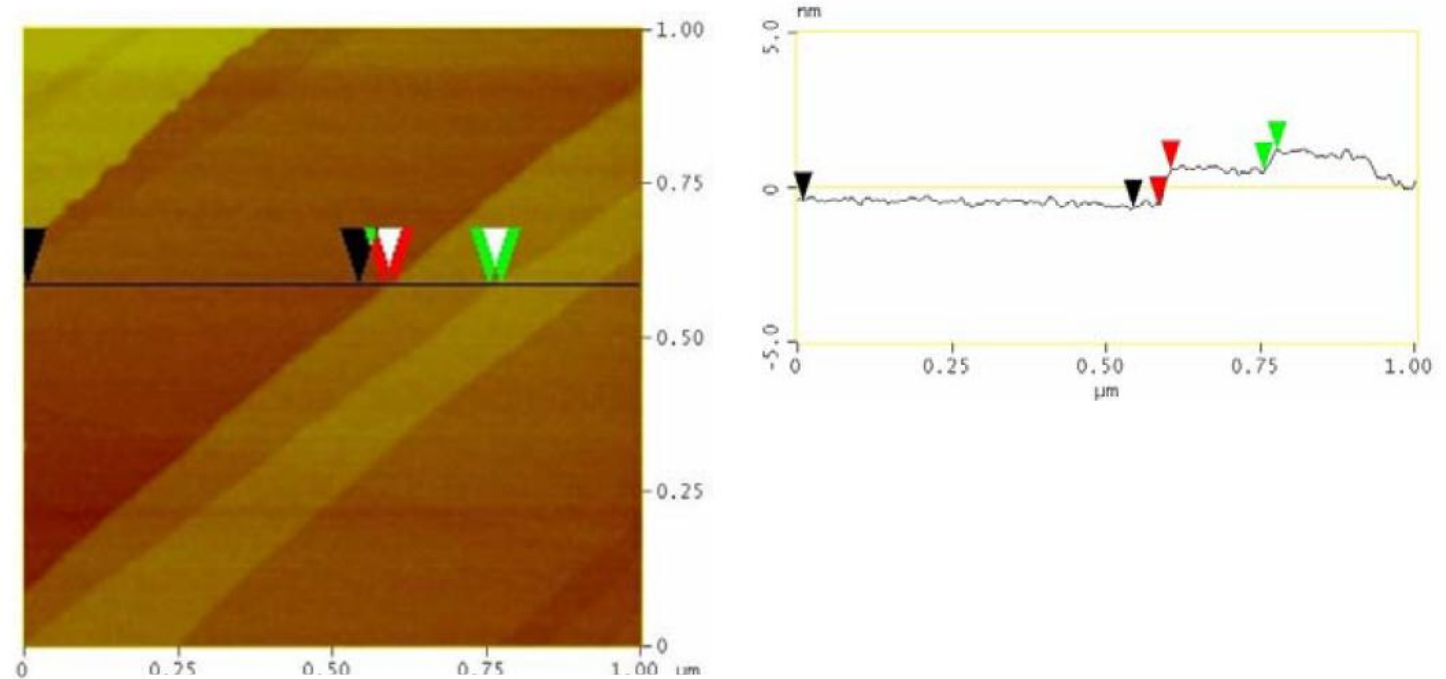
Supplementary Figure 2.
Morphology of the (001) surface of a $Pb_{0.77}Sn_{0.23}Se$ crystal. Atomic force microscopy (AFM) image of a (001) surface of a bulk crystal freshly cleaved in air at room temperature. The height differences between the points marked with green and red arrows equal 6.8 Å and 11.5 Å, respectively. The macroscopically large region between the black arrows is atomically flat.

Silicon Carbide (SiC)

In 1893 Dr. Moissan analyzed samples from Canyon Diablo Meteor Crater Later Named "Carborundum" or "Moissanite"

In 1896 Acheson attempted to create artificial diamond with silica and carbon powder but ended up with SiC subsequently used as abrasive by Westinghouse

Plik:BLW Carborundum crystals.jpg – Wikipedia, wolna encyklopedia

Moissanite – Wikipedia

In 1955 Lely Developed a Sublimation Method to Grow Small Hexagonal SiC "Lely" Platelets at 2250°C
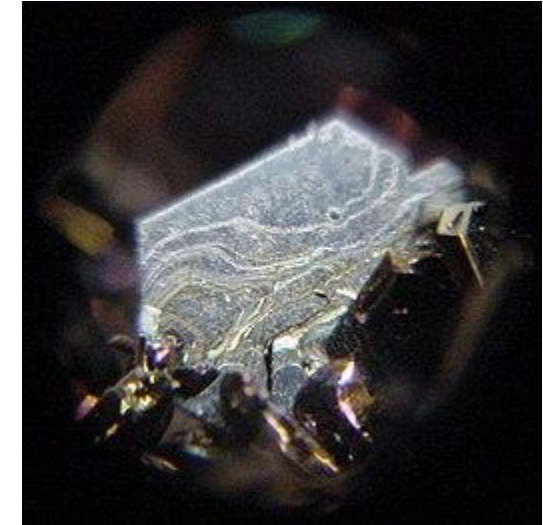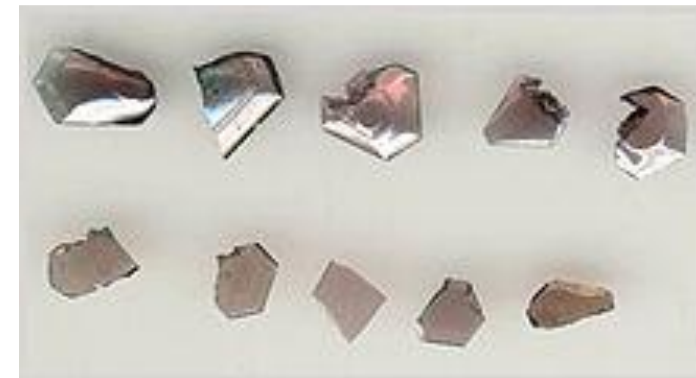
Silicon Carbide (SiC)

In 1978 Tairov Published First
Seeded SiC Crystal Growth Result

NCSU Licensed Key Patents to
Establish Cree Research in 1987

Tairov
Tsvetkov

1987

Cree

1991
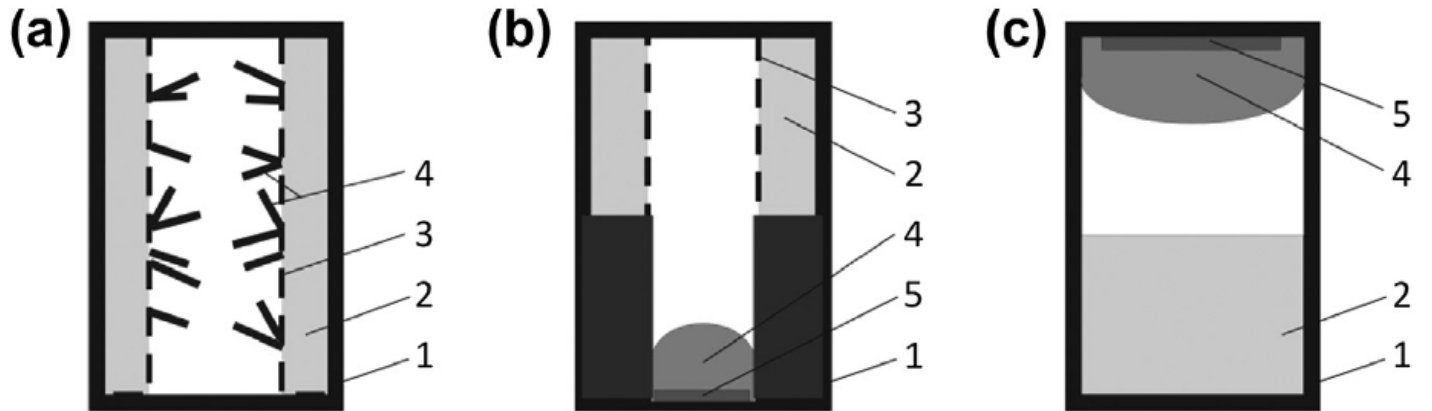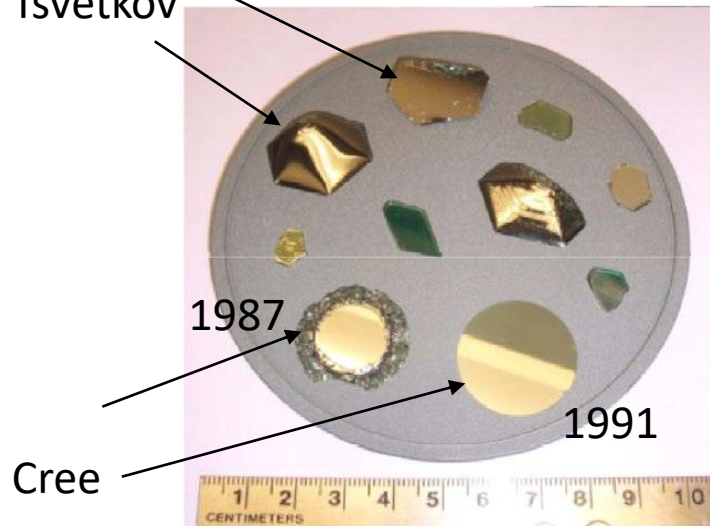
Schematic cross-section drawings of hot zone setups used for SiC bulk
crystal growth. (a) Lely setup, (b) Ziegler setup, (c) modified PVT setup as
typically used today, 1: graphite crucible, 2: SiC source material, 3: optional
porous graphite cylinder, 4: growing SiC crystal(s), 5: SiC seed

Silicon Carbide (SiC)

Silicon carbide (SiC) is a compound semiconductor, with its atomic crystal consisting of 50 % silicon (Si) and 50 % carbon (C) atoms. Each C has exactly four Si neighbors and vice versa, with a very strong C-Si bond strength of approximately 4.6 eV, which leads to impressive material properties.

SiC - an outstanding example for *polymorphism*

A certain polytype is defined by the Si-C bilayer stacking sequence along the c-axis of the hexagonal close-packed system.
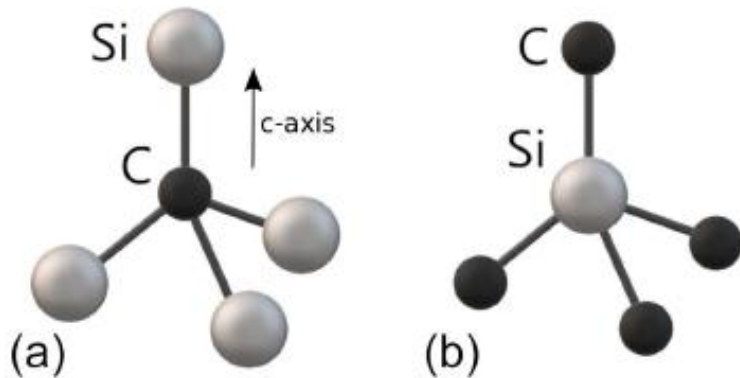
Figure 2.1: *The tetrahedron building block of SiC, that either can be represented with a C atom in the center bonded to four Si atoms (a) or a Si atom in the center bonded to four C atoms (b).*
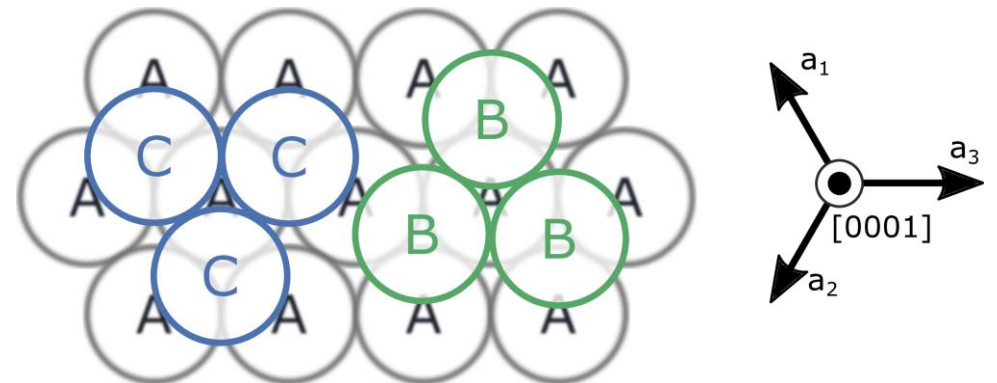
On each Si-C bilayer (A), there are two possible stacking sites (B, C).

Silicon Carbide (SiC)

SiC has lattice sites which differ in their structures of nearest neighbors. These lattice sites can either be hexagonal sites or cubic sites. Cubic and hexagonal sites mainly differ in their position of second-nearest neighbors. The relative concentration of hexagonal or cubic sites furthermore depends on the polytype: while only cubic sites are present in 3C-SiC, 4H-SiC has one hexagonal and one cubic site, whereas 6H-SiC has one cubic and two hexagonal sites.
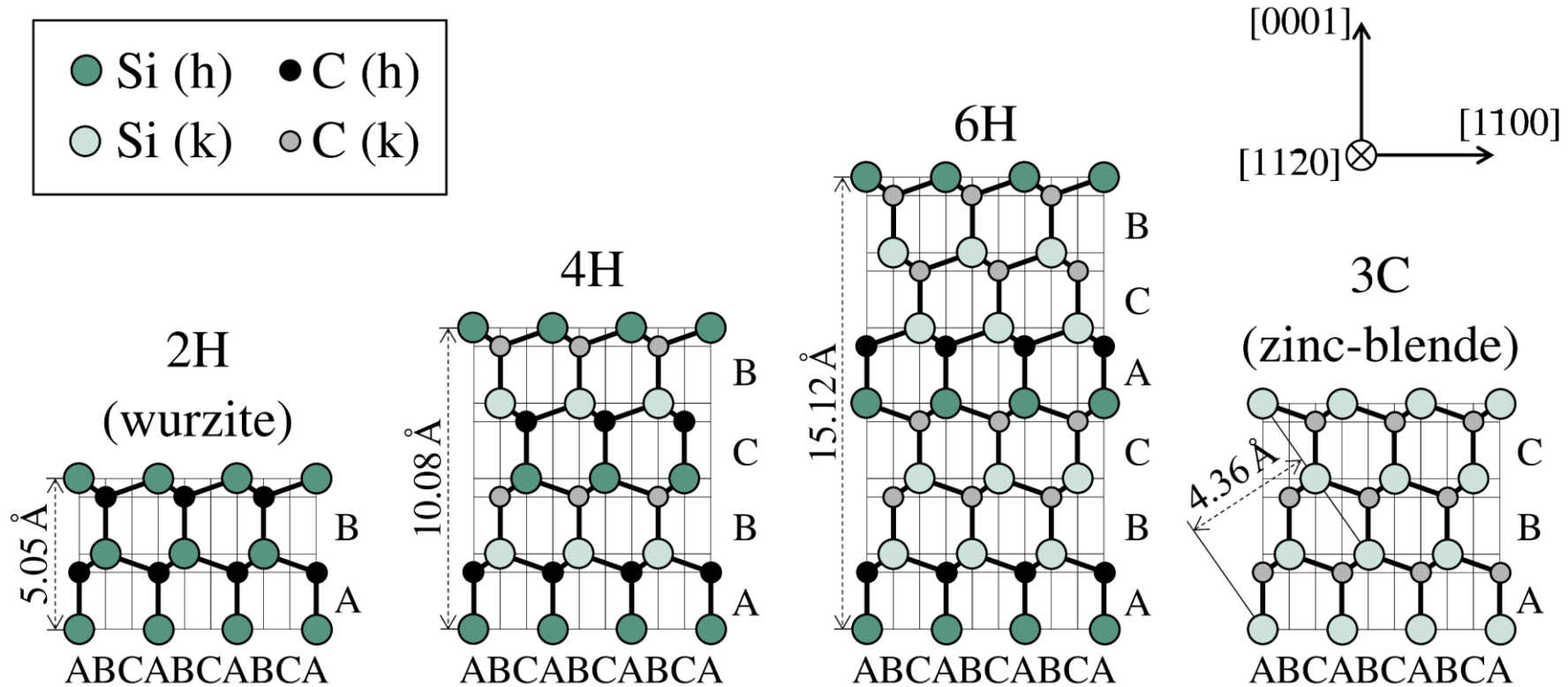
Silicon Carbide (SiC)

How are SiC crystals grown?
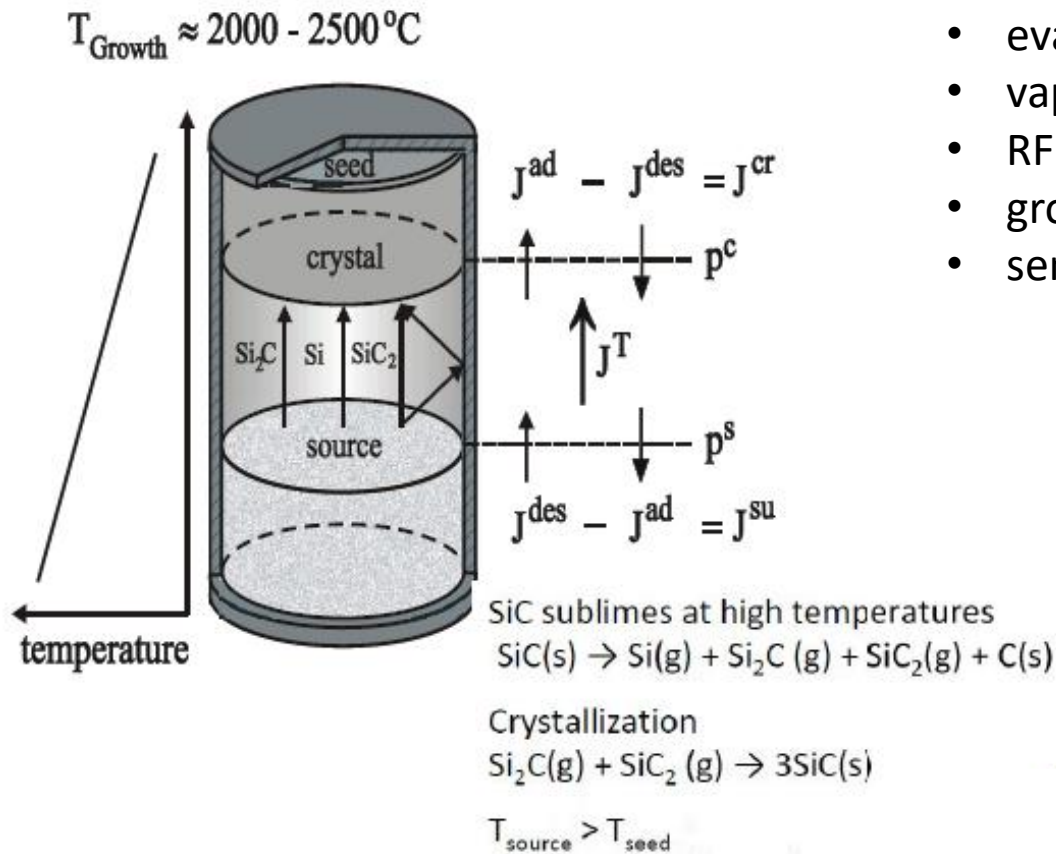
Seeded Sublimation Method:
- closed system
- evaporation of SiC charge
- vapor species transport to seed
- RF or resistive heating
- growth rate controlled by temp/pressure
- semi-insulating (SI) or n-type

$T_{Growth} \approx 2000 - 2500\,^{\circ}C$

seed

crystal

$J^{ad} - J^{des} = J^{cr}$

p^c

$Si_2C \quad Si \quad SiC_2$

J^T

source

p^s

$J^{des} - J^{ad} = J^{su}$

temperature

SiC sublimes at high temperatures
$SiC(s) \rightarrow Si(g) + Si_2C\,(g) + SiC_2(g) + C(s)$

Crystallization
$Si_2C(g) + SiC_2\,(g) \rightarrow 3SiC(s)$

$T_{source} > T_{seed}$
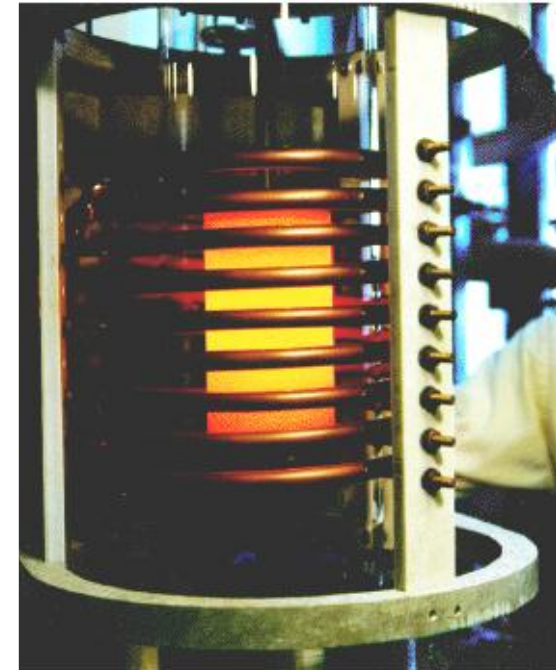
R=0.1-0.5 mm/hour

Silicon Carbide (SiC)

(a)
- Upper pyrometer
- Inert/doping gas inlet
- Water cooled double-walled quartz tubing
- Water cooled induction coil
- Seed
- Growing crystal
- Susceptor
- Crucible
- Source material
- Crucible/susceptor support
- Thermal insulation
- Exhaust/pump line
- Lower pyrometer
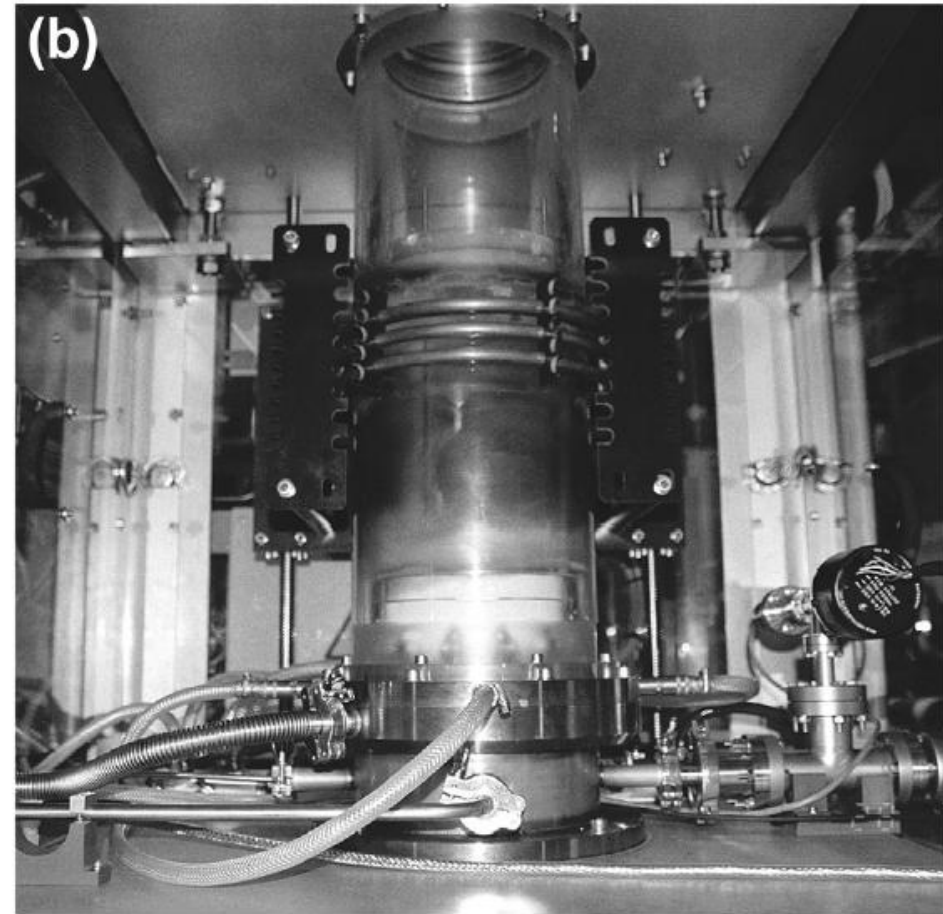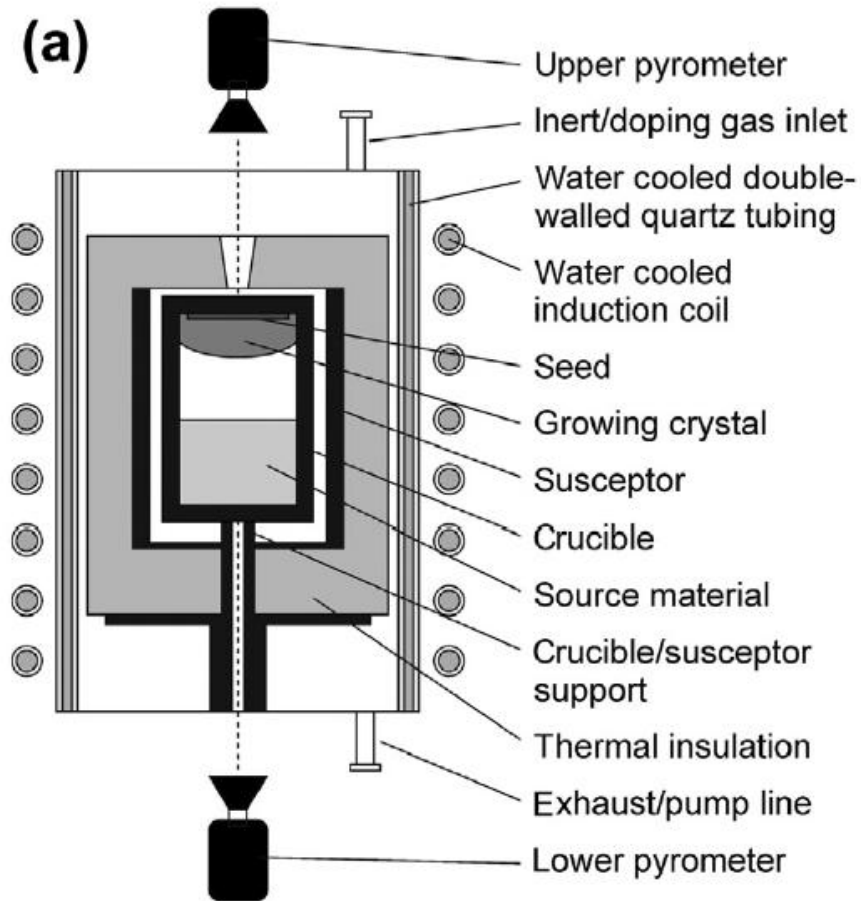
FIGURE 16.7 (a) Schematic and (b) photograph of a typical PVT growth setup.

Silicon Carbide (SiC)

Crucible

TaC crucible
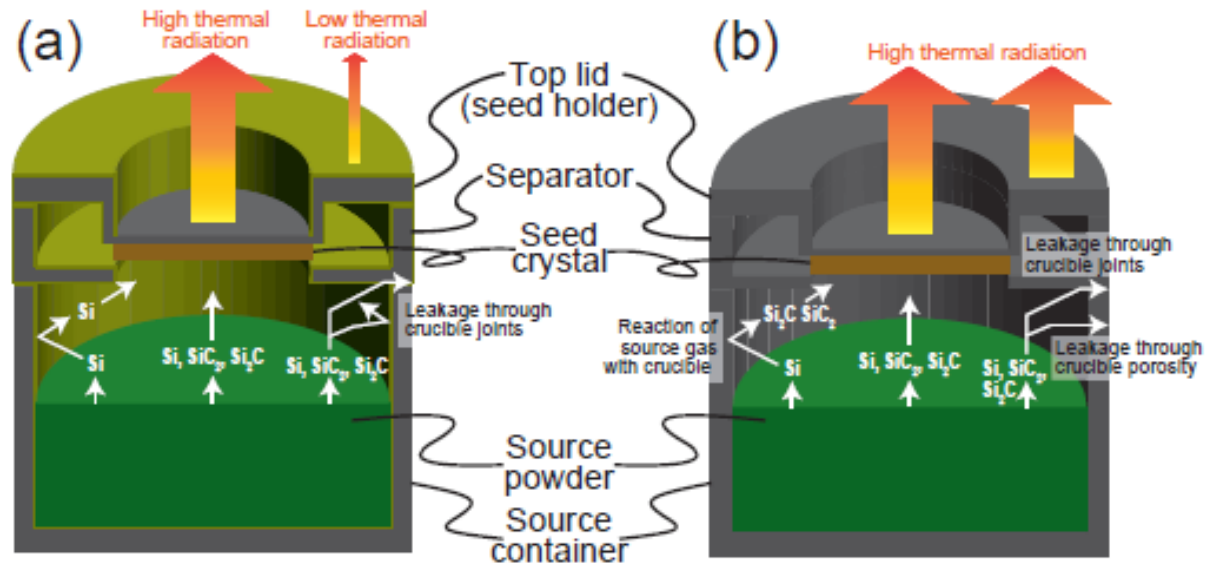
graphite crucible

TaC crucible
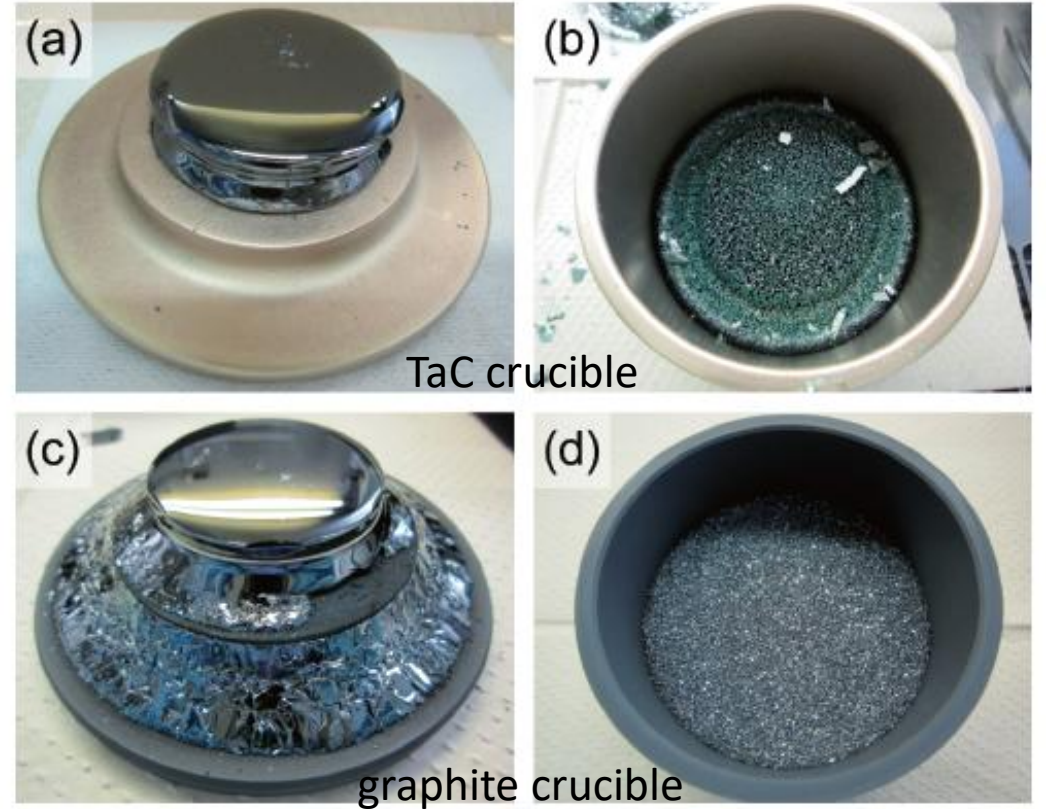
graphite crucible

Growth with the TaC-coated graphite crucibles reduced source gas leakage and increased the material yield for single crystals because the TaC layers were gas-tight and had a low emissivity.

Silicon Carbide (SiC)
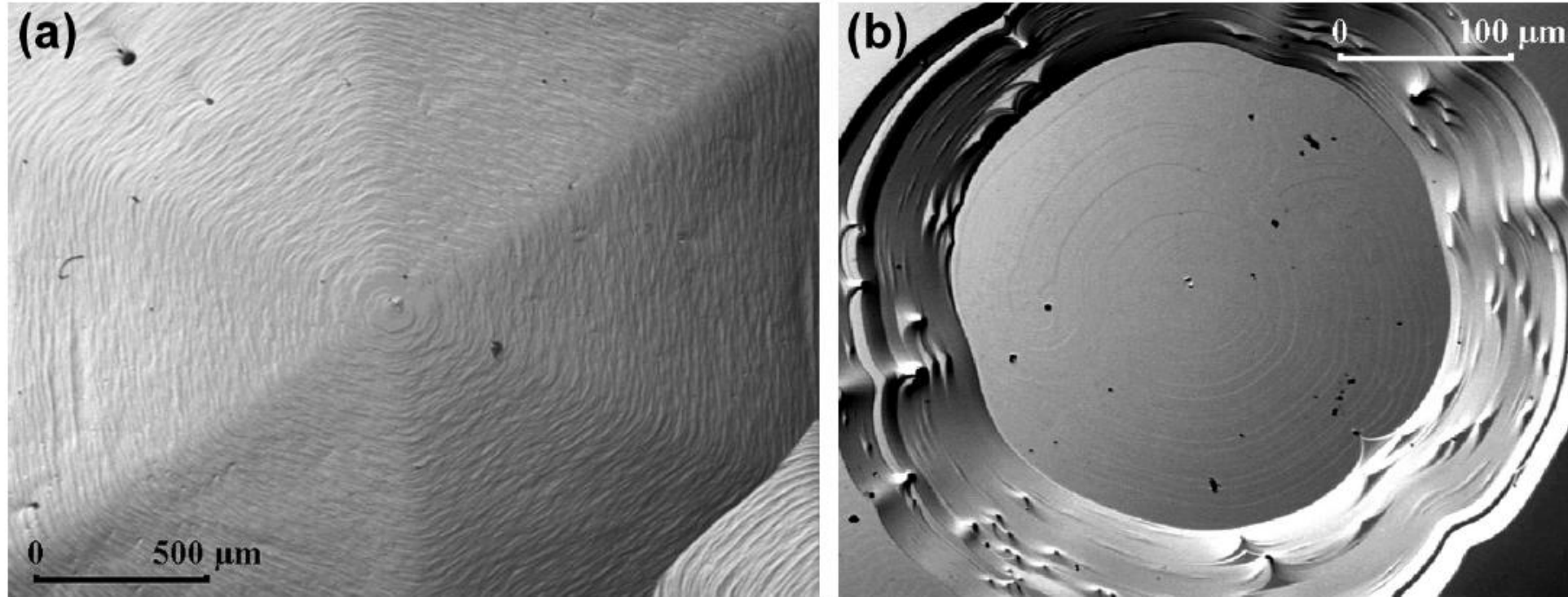
FIGURE 16.6 Spiral growth and step bunching on basal planes of SiC (optical microscopy images): (a) C-polar face, (b) Si-polar face.

Silicon Carbide (SiC)
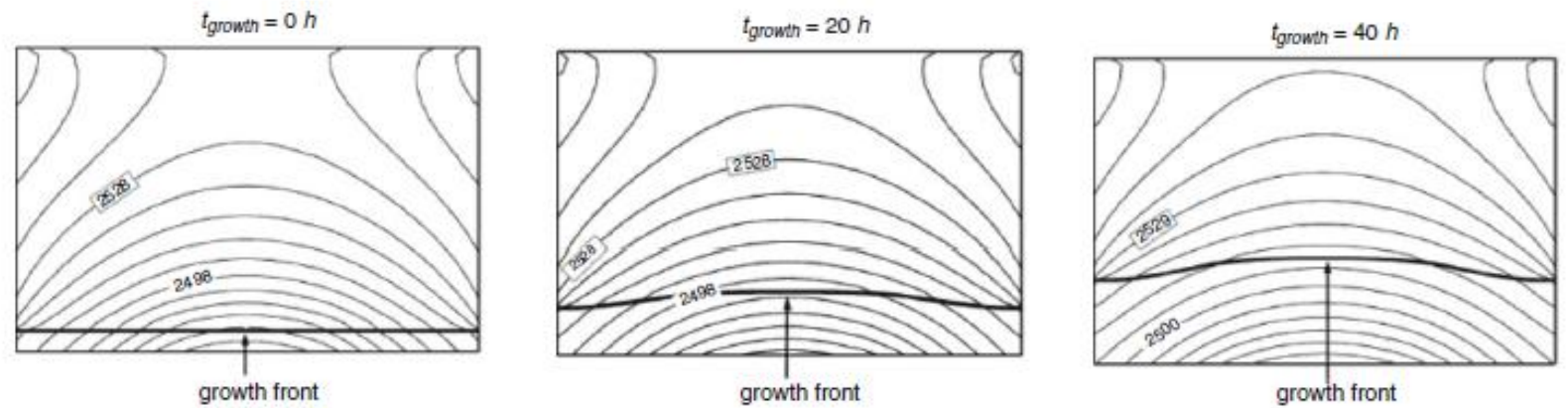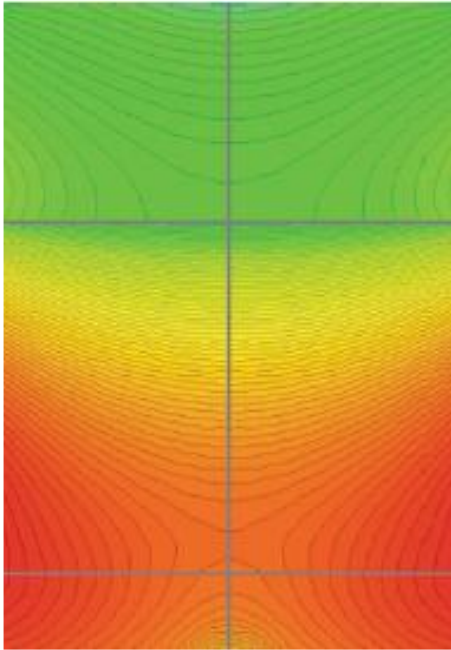
Temperature distribution and growth front for three different points in time during SiC PVT growth. The seed is positioned at the bottom of the individual images. The SiC source is on the top.

Typical thermal field of SiC PVT growth

Silicon Carbide (SiC)

Various defects observed in bulk SiC and their relationship
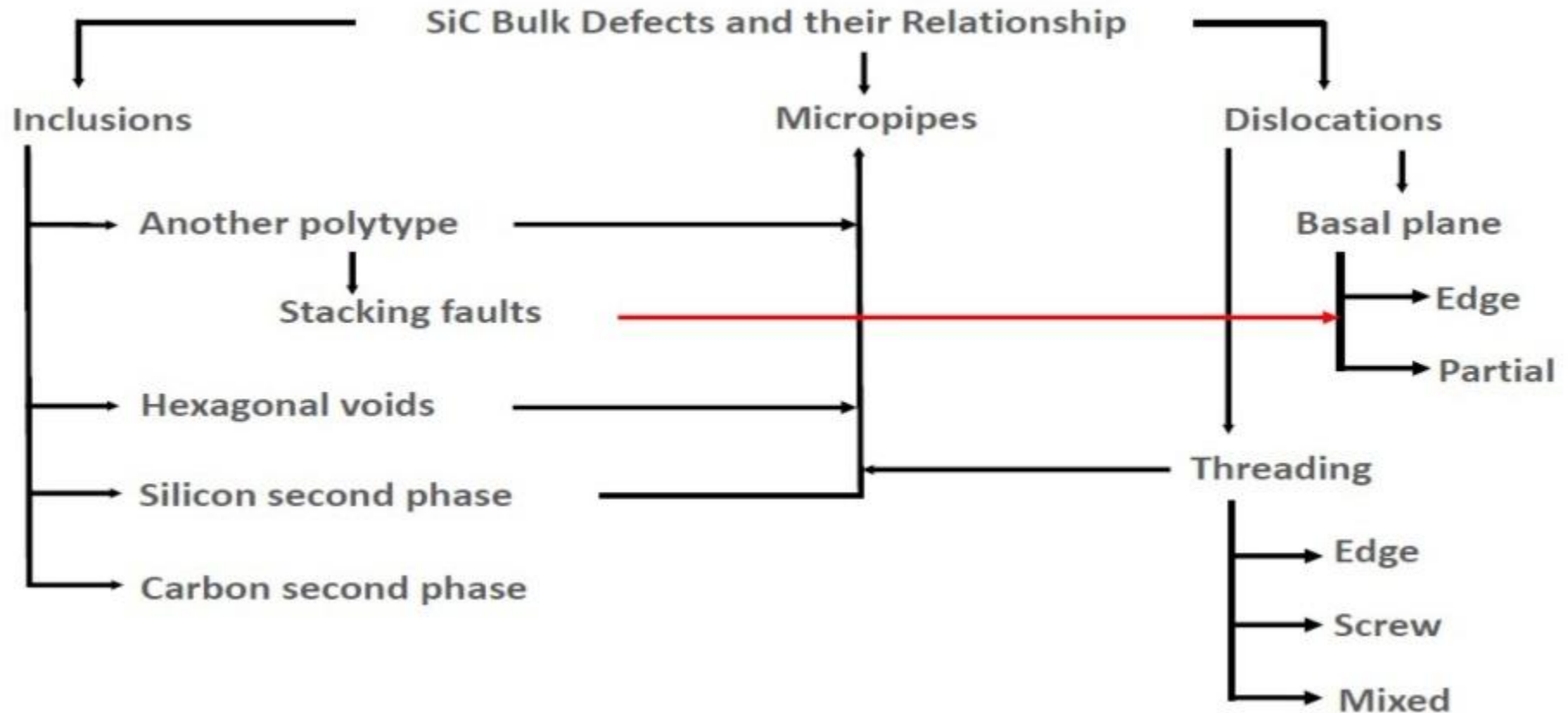
Silicon Carbide (SiC)
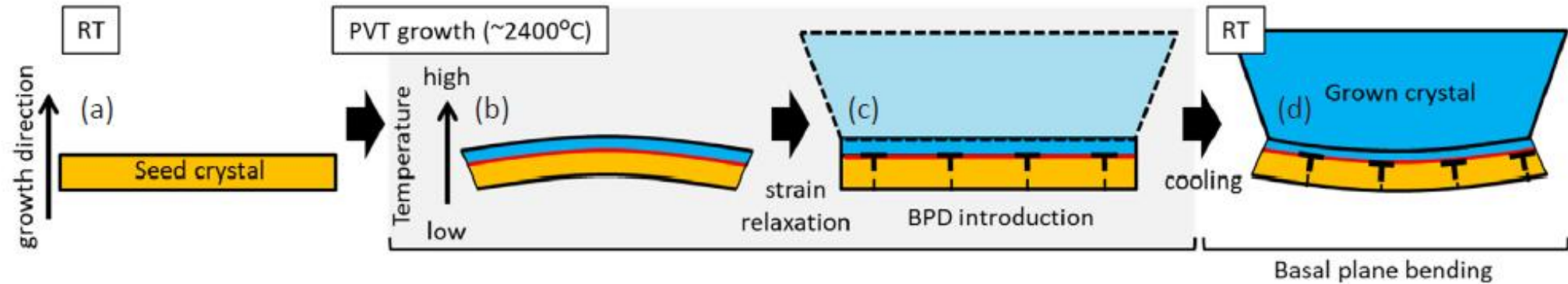
- (a) seed crystal prior to PVT growth

- (b) basal plane bending associated the large temperature gradient at the initial stage of growth, which occurs in a convex manner toward the growth direction

- (c) introduction of BPDs to relax the misfit strain within the basal plane at the grown crystal/seed interface

- (d) concave-shape basal plane bending toward the growth direction after cooling to room temperature, are sequentially depicted.

Silicon Carbide (SiC)
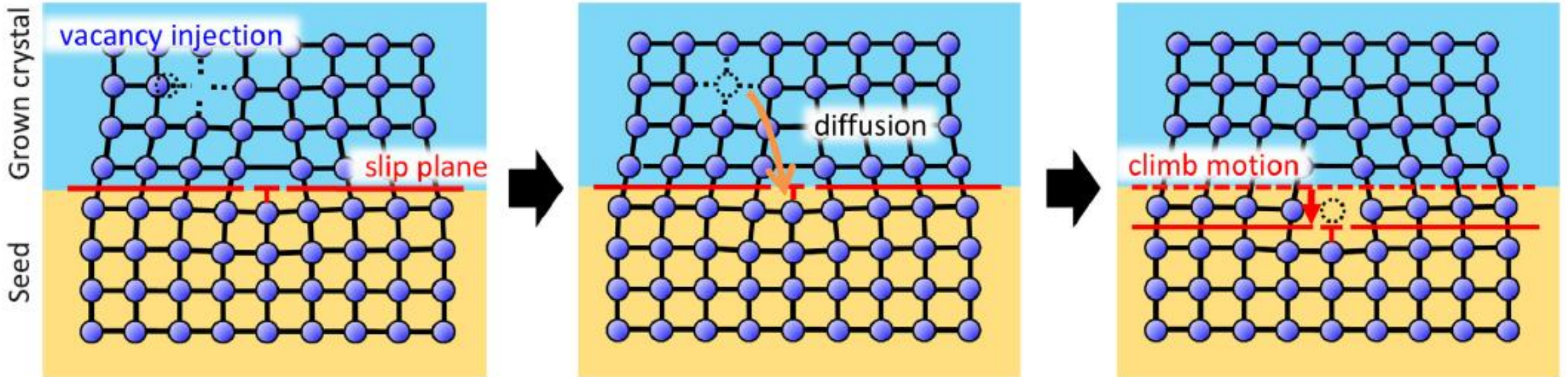
Schematic illustration of the climb motion of a BPD toward the back side of the seed crystal due to the vacancy injection into the growing crystal during PVT growth

Silicon Carbide (SiC)
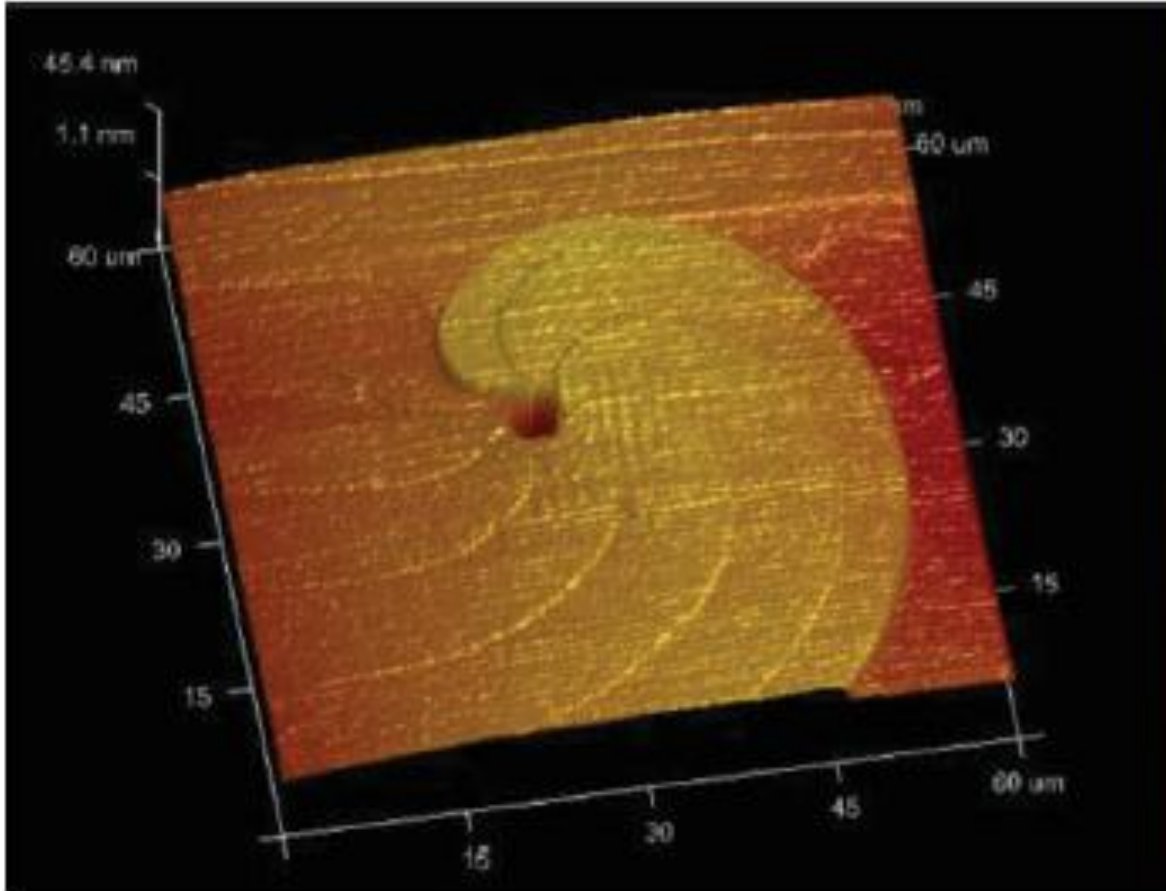
An AFM image of a micropipe in 6H-SiC single crystal

A micropipe is a hollow core associated with a super-screw dislocation. It penetrates through the entire crystal along the c-axis with diameter from tens of nanometers to several micrometers. According to the Frank theory [19], a dislocation whose Burgers vector exceeds a critical value, of the order of magnitude 10 Å, is only in equilibrium with an empty tube at its core. When a micropipe was formed, the elastic strain energy released by the formation of hollow core and surface free energy created by the interior cylindrical surface of hollow core reached a balance.

- Micropipes can be generated due to the instability growth conditions or other defects such as seed back-side void, foreign polytype, C or Si inclusion, etc.

- Micropipes have the heredity.

Silicon Carbide (SiC)
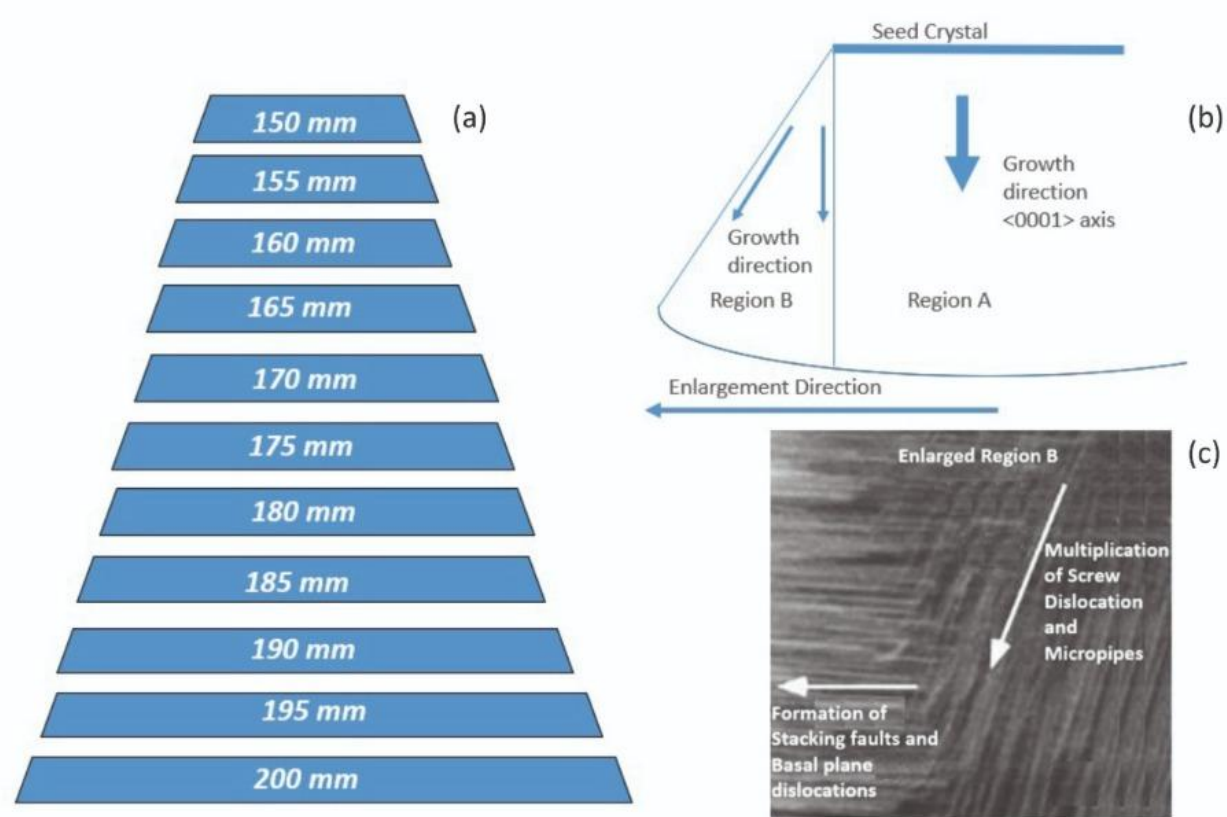
Seed enlargement lies at the heart of the introduction of larger wafer sizes. Shown here are illustrations of: (a) a seed expansion process from 150-200 mm, and (b), the defects that can develop during the seed expansion process. The newly expanded region is susceptible to the formation of more defects (c)

Silicon Carbide (SiC)

Fig. 2.21 Defect propagation on the 4H-SiC {0 3—3 8} seed
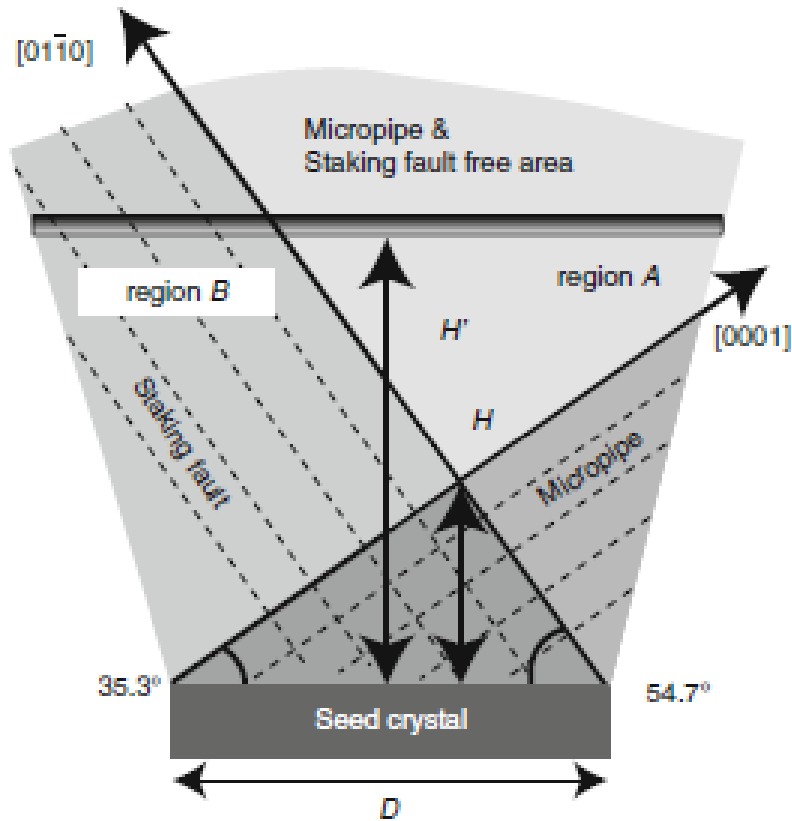
Silicon Carbide (SiC)
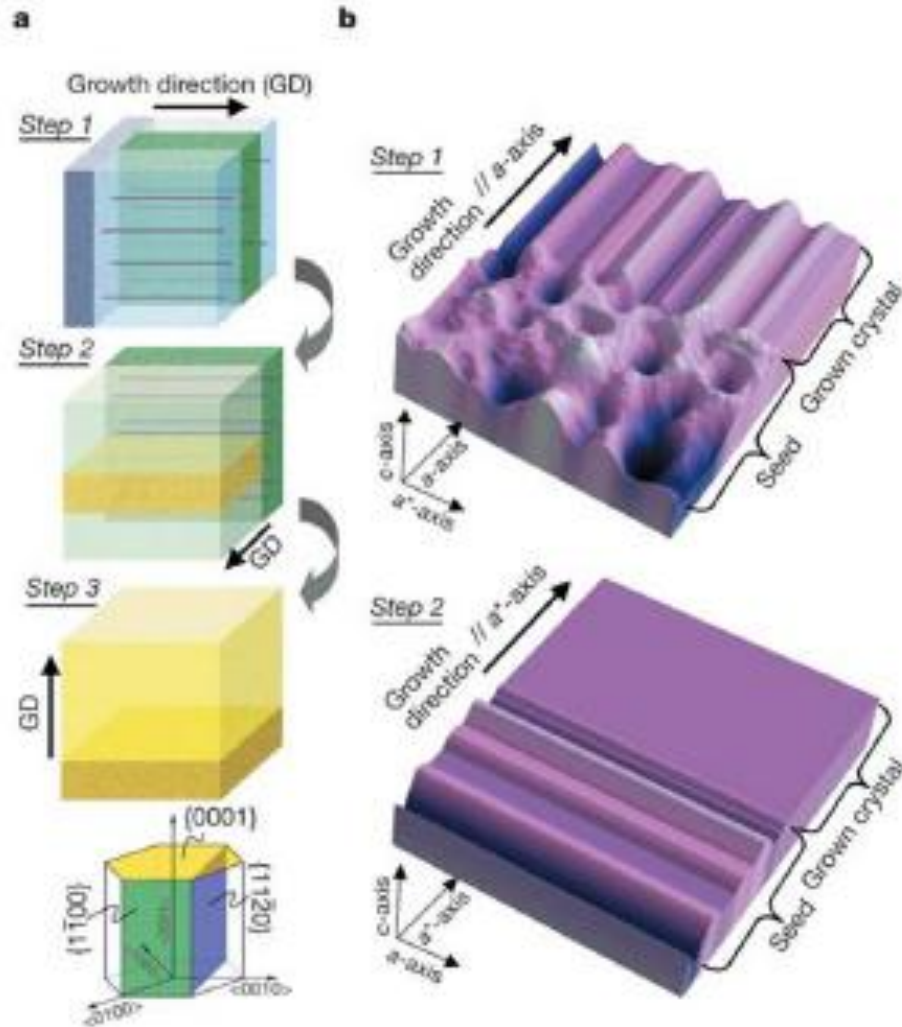
Schematic illustrations of 'repeated a-face' (RAF) growth process. The growth sequences are as follows.

Step 1: first a-face growth (seed and grown crystal are shown dark blue and light blue, respectively). GD, growth direction.

Step 2: second a-face growth perpendicular to first a-face growth (seed sliced from first a-face growth crystal, and the grown crystal are shown dark green and light green, respectively).

Step 3: c-face growth with offset angle of several degrees (seed sliced from second a-face growth crystal, and the grown crystal are shown dark yellow and light yellow, respectively)

a.   In this figure, the first and second a-faces are {11-20} and {1-100} faces. At the bottom of panel a are shown the major crystallographic axes and lattice planes in the RAF process. Dislocation characteristic of a-face growth crystal (first a-face growth crystal and second seed crystal of panel a) is shown by purple line.

b.   Top side view, showing {0001} lattice plane irregularities of seed and grown crystal in steps 1 and 2. The a*-axis is perpendicular to both the a-axis and the c-axis.

Silicon Carbide (SiC)

GT Advanced Technologies (GTAT)

Shifting to 200 mm silicon carbide - News (compoundsemiconductor.net)

Silicon Carbide (SiC)

by J.D. Blevins, Petersen Peer Review Presentation; 2nd - 5th Nov. 2021

Silicon Carbide (SiC)

Progress in crystal growth from 50 mm to 200 mm

Silicon Carbide (SiC)

1. Teal and Little (1950)
2. Mullin, Heritage, Holiday, and Straughan (1968)
3. Tairov and Tsvetkov (1978)
4. Davis, Carter, and Hunter (1989)

by J.D. Blevins, Petersen Peer Review Presentation; 2nd - 5th Nov. 2021
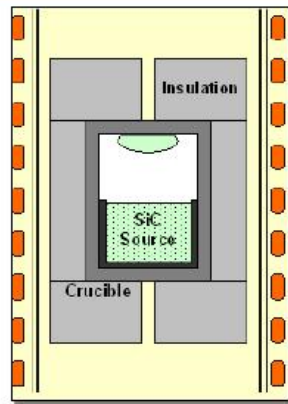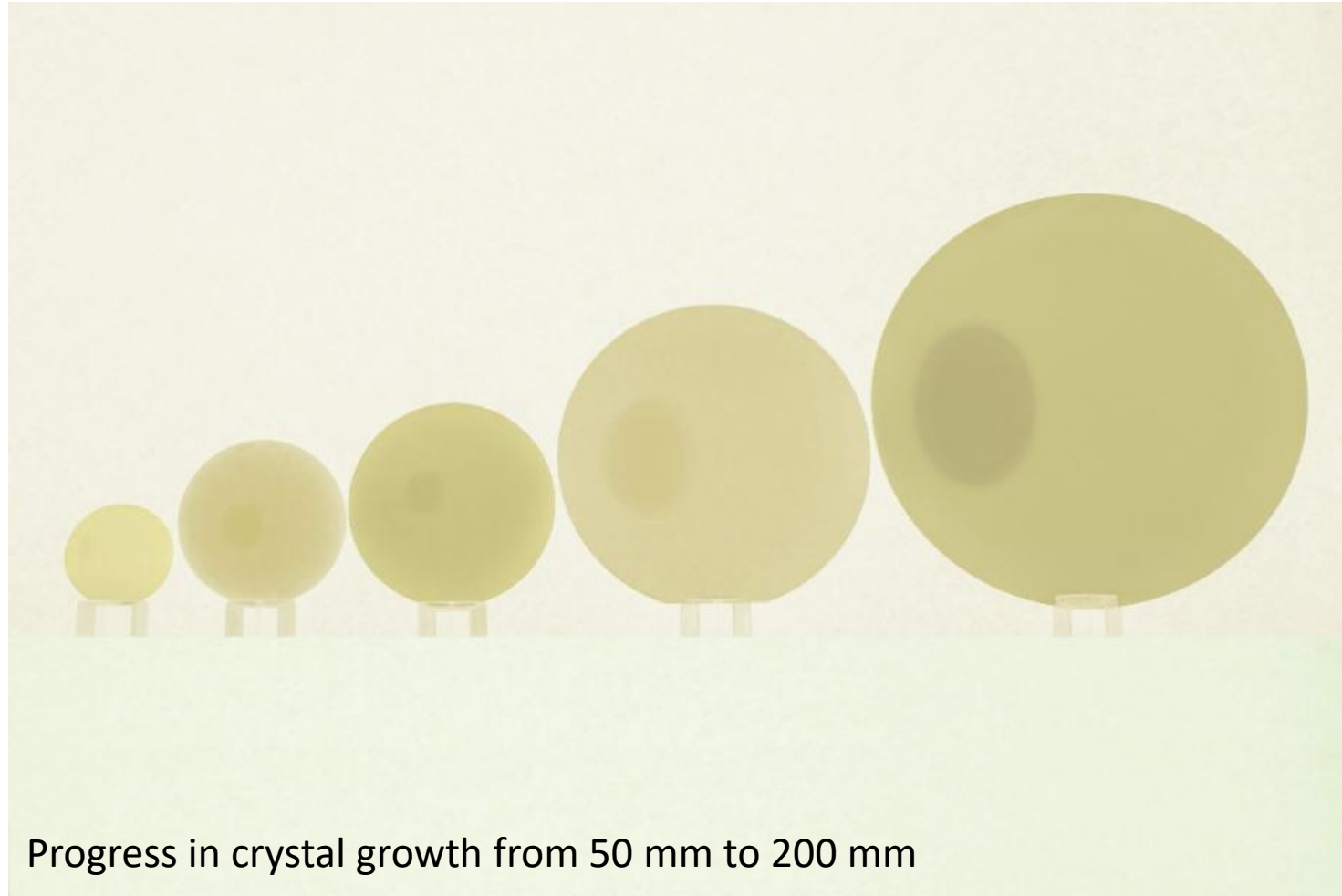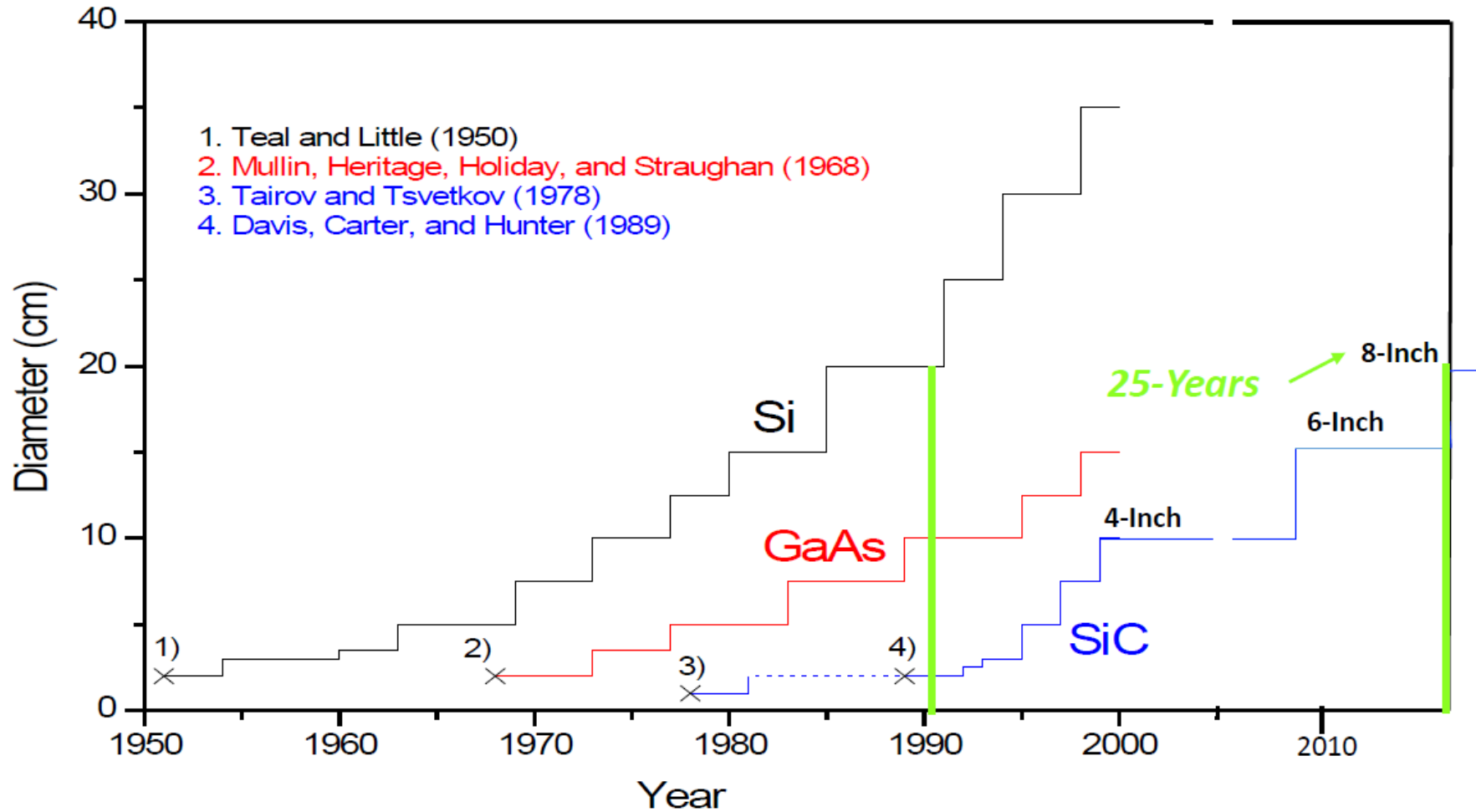
Silicon Carbide (SiC)

SiC crystal growth

SiC boule

seed crystal

[0001]

[11$\bar{2}$0]

off-axis SiC(0001) wafer

top view

[$\bar{1}$100]

[11$\bar{2}$0]

off-angle

[0001]

[11$\bar{2}$0]

side view
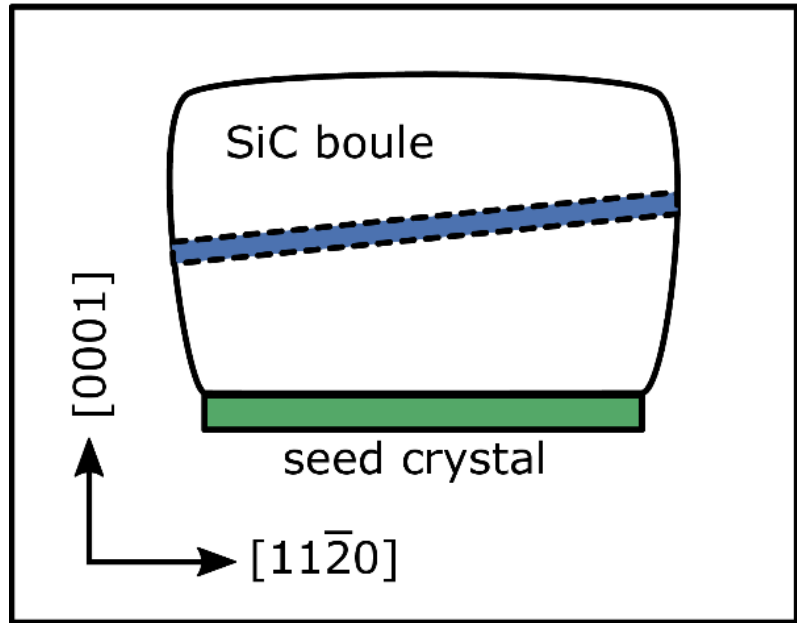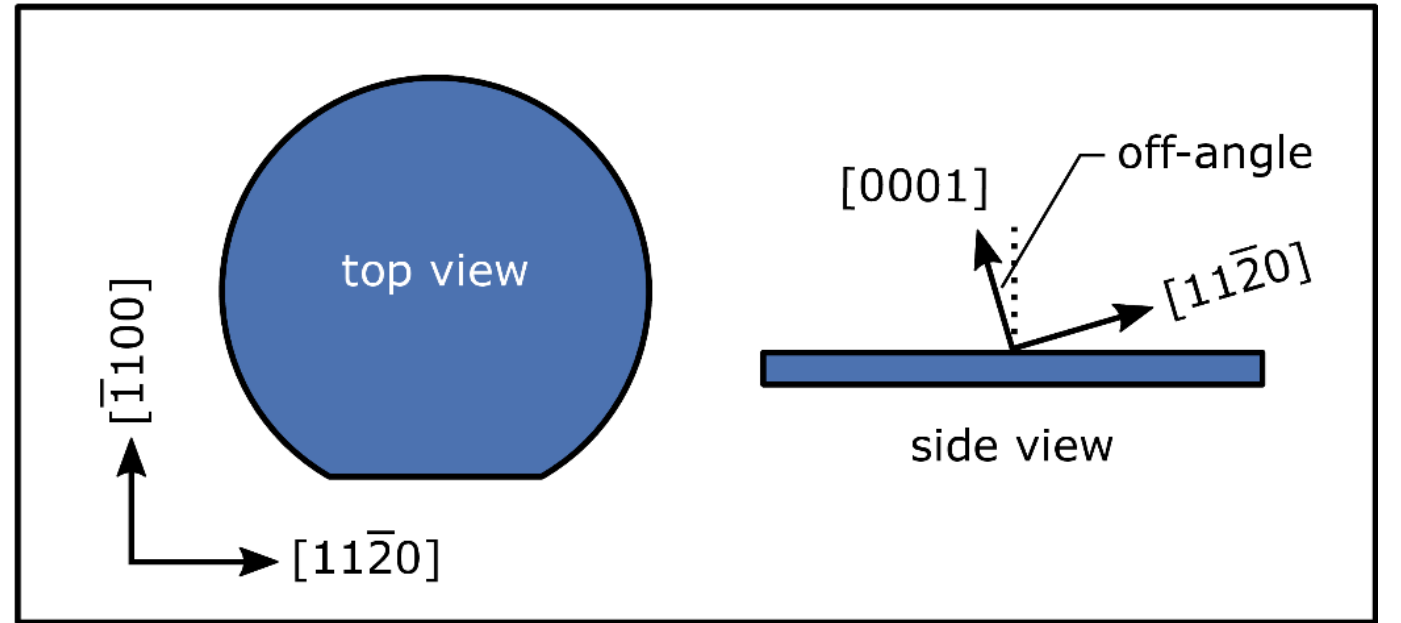
off-angle = 4°

Silicon Carbide (SiC)
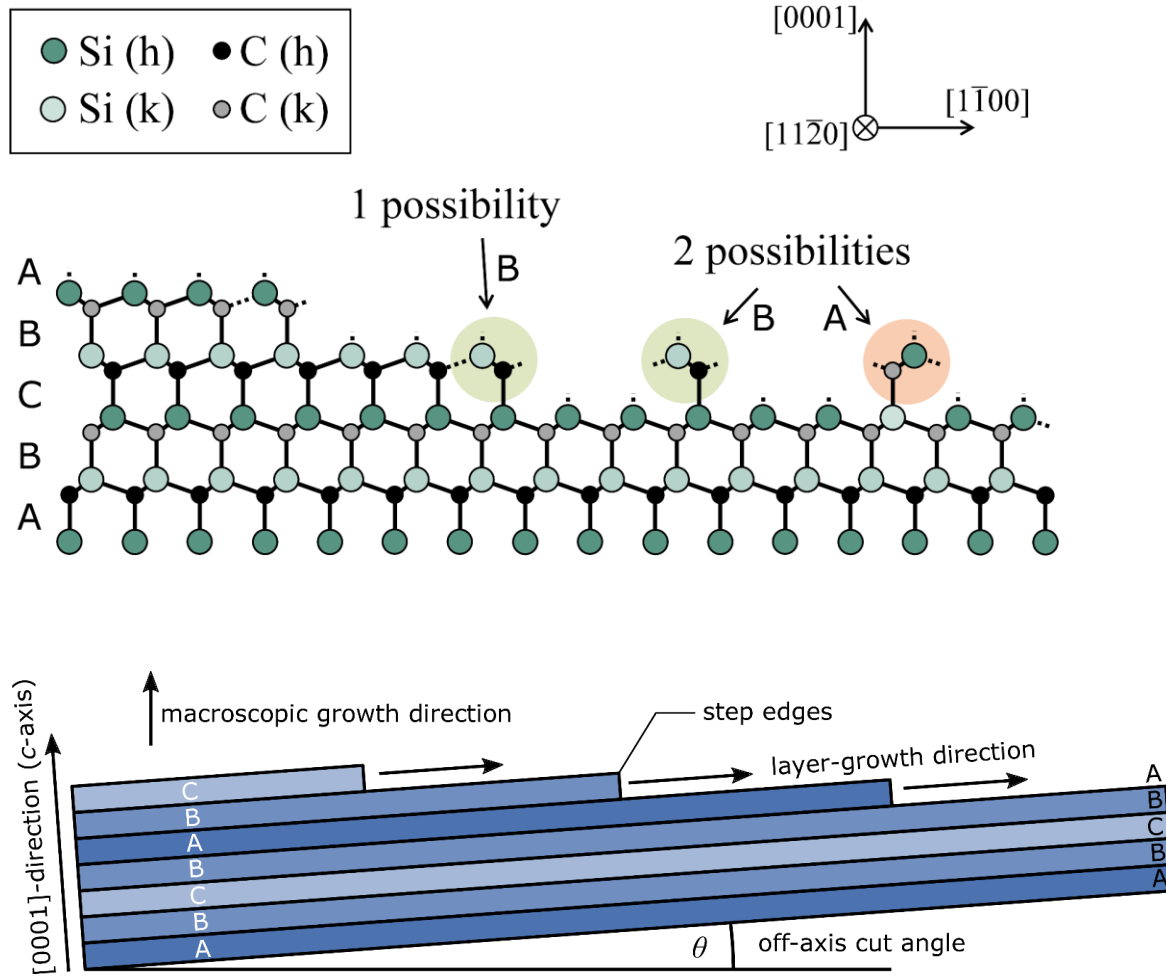
- The main reason for the off-axis cut is to enable polytype preservation during the homoepitaxial growth process. Without an off-axis wafer cut, all stacking information of the polytype is lost and two arrangements, A or B, are possible for the atomic bilayer, which follows C.

- Due to the step edges, which arise on the surface of an off-axis wafer, only a single possible bond configuration remains (B) because the stacking information is transfered along the crystal growth direction.

- The microscopic crystal growth takes place along the step edges, which results in a macroscopic growth along the c-axis.

Silicon Carbide (SiC)

Material properties of 4H-SiC compared to other semiconductors

Property	4H-SiC	Si	GaAs	Diamond	GaN
Band gap energy (eV)	3.26	1.12	1.43	5.45	3.45
Breakdown field (10^6 V cm^{-1})	3.2	0.3	0.4	5.7	3.0
Therm. conductivity (W cm^{-1} K^{-1})	4.9	1.5	0.46	22	2.2
drift velocity (10^7 cm s^{-1})	2.2	1.0	1.0	2.7	2.2
mobility (cm^2 V^{-1} s^{-1})	1200	1500	8500	2200	1250
Melting point (°C)	2830	1420	1240	4000	2500
BFOM (relative to Si)	626	1	16	27000	650

Silicon Carbide (SiC)

BFOM calculates and compares, based on the materials' mobility (μ_r), permissivity (ε_r), voltage breakdown (V_B), and band gap (E_G), the on-resistance of each material per surface area.

$$\begin{cases} BFOM = \epsilon_r \mu_r E_G^3 \\ R_{ds-on} = \dfrac{4V_B^2}{BFOM} \end{cases}$$
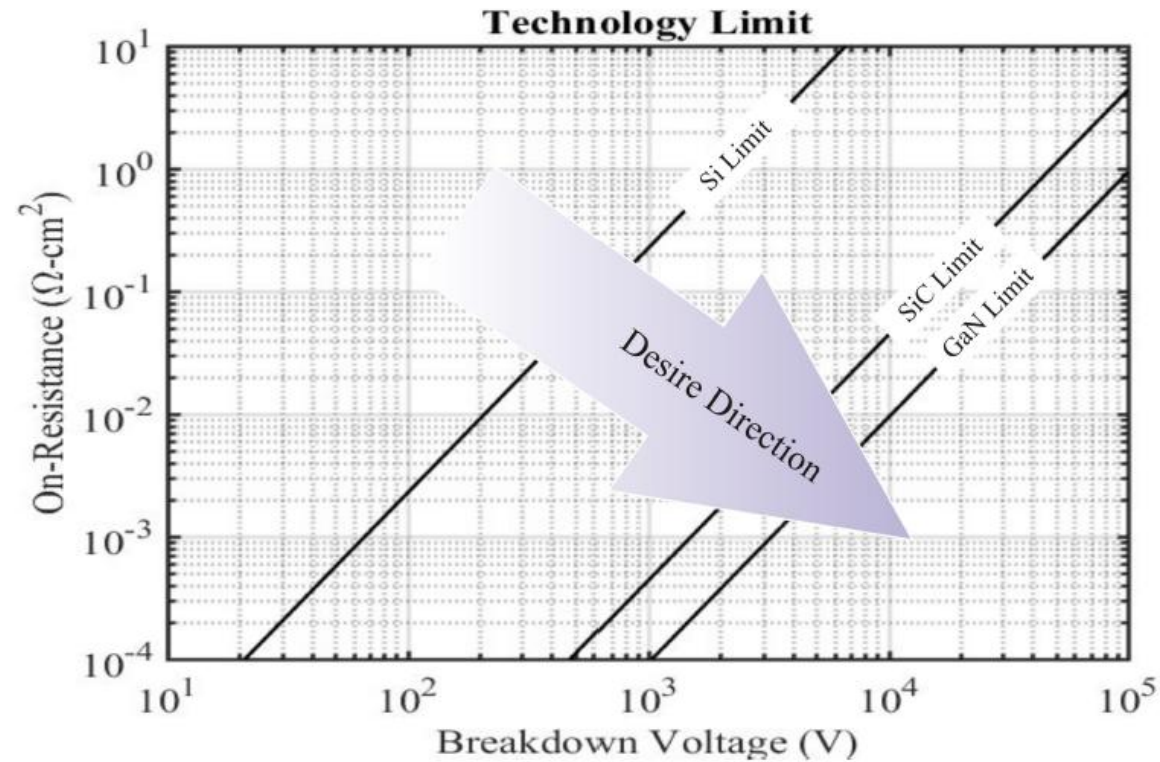
Baliga's figure-of-merit to show the technological limit of each semiconductor material.

M. D. Vecchia et al., Energies 2019, 12, 2663;

Silicon Carbide (SiC)

- The Johnson FoM outlines the power frequency for low-voltage transistors.
- The Keyes FoM establishes thermal limits to transistors' switching behavior in ICs.
- The Baliga FoM identifies material parameters that minimize conduction losses in low-frequency unipolar transistors.
- The Baliga high-frequency FoM shows that using SiC devices for high-frequency applications (in contrast to conventional semiconductors) can significantly reduce power loss.

$$\text{JFOM} = \frac{E_B^2 \cdot v_s^2}{4\pi^2} \qquad \text{BFOM} = \varepsilon_s \cdot \mu \cdot E_g^3$$

$$\text{KFOM} = \kappa \cdot \sqrt{\frac{c \cdot v_s}{4\pi\varepsilon_s}} \qquad \text{BHFFOM} = \mu \cdot E_B^2 \cdot \sqrt{\frac{V_G}{4V_B^3}}$$
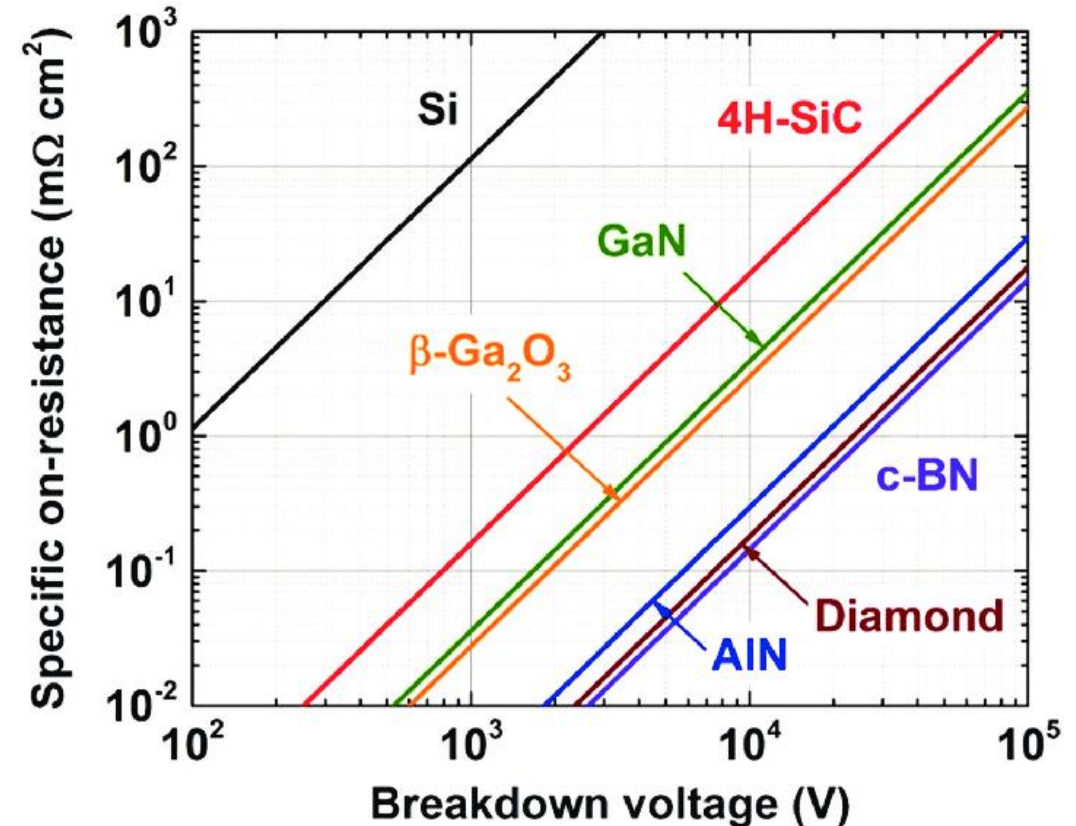
Contours of constant Baliga figure-of-merit (BFOM) for various… | Download Scientific Diagram (researchgate.net)

https://www.allaboutcircuits.com/news/figures-of-merit-power-design-reliable-benchmark-evolving-standard/

Silicon Carbide (SiC)

How are SiC Substrates Used

RF Power

4H/6H Semi-Insulating SiC — GaN HEMT

GaN HEMT

Source	Gate	Drain

AlGaN

GaN Buffer

Nucleation Layer

4H/6H-SiC

Power Switching

4HN Semi-Conducting SiC — MOSFET, Schottky Diode, JFET

SiC DMOSFET

Source — Gate — Source

P+ N+ R_{ch} P-well — R_{ch} N+ P+ P-well

R_{JFET}

depletion — depletion

R_{spread}

R_{drift}

N- drift layer

N+ 4H-SiC substrate

Drain
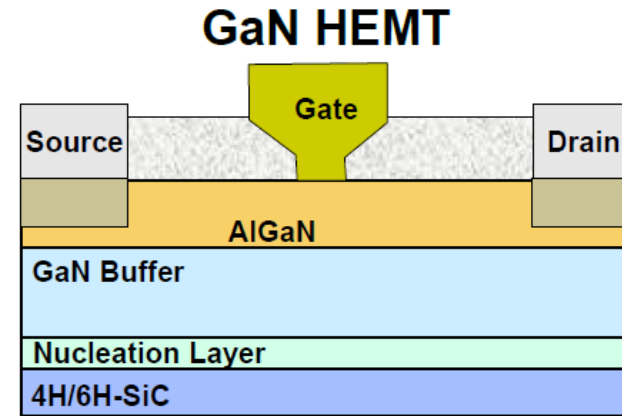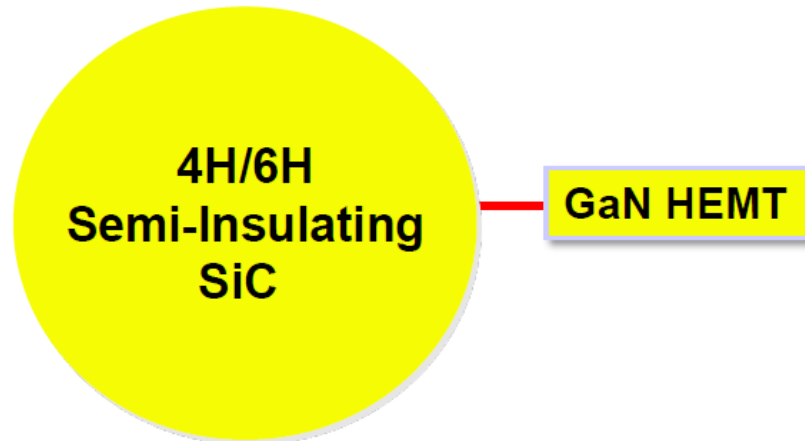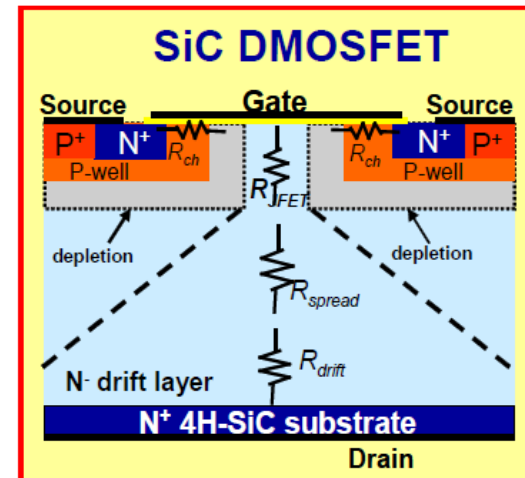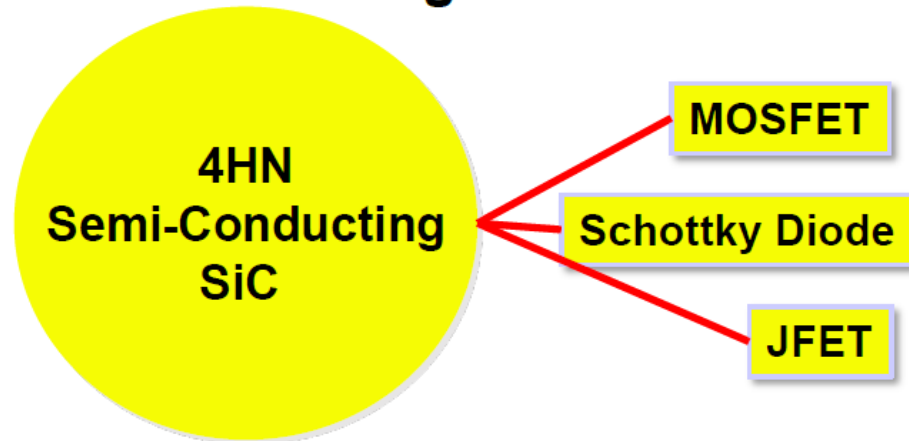
Silicon Carbide (SiC)
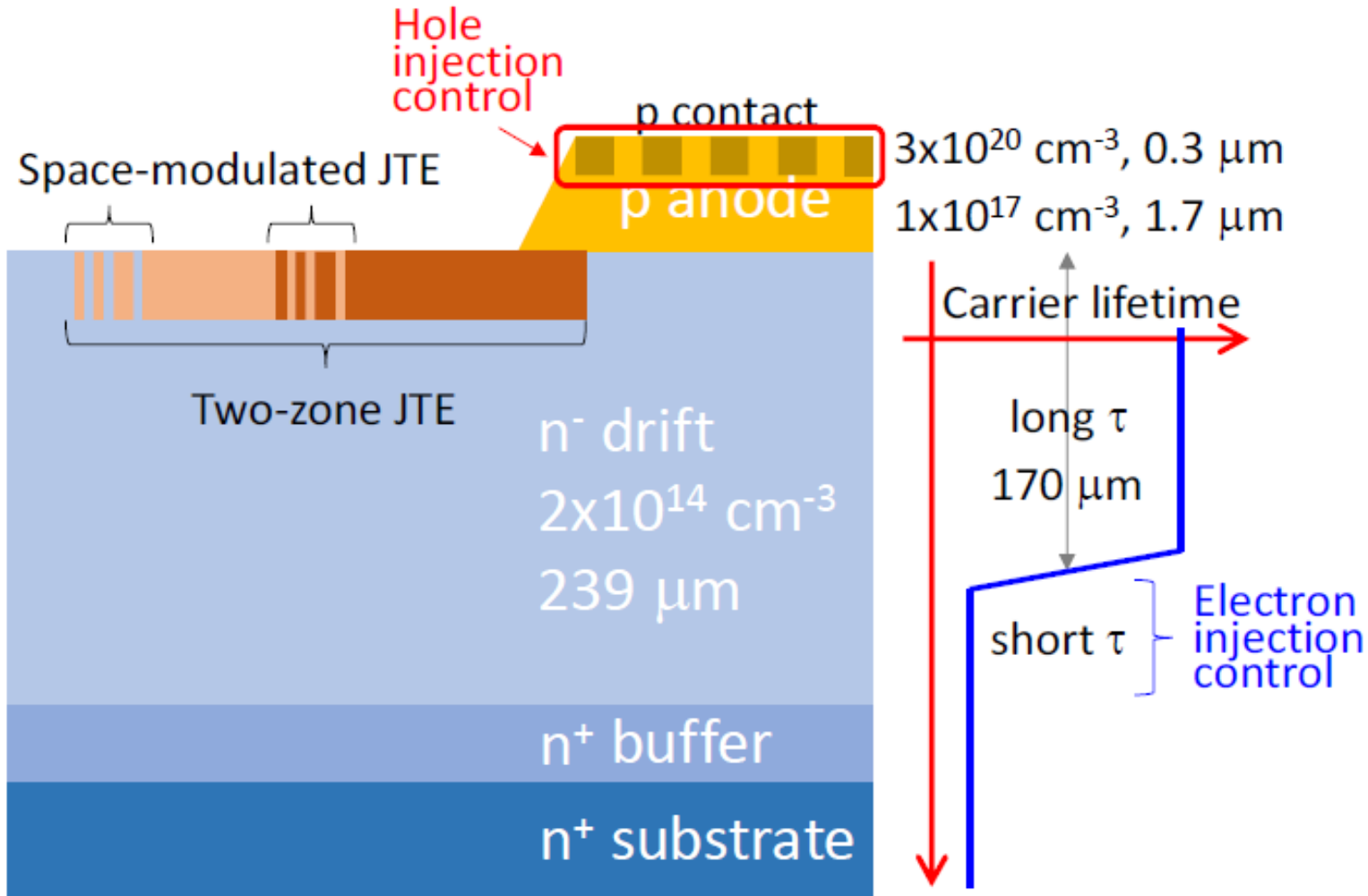
27.5 kV 4H-SiC PiN Diode

Device structure of developed UHV 4H-SiC PiN diode with three features:

- two-zone and space-modulated JTE,
- electron injection control from the cathode,
- hole injection control from the anode.

Active area of fabricated diodes is 5.75 mm^2.

K. Nakayama et al., 27.5 kV 4H-SiC PiN Diode with Space-Modulated JTE and Carrier Injection Control , Proceedings of the 30th International Symposium on Power Semiconductor Devices & ICs May 13-17, 2018, Chicago, USA

Silicon Carbide (SiC)

WILEY-VCH

Edited by Peter Wellmann, Noboru Ohtani, and Roland Rupp

Wide Bandgap Semiconductors for Power Electronics

Materials, Devices, Applications

Volume 1
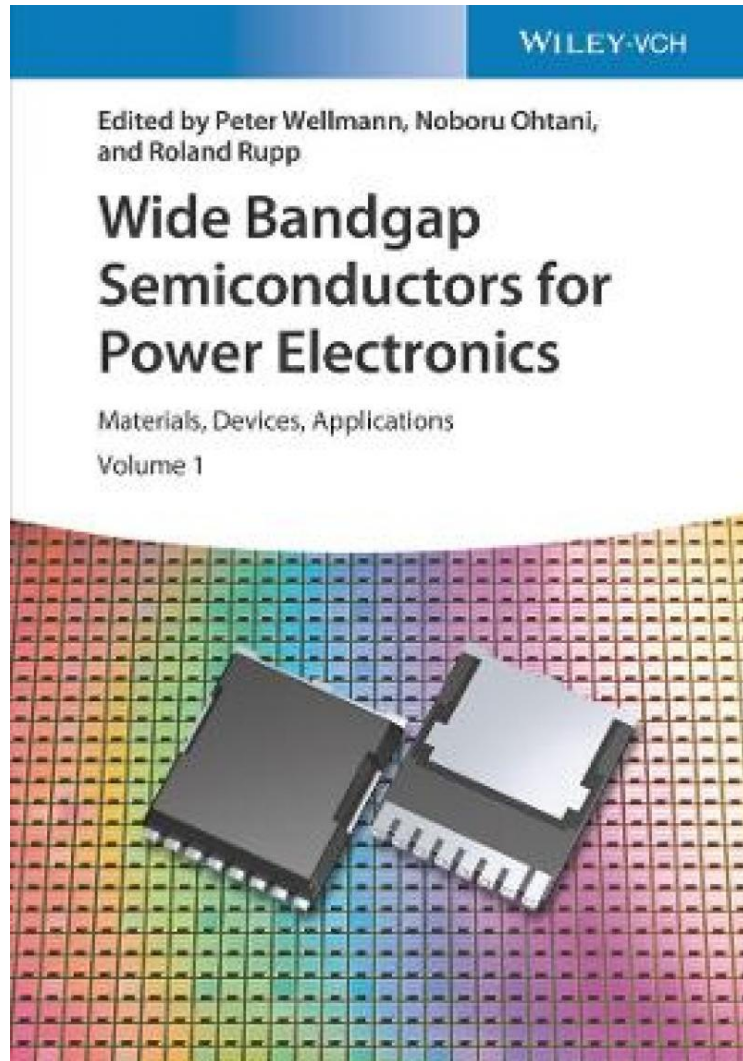
PART I. SILICON CARBIDE (SiC)

Bulk Growth of hex-SiC

Industrial Perspectives on hex-SiC Bulk Growth

CVD Epitaxy of hex-SiC

Industrial Perspective on CVD Epitaxy of hex-SiC

Bulk and Epitaxial Growth of c-SiC

Intrinsic Defects in SiC

Dislocations in SiC Bulk Wafers and Epitaxial Layers: Characterization Using X-Ray Techniques

Dislocations in SiC Bulk Wafers and Epitaxial Layers: Characterization Using Photoluminescence and Two-Photon Absorption Microscopy

Theoretical Approaches to Understanding Evolution and Propagation of Dislocations in SiC

MOS Gate Oxide Interface Defects in SiC

SiC-Graphene Interfaces

Device Processing Using c-SiC and hex-SiC

Unipolar SiC Devices

Bipolar SiC Devices

Reliability of SiC Devices

Industrial Systems Using SiC Circuits

Hybrid Electric Vehicles and Electric Vehicles Applications of SiC

Novel Applications of SiC in Quantum Information

PART II. GALLIUM NITRIDE (GaN), DIAMOND, AND Ga2O3

Aluminum Nitride (AlN)

Al pallet

BN

AlN

W

RF coil
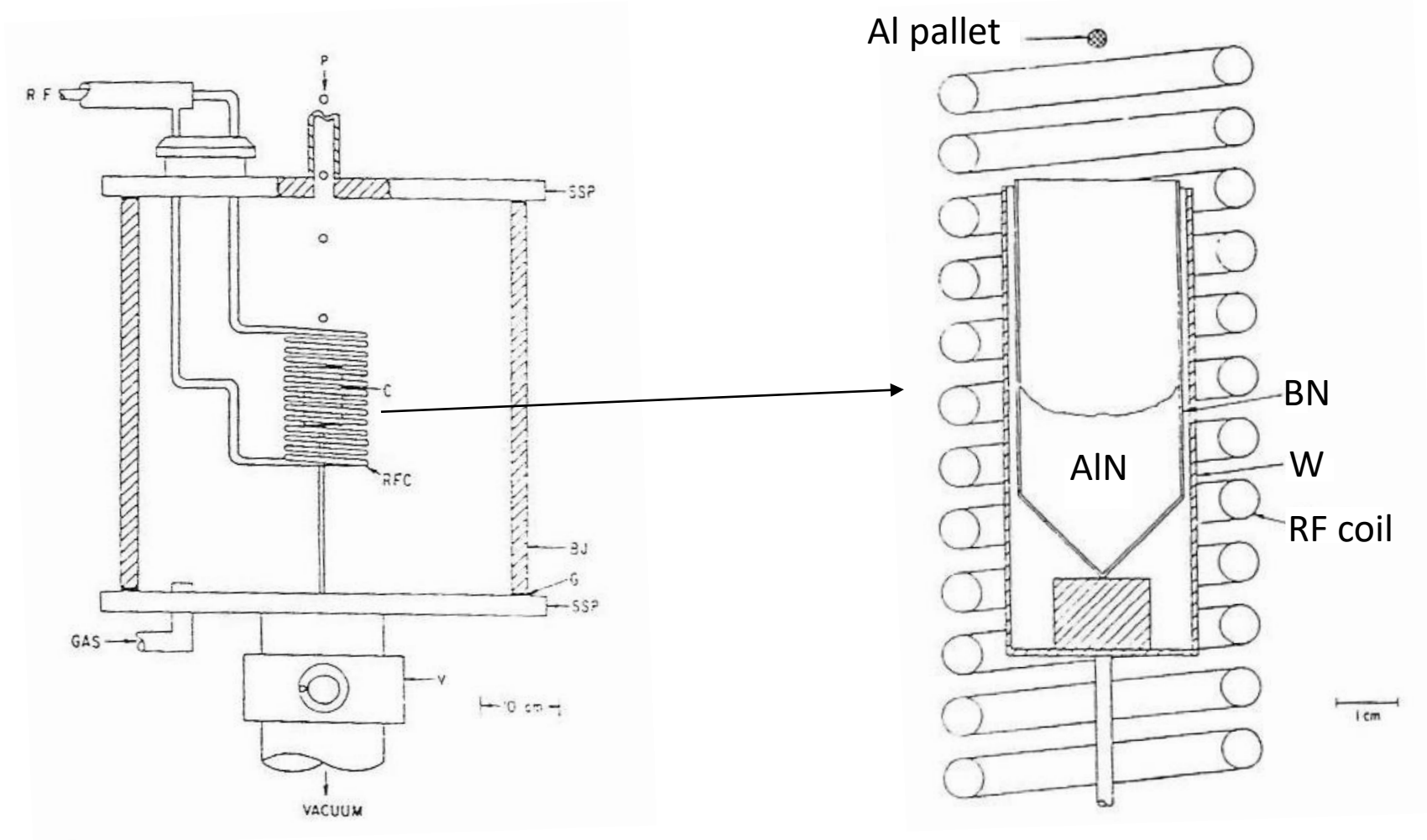
- The starting material was prepared by the direct reaction of aluminum and nitrogen at 1850°C.

G.A. Slack, T.F. McNelly, Journal of Crystal Growth 42 (1977) 560-563

Aluminum Nitride (AlN)
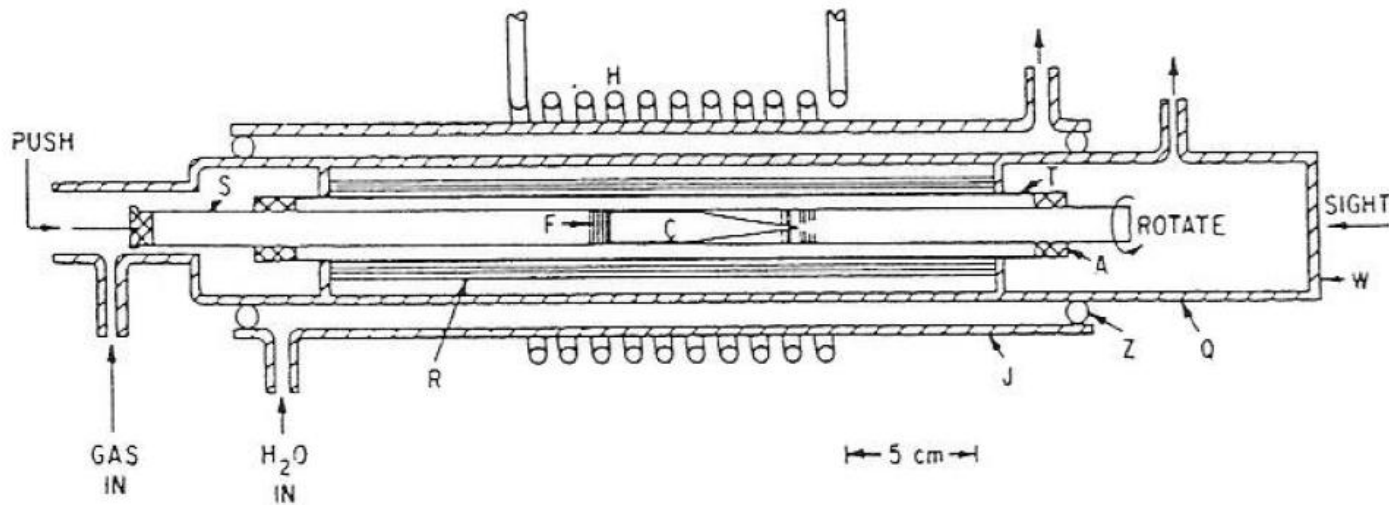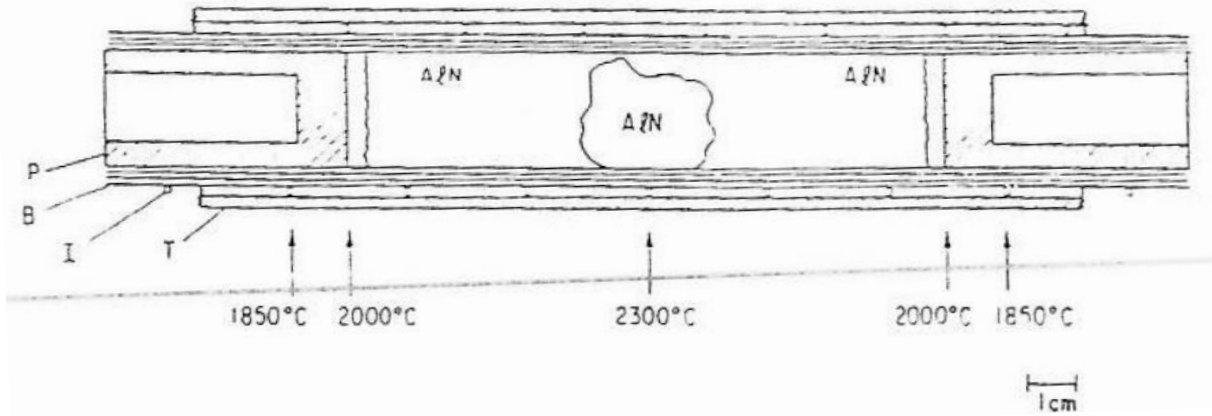
- The AlN charge of about 70 g was held at 2300°C for 12 to 24 h.
- The charge has evaporated to the ends of the chamber where it condensed out as AlN at about 2000 °C.
- The material was ready to be placed into sealed tungsten crucible for the final growth process.

- Single crystals of aluminum nitride up to 1 cm long and 0.3 in diameter were grown by a sublimation-recondensation technique at about 2250°C.
- The crystals were grown at a rate of 0.03 cm/hr. in sealed tungsten crucible in an rf heated tungsten furnace.
- The crystals were amber in color and had the wurtzite structure.

G.A. Slack, T.F. McNelly, Journal of Crystal Growth 42 (1977) 560-563

Aluminum Nitride (AlN)

$$SiC(s) \rightleftharpoons Si(g) + Si_2C(g) + SiC_2(g)$$

$$AlN(s) \rightleftharpoons Al(g) + 1/2 N_2(g)$$
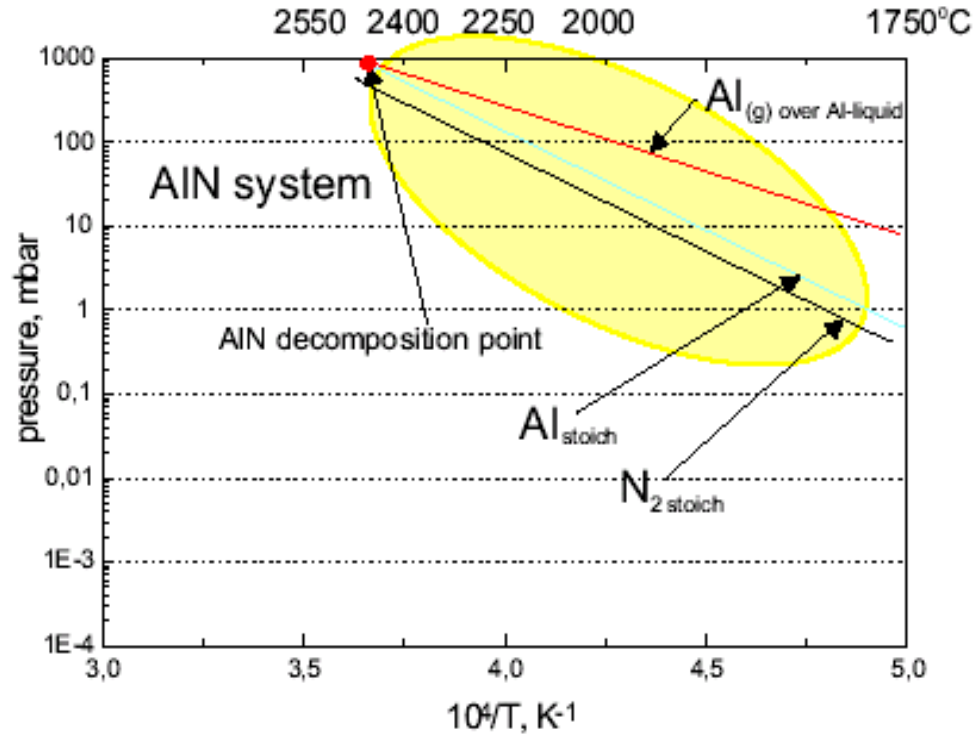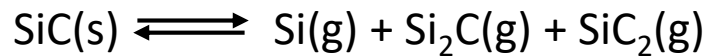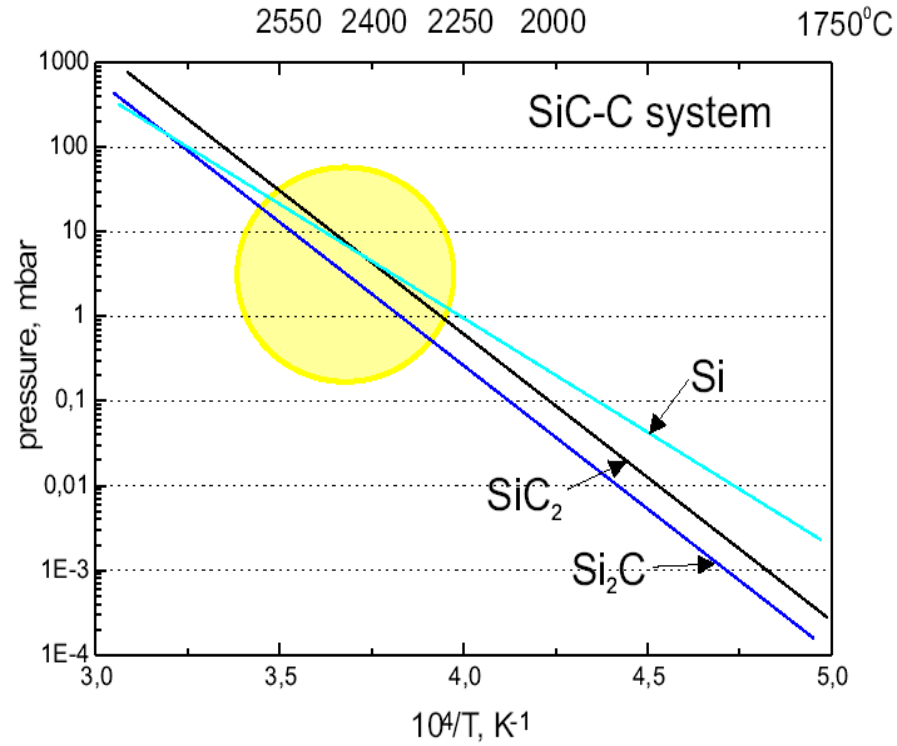
Below 2000C needle and prismatic growth occurs
Desired growth window 2000C < T < 2493
Free energy of formation of Al_2O_3 is much lower than that of AlN

Aluminum Nitride (AlN)

Sandwich Configuration

Crucible

CRYSTAL(colder)!

δ

Vapor

Source(hotter)
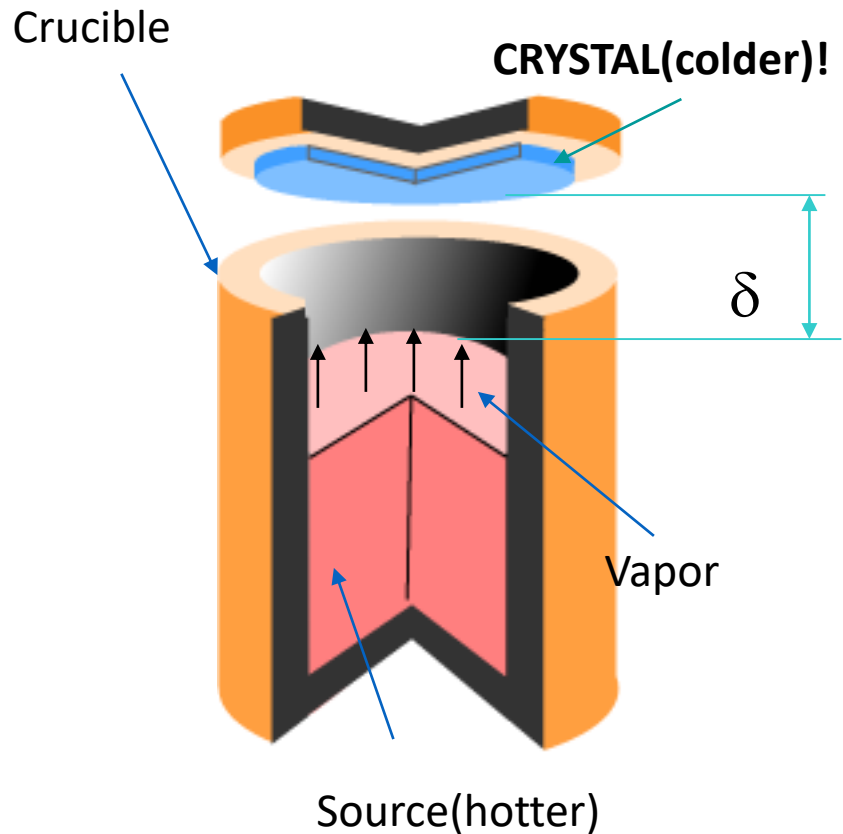
- Sublimation of AlN

  - start ~1700° C; appreciable >2200° C

  - AlN => Al + 1/2 N$_2$

  - Al and Al vapor are very reactive at high temperature
    - reactor parts
    - crucibles: **TaC**, W

  - Growth rate
    - $\Delta T = T_{source} - T_{seed}$

Aluminum Nitride (AlN)

Unit cell diagram of single-crystal AlN
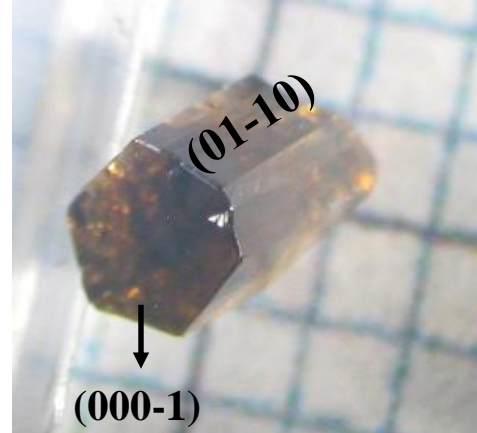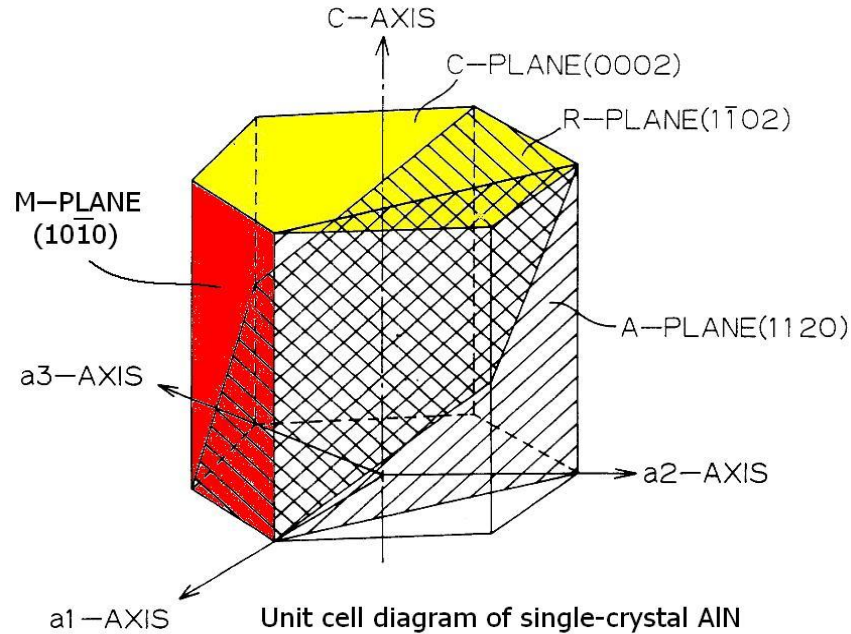
Free standing prismatic crystal showing m- and the (000-1) facet
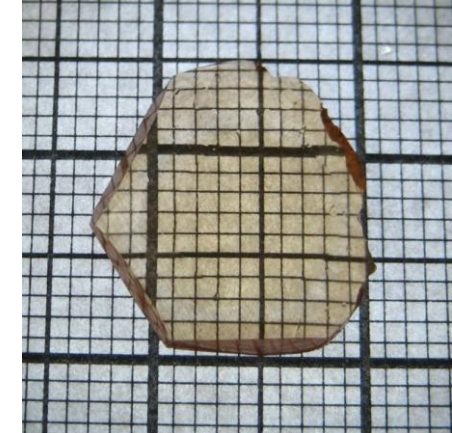
Free-standing AlN "Lely" platelet

- Natural crystal habit determined from spontaneously nucleated crystals
  - m- and c-facets are stable
    - aqueous KOH etching (60ºC for 5 min): all flat c-faces are N-polar
  - crystal size ~5-10 mm, $FWHM_{DRC}$ < 15 arc sec, DD < 100
- These crystals are excellent starting seeds

Aluminum Nitride (AlN)
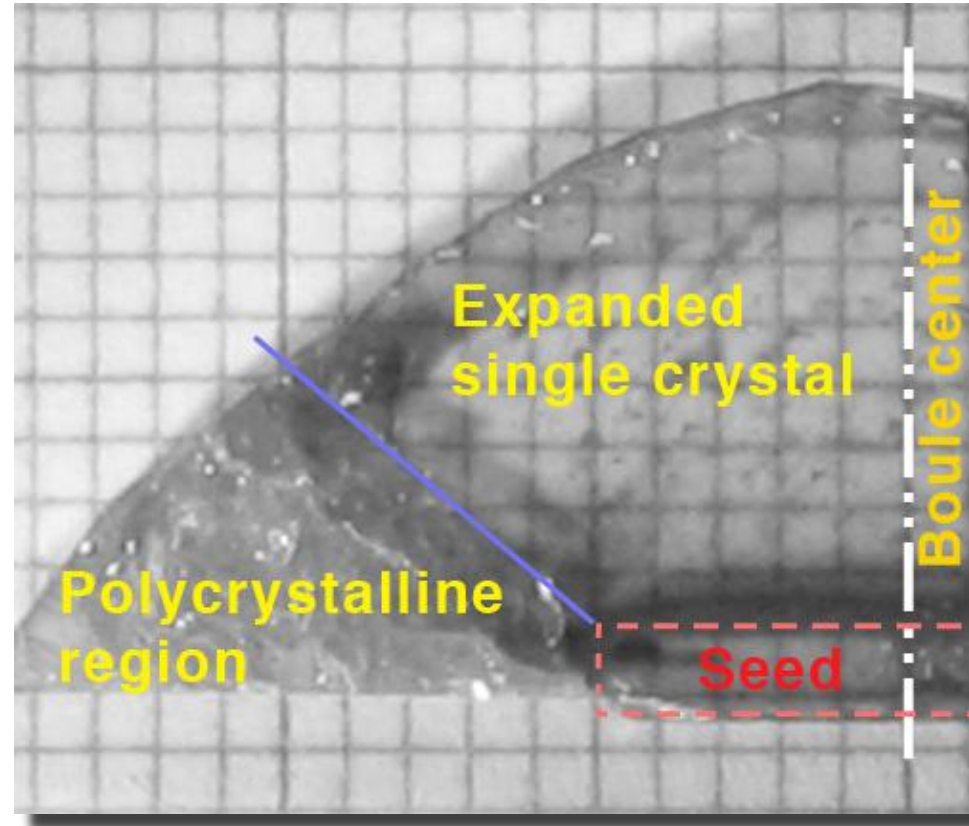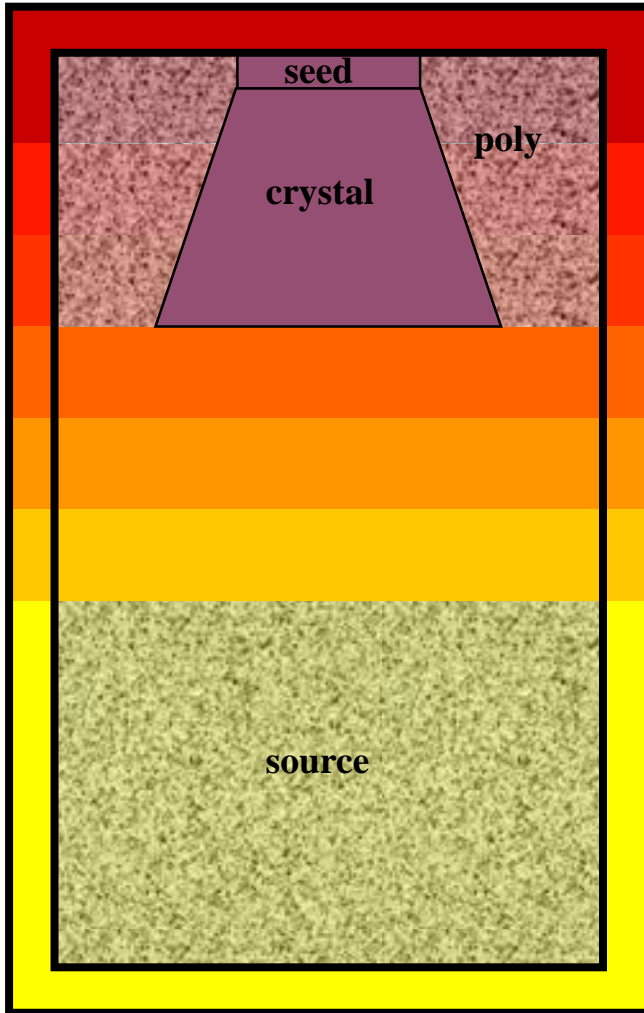
- Longitudinal cut, i.e. (11-20) plane, showing crystal expansion
- The crystal size more than doubled in 5 mm of growth
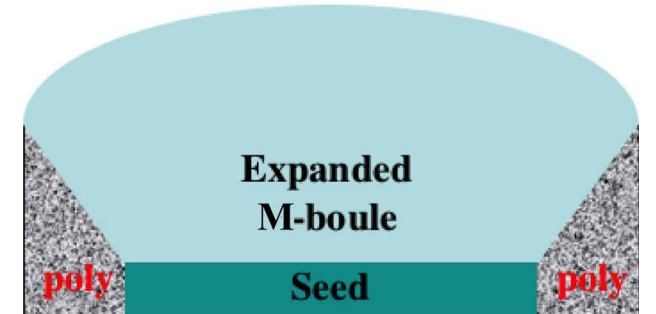
Expansion angle: 25-45°

Expansion angle: 10-20°

Z. Sitar (NCSU), IWBNS VI (2009)
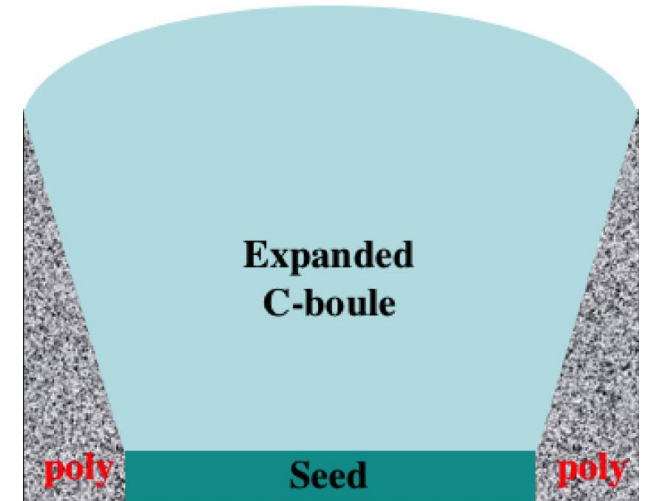
Aluminum Nitride (AlN)

Conventional thermal profile

Convex thermal profile

seed
poly
crystal
source

seed
NO-poly
crystal
source
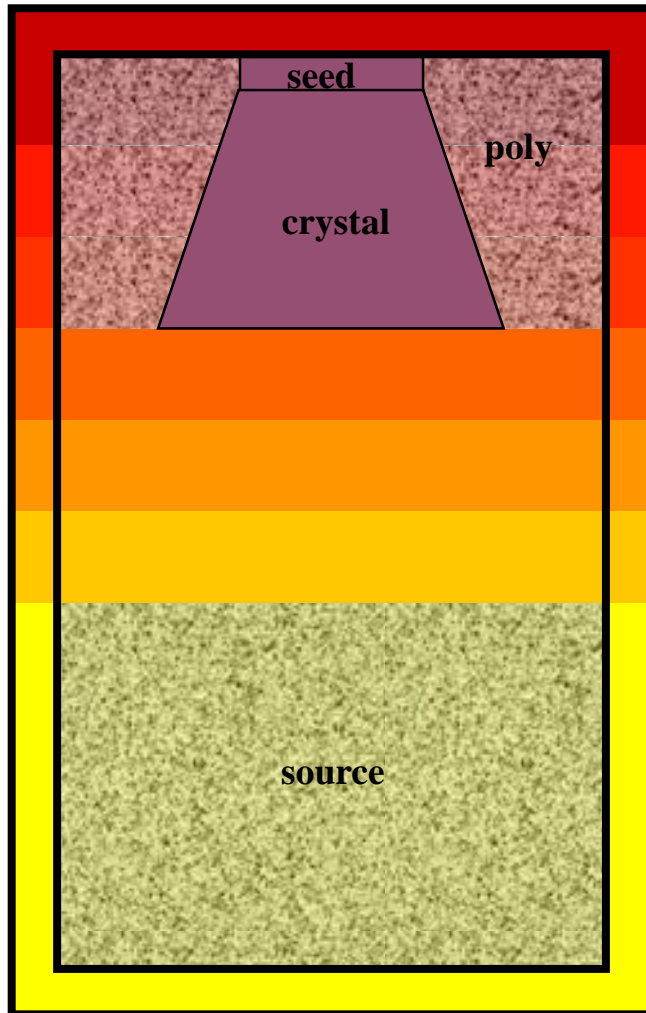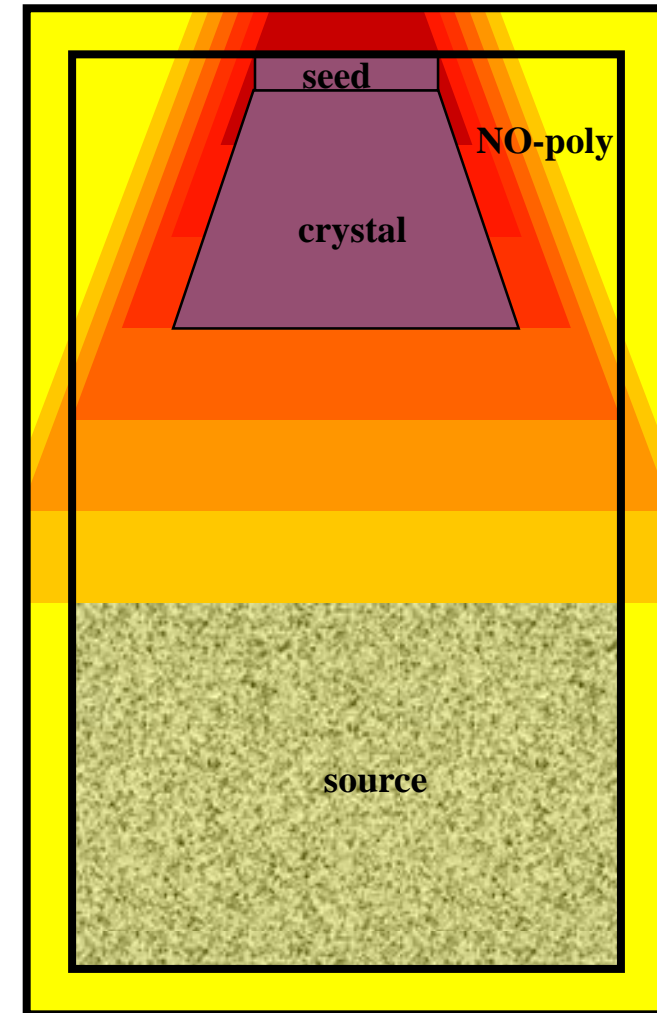
Aluminum Nitride (AlN)

c-plane growth
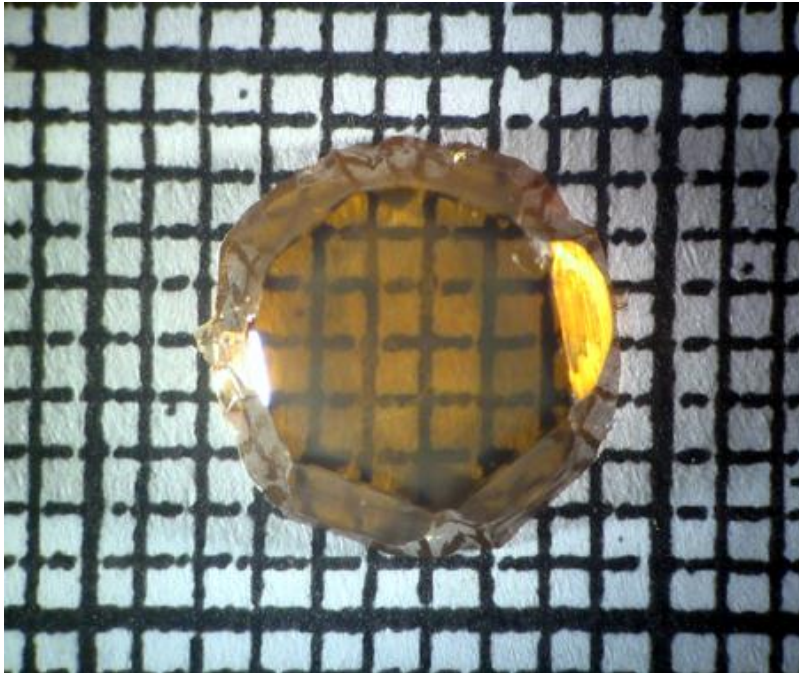
- Smooth, hexagonal c-facet
- 6 smooth m-facets
- Occasional appearance or r-facets at the top of the boule

m-plane growth
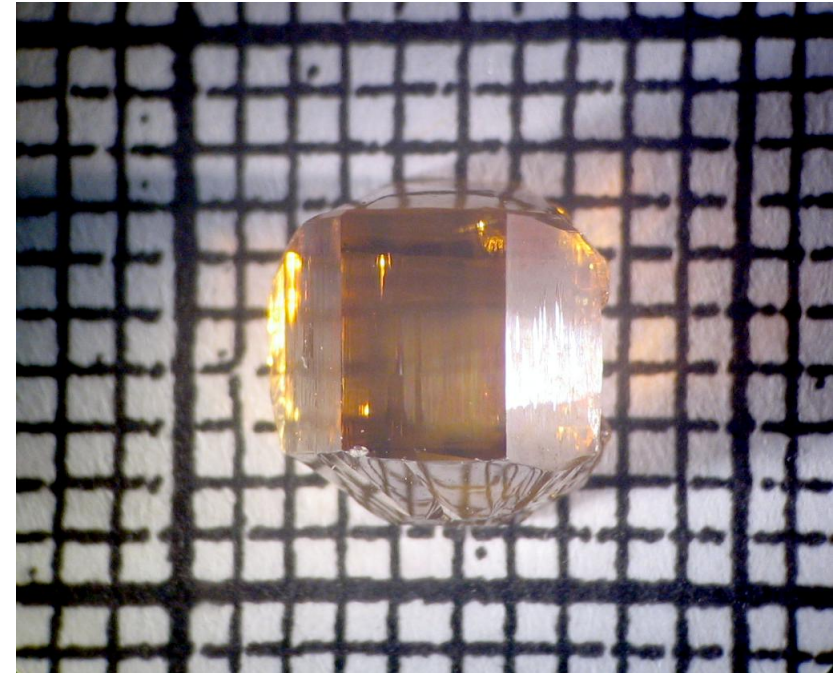
- Smooth, rectangular m-facets
- Smooth –c-facet; rough +c-facet
- Occasional appearance or r-facets between c and m

81

Aluminum Nitride (AlN)
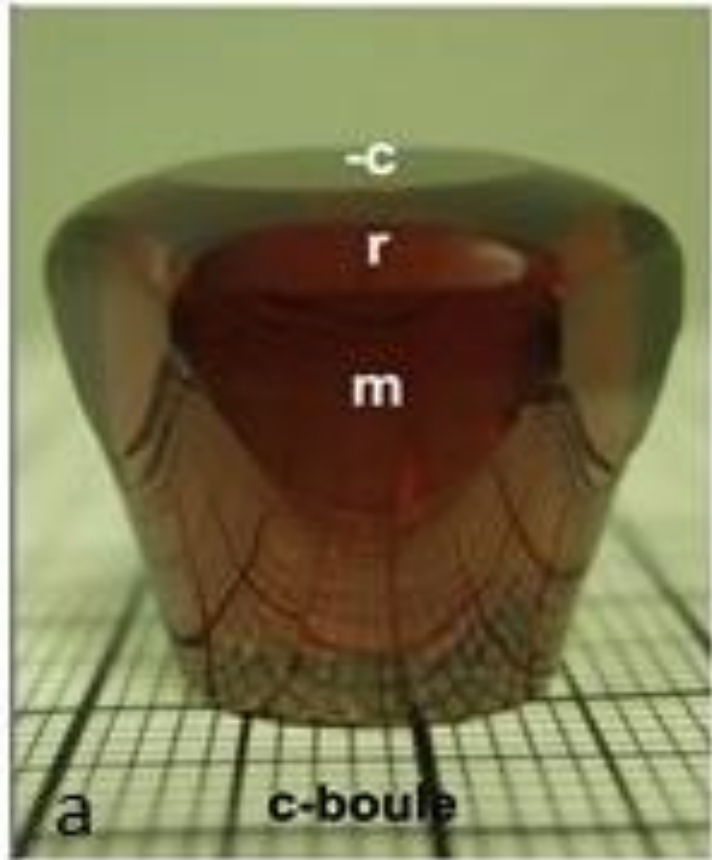
Z. Sitar, NCSU

- Round c-boule
- Shape controlled by the thermal field
- Flat c-facet; 6 r-facets
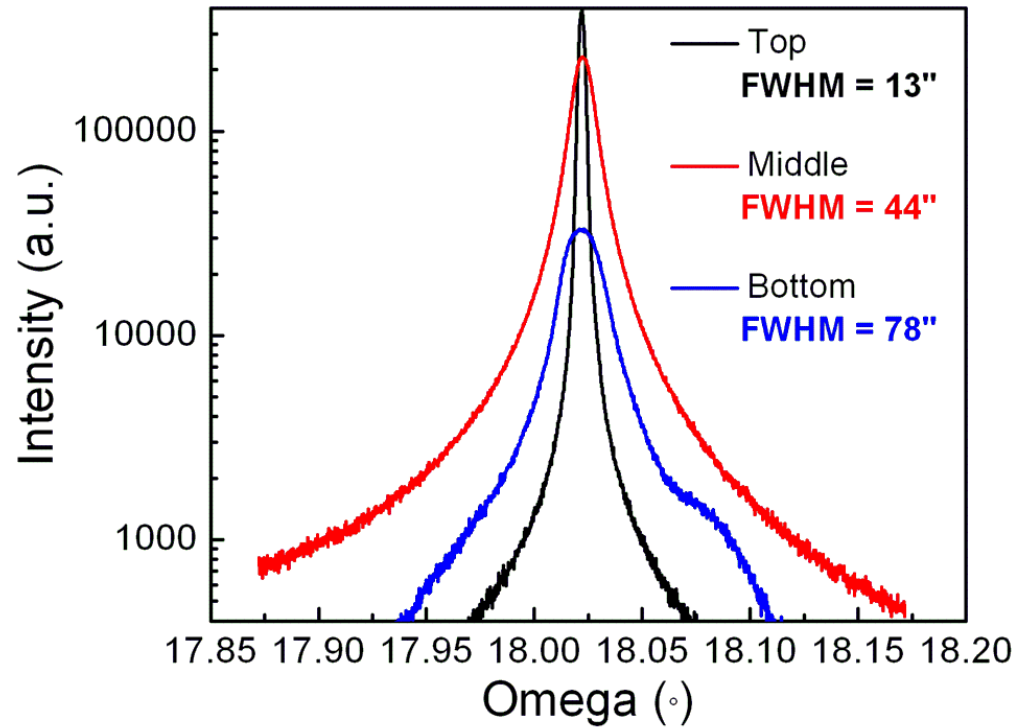
- Crystalline quality increases with the distance from the seed
- The change in the top graph is over a length of ~10 mm

Z. Sitar (NCSU), IWBNS VI (2009)

Aluminum Nitride (AlN)

Non-transparent

Transparent

HEXATECH, INC. - Company (hexatechinc.com)

Aluminum Nitride (AlN) Technology Overview - Crystal IS - CISUVC
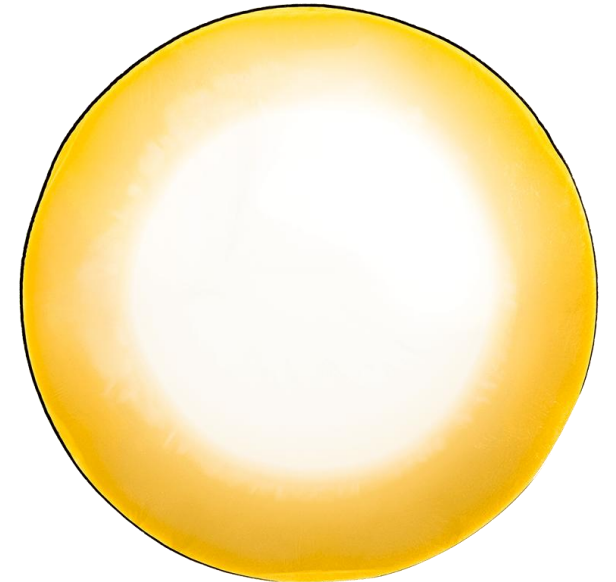
Aluminum Nitride (AlN)
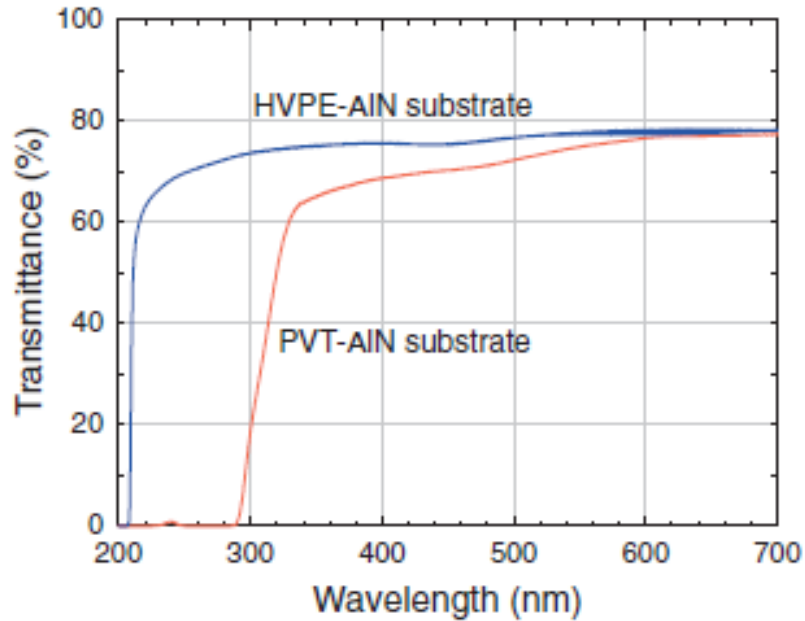
Fig. 4. External optical transmission spectra of PVT- and HVPE-AlN substrates measured at RT in air. Substrates of the same thickness and surface polish state were used.
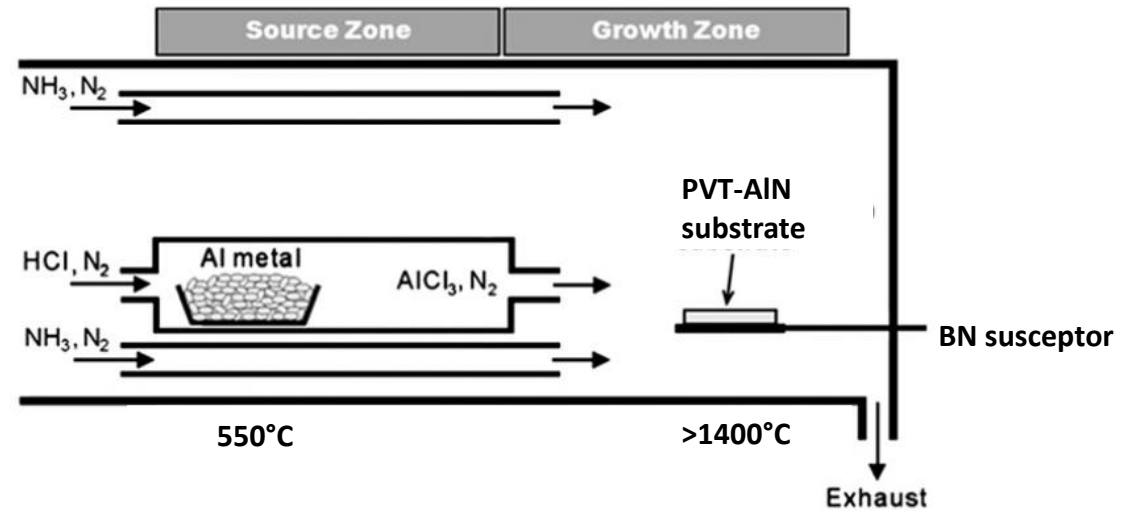
Table I. Impurity concentrations in PVT- and HVPE-AlN substrates (atoms/cm^3) measured by SIMS. The B concentration in the PVT-AlN substrate was not measured.

	H	B	C	O	Si	Cl
PVT-AlN	$<5 \times 10^{17}$		3×10^{19}	2×10^{19}	5×10^{18}	$<3 \times 10^{14}$
HVPE-AlN	$<5 \times 10^{17}$	5×10^{15}	$<2 \times 10^{17}$	$<4 \times 10^{17}$	2×10^{17}	1×10^{15}

Y. Kumagai et al., Applied Physics Express 5 (2012) 055504

Aluminum Nitride (AlN)

UV-C (100–280 nm) laser diodes (LDs) are strong candidates for health care applications, such as bio-/chemical sensing and sterilization devices

270 nm
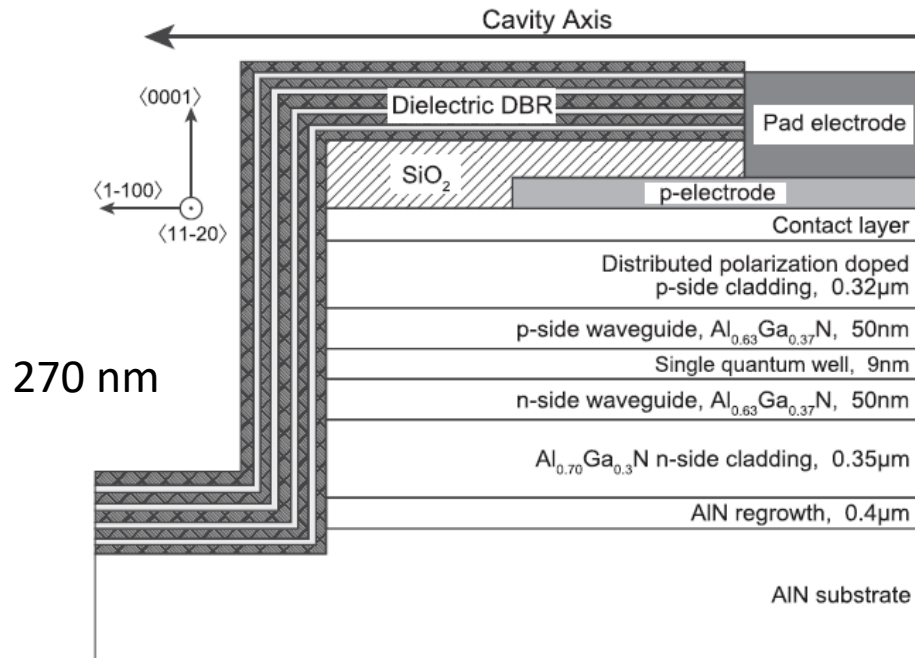
FIG. 1. Schematic cross section of the fabricated UV-C LD.

T. Sakai et al., Appl. Phys. Lett. 116, 122101 (2020); doi: 10.1063/1.5145017

High-power radio frequency (RF) operation of AlGaN/GaN high electron mobility transistors (HEMTs) fabricated on free-standing AlN substrate at X-band.
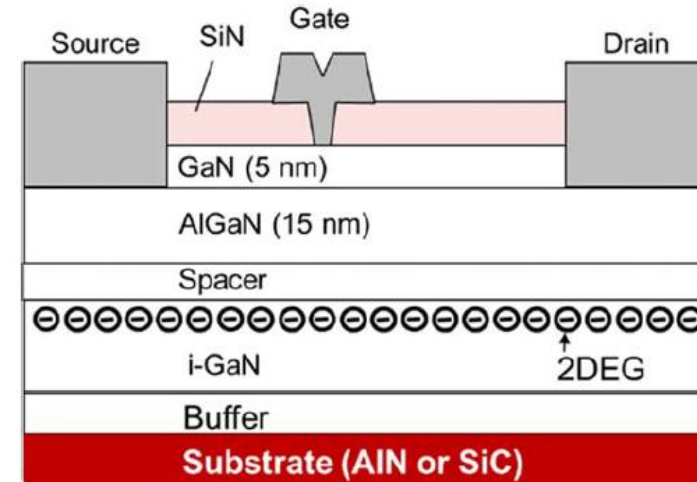
Fig. 1. (Color online) AlGaN/GaN HEMT structure grown on AlN or SiC substrate.

The X band is used for radar, satellite communication, and wireless computer networks (8.0–12.0 GHz.).

S. Ozaki et al., Applied Physics Express 14, 041004 (2021)

Gallium Nitride (GaN)

- Melting temperature and pressure of most typical semiconductor materials

crystal	T_M , ^oC	p_M , atm
Si	1400	< 1
GaAs	1240	2
GaP	1465	30
GaN	**2225**	**60 000**
AlN	3200	> 100
InN	1900	60 000

W. Utsumi et al. Nature Materials 2 (2003) 735

- Multi-anvil high-pressure apparatus Spring-8 synchrotron

Gallium Nitride (GaN)

temperature, K

$Ga + 1/2 N_2 = GaN$

$G = H - TS + pV$

$\Delta G = G_{GaN} - (G_{Ga} + 1/2 G_{N_2})$

in equilibrium $\Delta G = 0$

Gibbs free energy, kcal/mole

GaN

$Ga + 1/2 N_2$

1 GPa

0.1 MPa

crucible

N_2 molecules under pressure

Dissociative adsorption of N_2 on liquid metal surface

Dissolution and transport to the crystallization zone

Spontaneous crystallization

Ga

GaN

10 000 atm
1500°C

ΔT

T
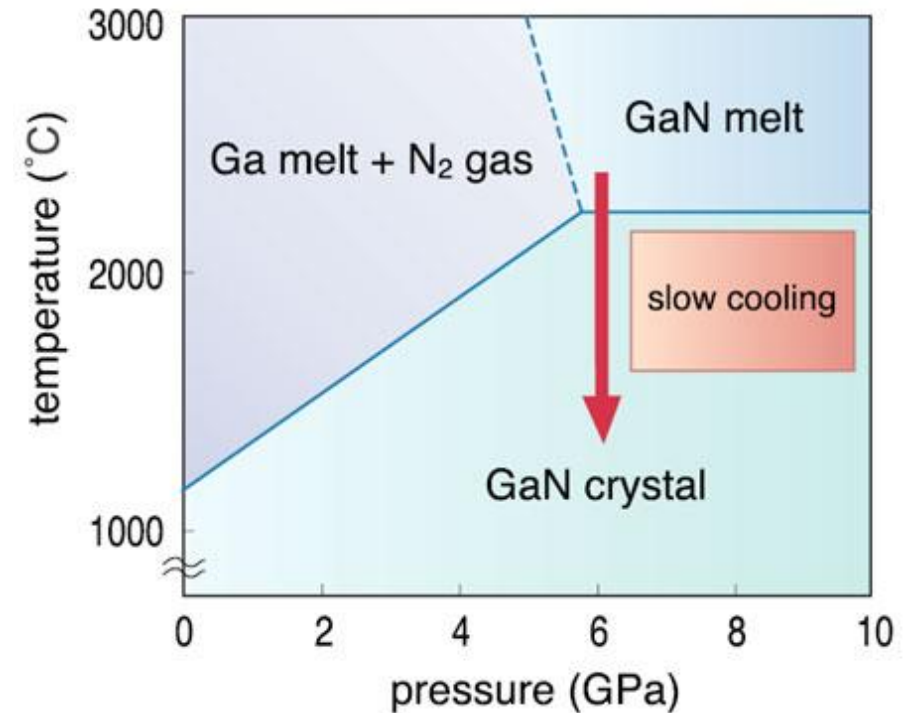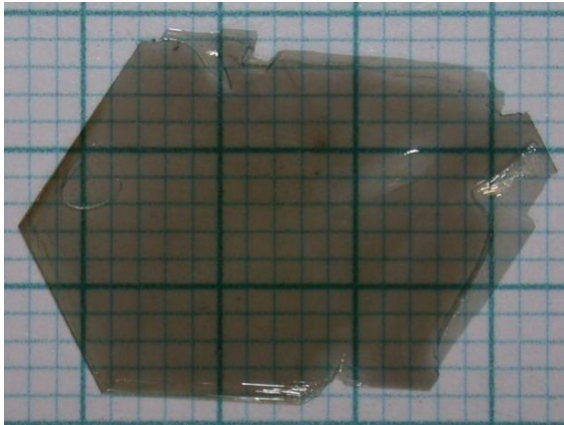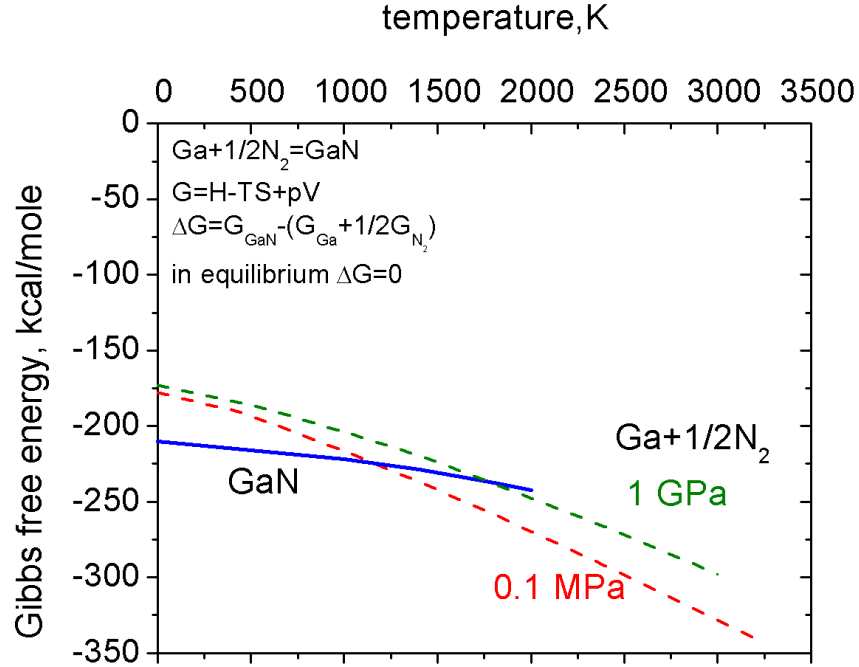
Perfect crystallographic quality but...too small!

I. Grzegory et al. in Bulk Crystal Growth of Electronic, Optical and Optoelectronic Materials, ed. by P. Capper, Wiley&Sons, (2005), 173
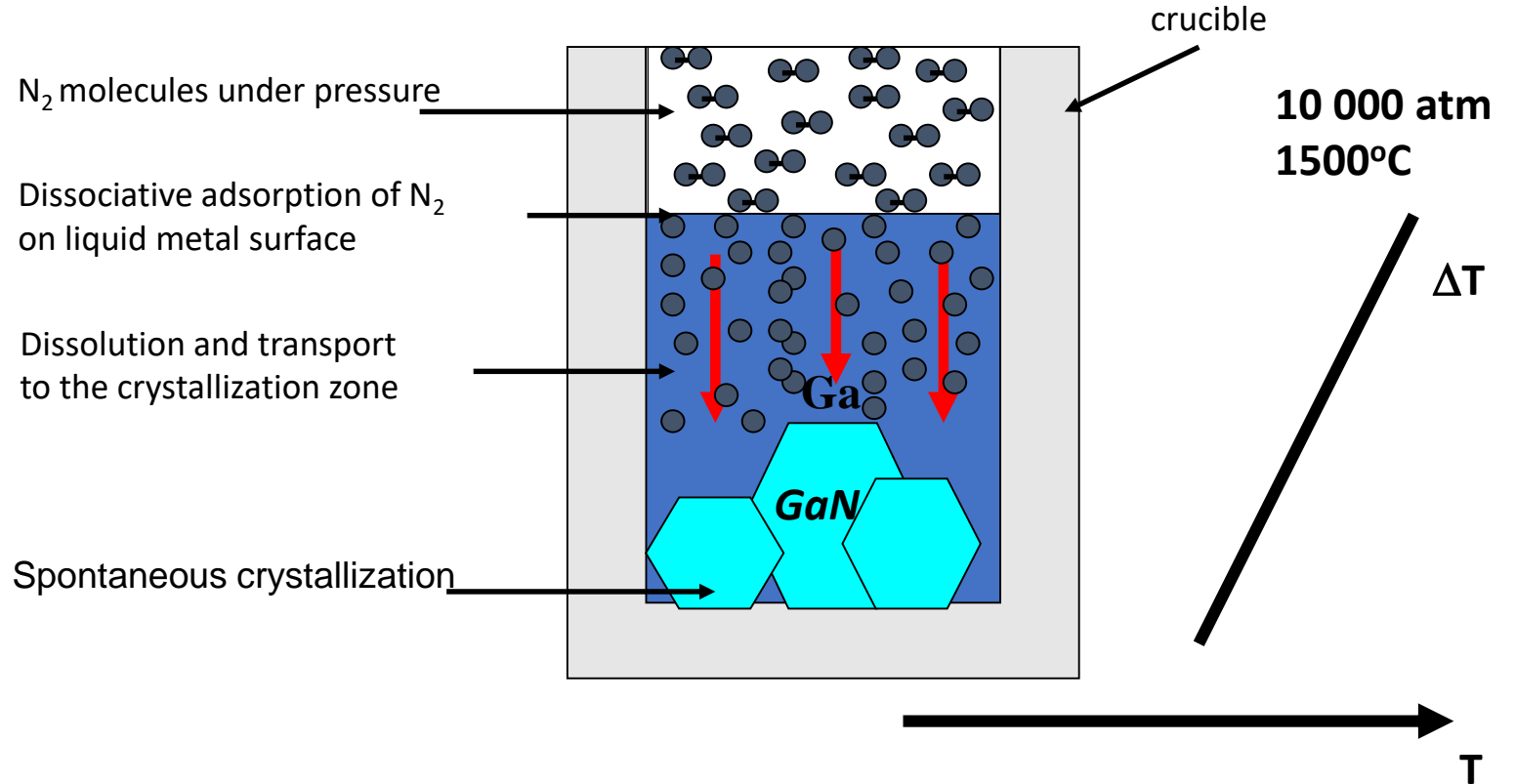
Gallium Nitride (GaN)

Point seed technique
Switching from 3D to 2D growth – the seed is pulled out from the solution when GaN is pyramidal

1

Ga+Na melt

GaN seed — Sapphire wafer

2

3D

3

4

5

6

2D
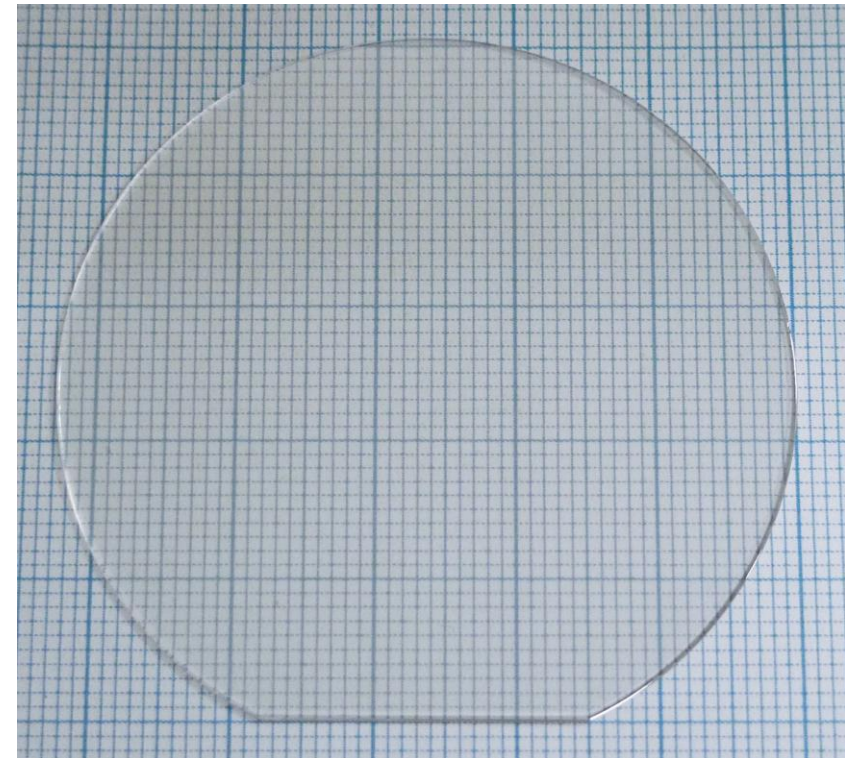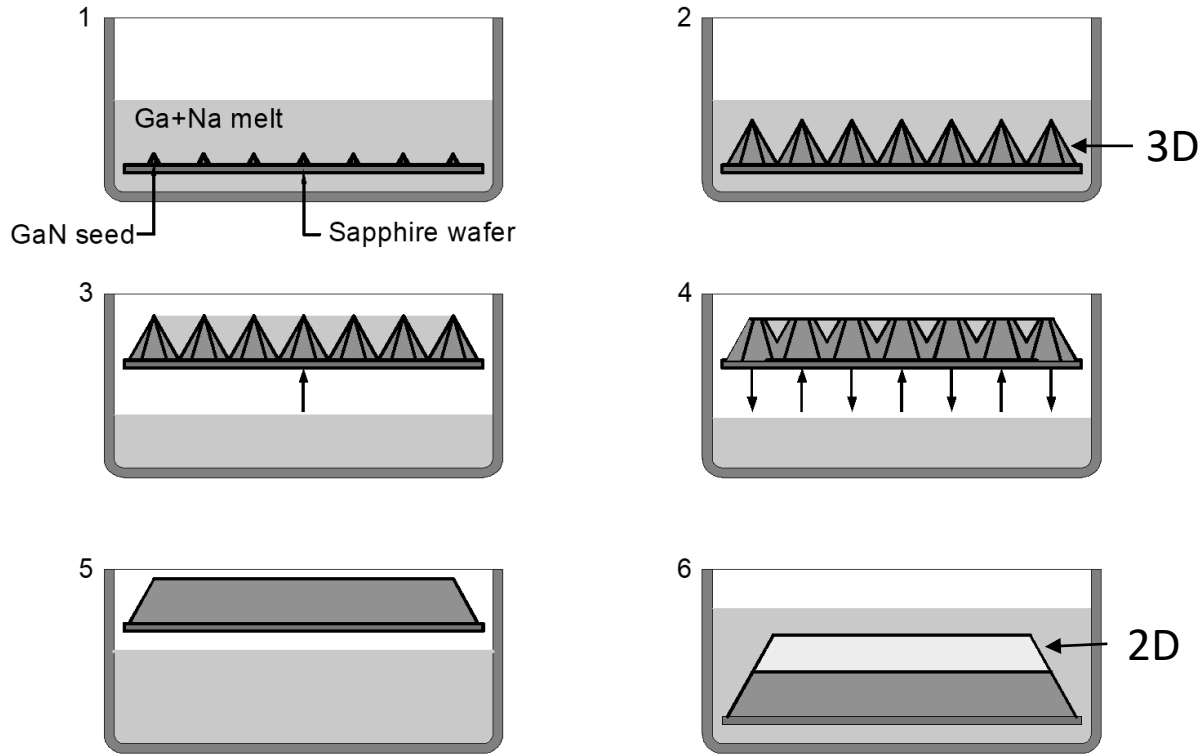
2-inch Na flux GaN wafer
Perfect structural quality

M. Imanishi et al., Applied Physics Express 12, 045508 (2019)

Gallium Nitride (GaN)

6-inch Na flux GaN

Y. Mori

Gallium Nitride (GaN)

Basic

GaN feedstock

NH₃ with mineralizer

Baffle

Seed crystals

Dissolving zone

Growth zone

Temperature

Acidic

Seed crystals

Baffle

GaN feedstock

NH₃ with mineralizer

Growth zone

Dissolving zone
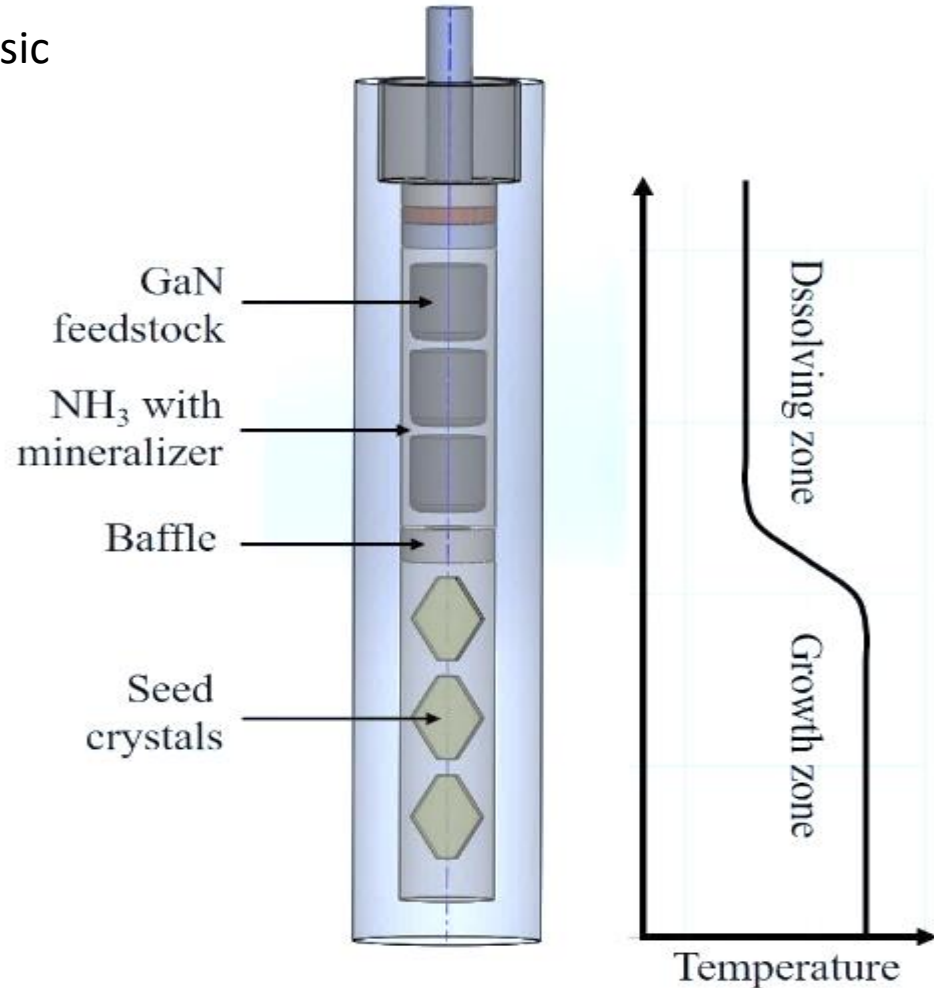
Temperature
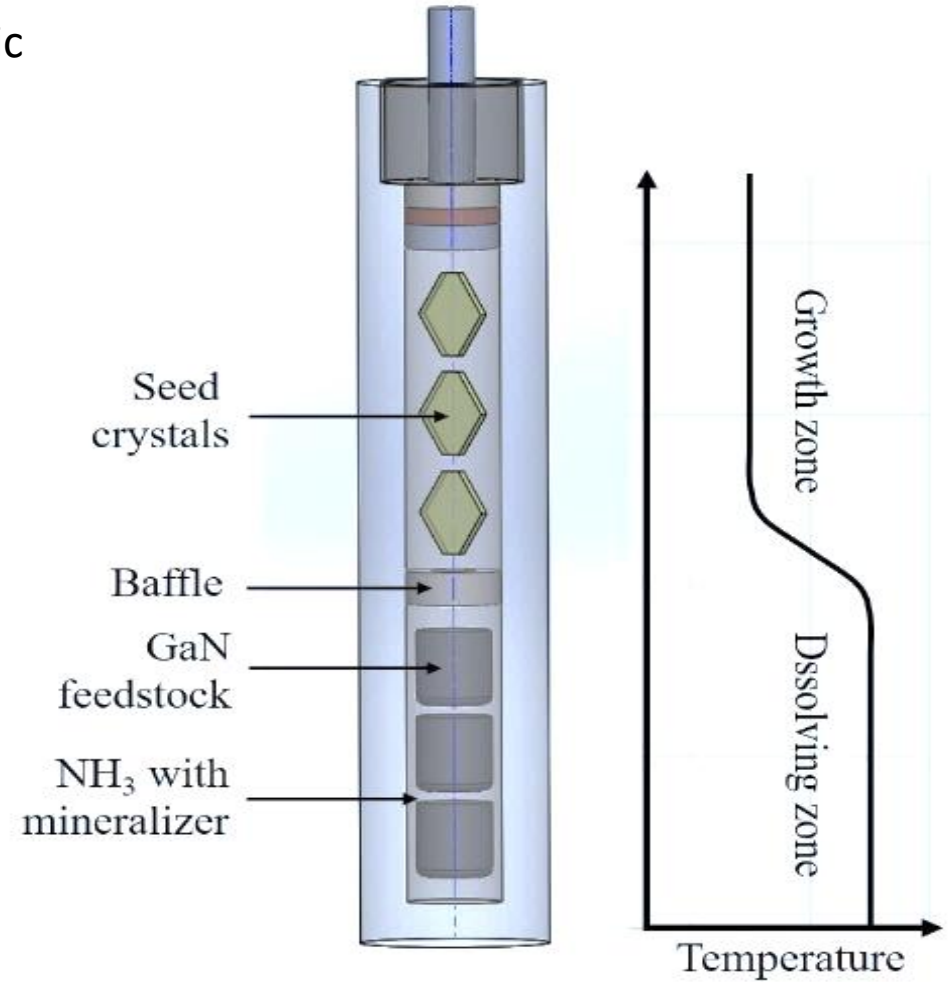
Mineralizers: Alkali metals   Halide compounds

Gallium Nitride (GaN)

Applied pressure and temperature: 300-400 MPa and 450–600°C,

mineralizers (alkali metals) - increased solubility of GaN feedstock.
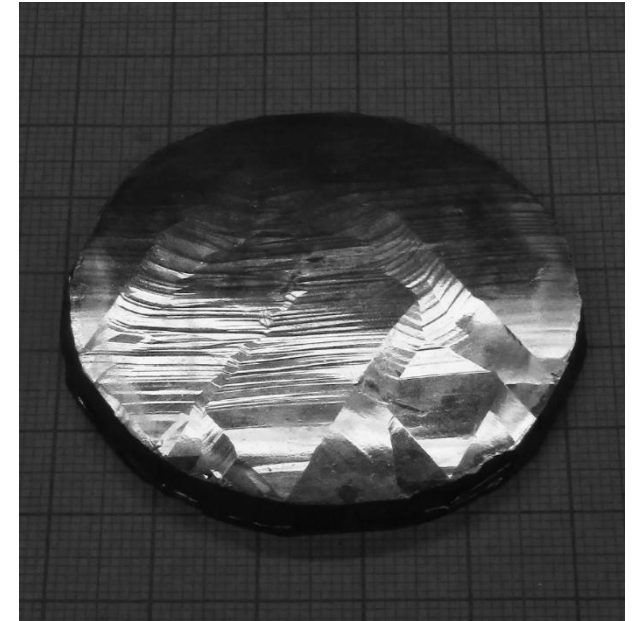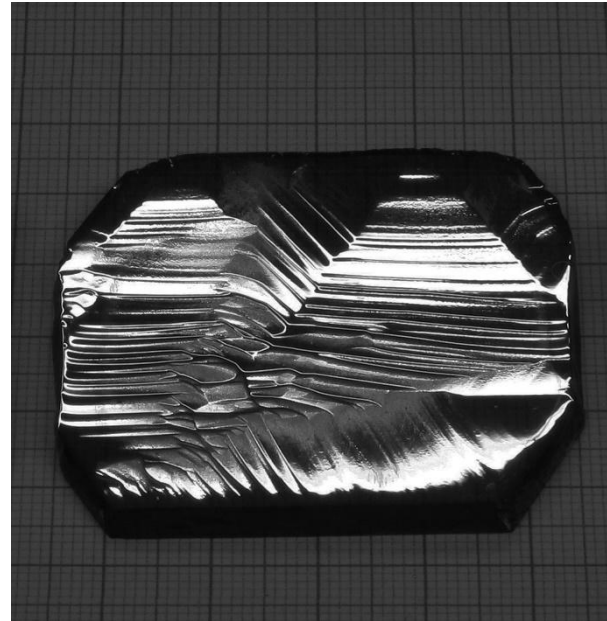
Gallium Nitride (GaN)
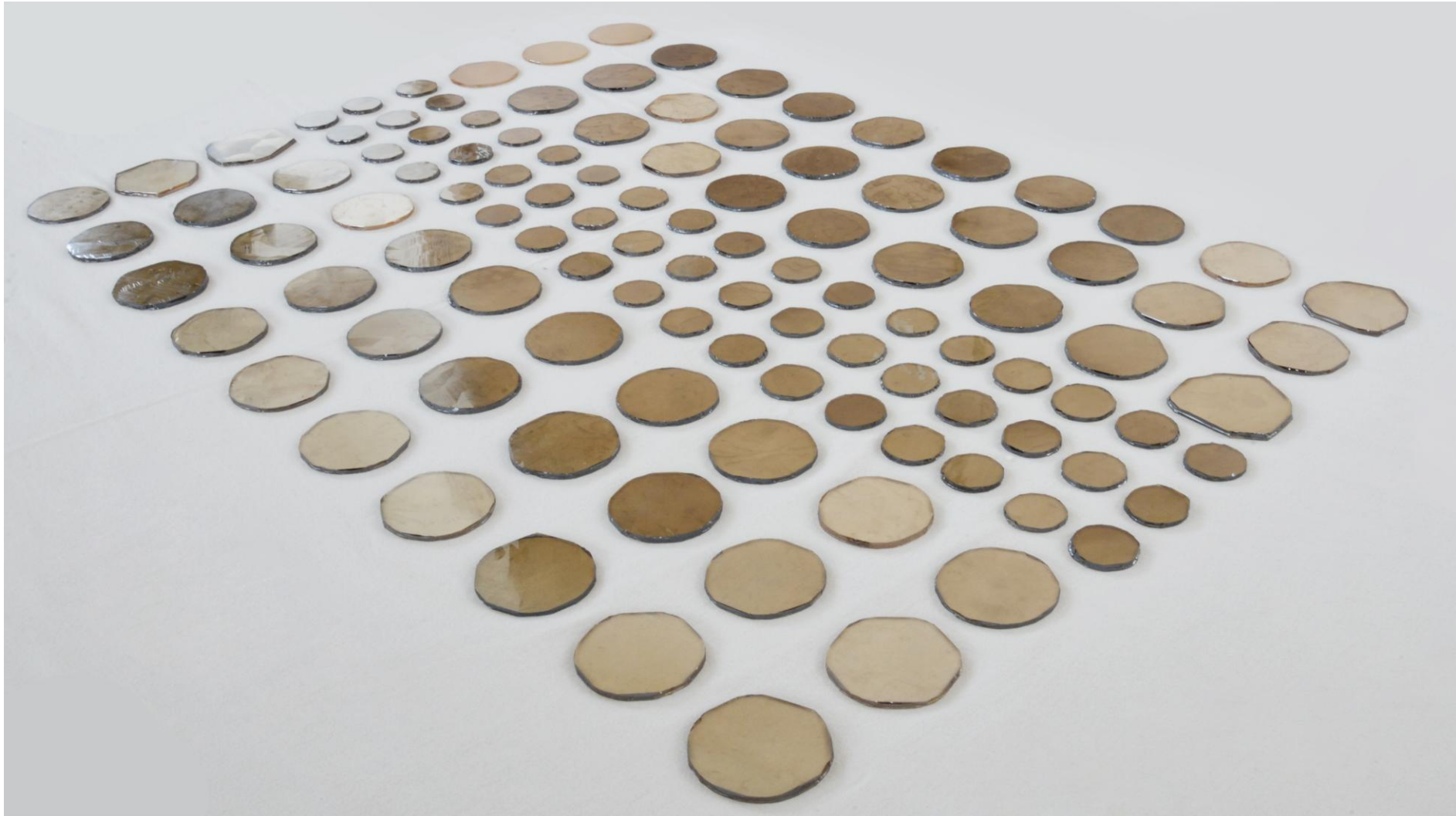
K. Grabianska, T. Sochacki, R. Kucharski

Gallium Nitride (GaN)

THE PREPARATION AND PROPERTIES OF VAPOR-DEPOSITED SINGLE-CRYSTAL-LINE GaN
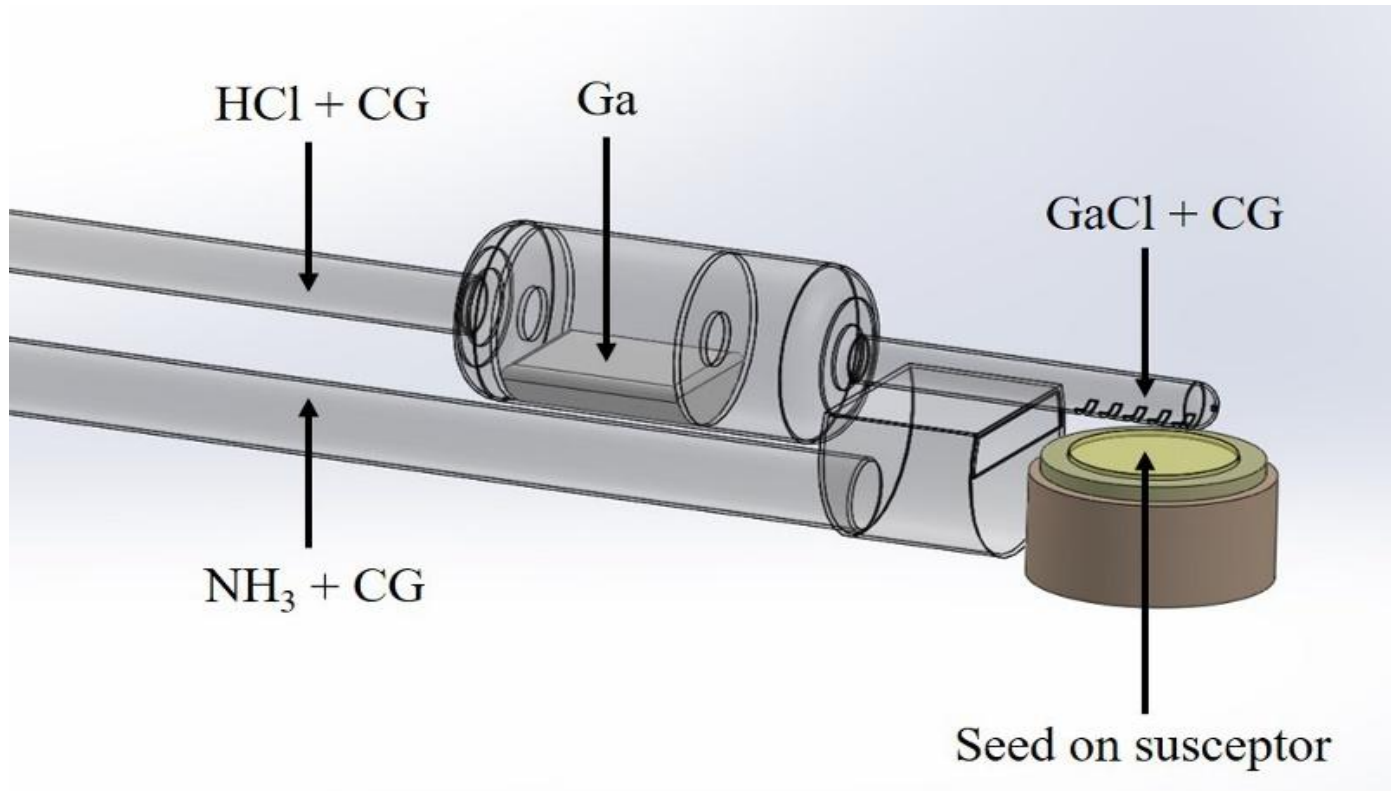
H. P. Maruska and *J. J. Tietjen*
RCA Laboratories
Princeton, New Jersey 08540
(Received 18 August 1969)

HCl + CG

Ga

GaCl + CG

NH$_3$ + CG

Seed on susceptor

$2HCl + 2Ga \rightarrow 2GaCl + H_2$

$GaCl + NH_3 \rightarrow GaN + HCl + H_2$

Gallium Nitride (GaN)
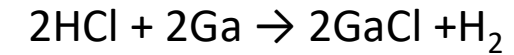
Secondary ion mass spectrometry (SIMS)
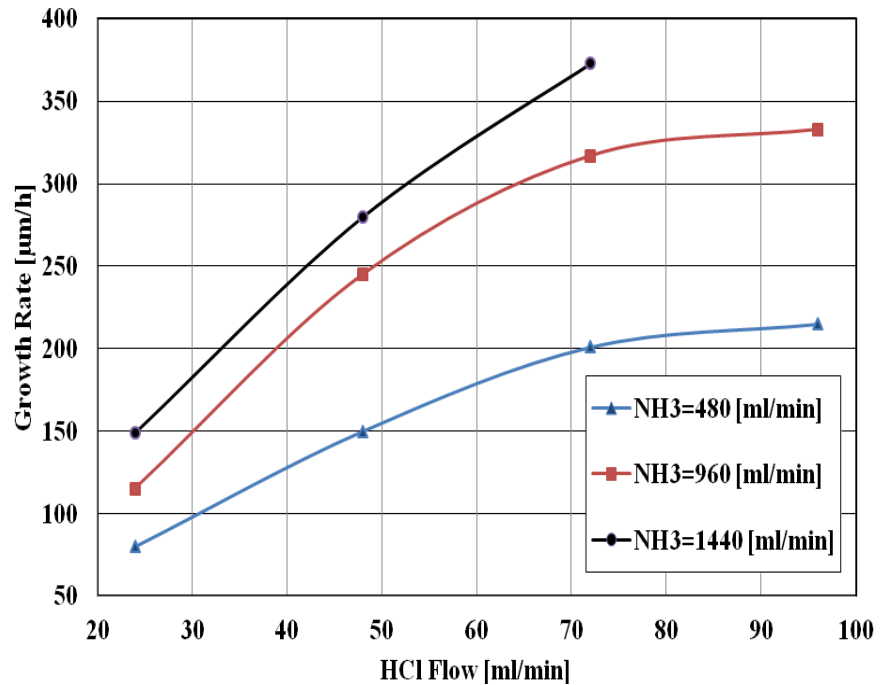
T. Sochacki et al., Journal of Crystal Growth 407, (2014) 52–57
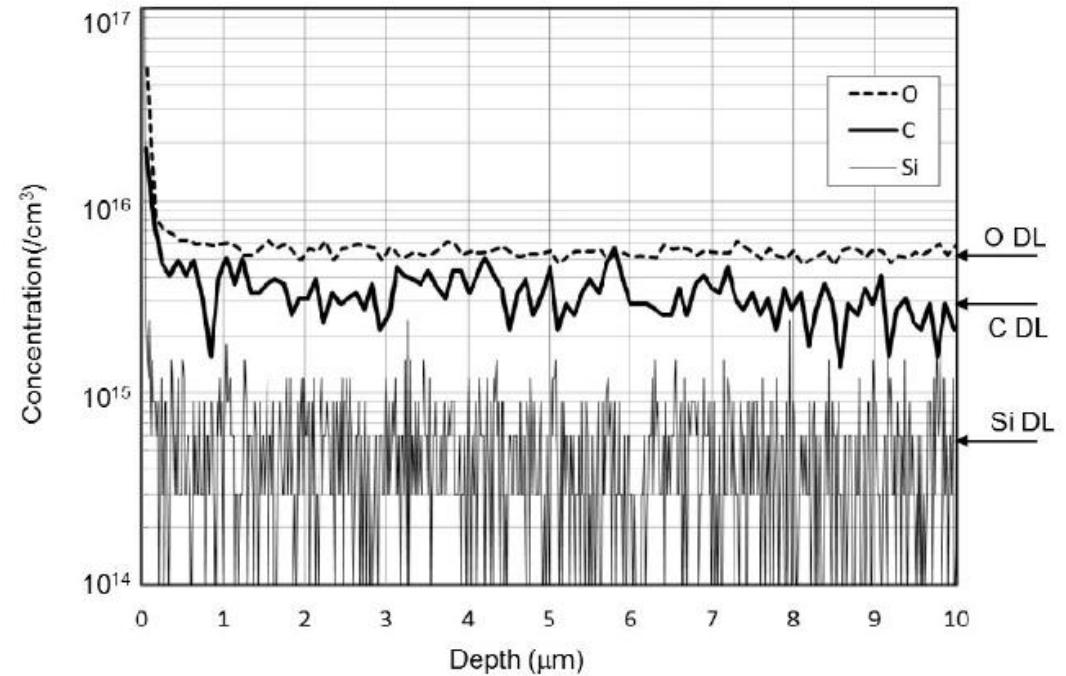
H. Fujikura et al., Japanese Journal of Applied Physics 56, 085503 (2017)

94

Gallium Nitride (GaN)

Highly conductive (n-type)

- Si doping (H_2Cl_2Si; $SiCl_4$)

- Ge doping ($GeCl_4$)

- Si/Ge doping
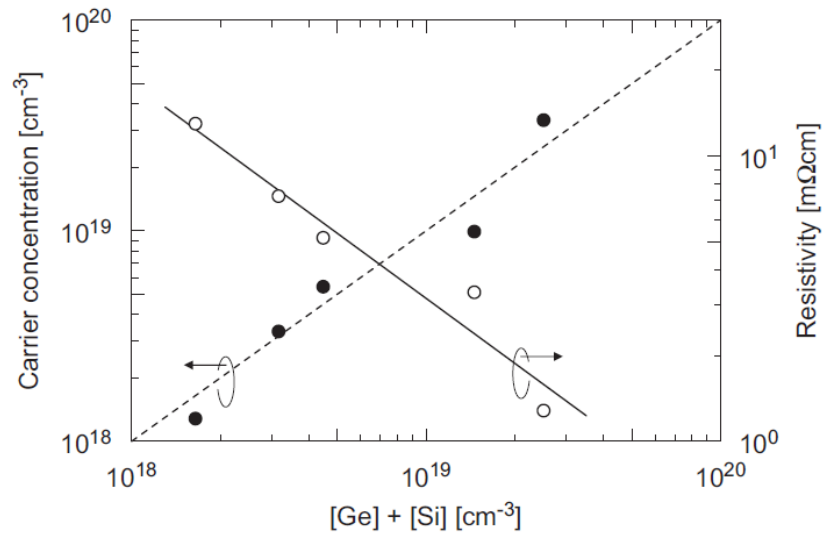
Semi-insulating (SI)

- Fe ($C_{10}H_{10}Fe$; solid metal)

- Mn (solid metal)

- C (CH_4; C_2H_2)
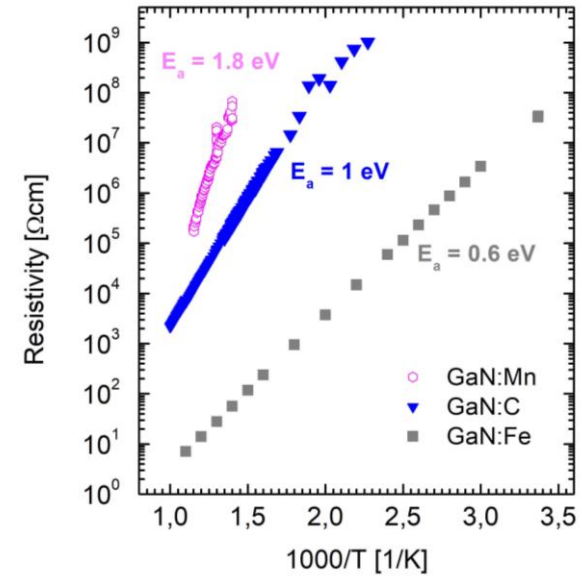
Y. Oshima et al. Journal of Crystal Growth 312 (2010) 3569–3573

M. Bockowski et al., J. Cryst. Growth 499 (2018) 1-7

Gallium Nitride (GaN)

1-inch Ammono-GaN substrates for HVPE growth

1. Thickness from 300 to 700 µm
2. Misorientation ~ 0,3° to the m direction
3. FWHM = 40 – 80 arcsec (beam size = 1x10 mm)
4. Bowing radius R > 20 m
5. TDD= 5×10^4 cm^{-2}
6. n = $2 \times 10^{17} - 5 \times 10^{18}$ cm^{-3}

Gallium Nitride (GaN)

RMS < 0.1 nm

Visible atomic steps
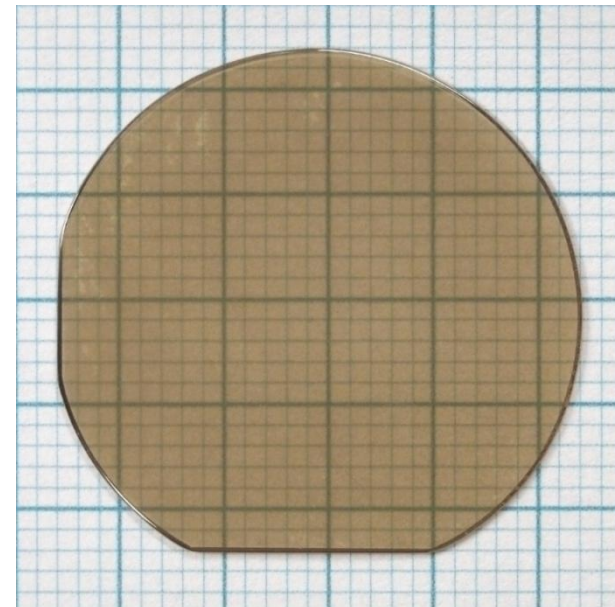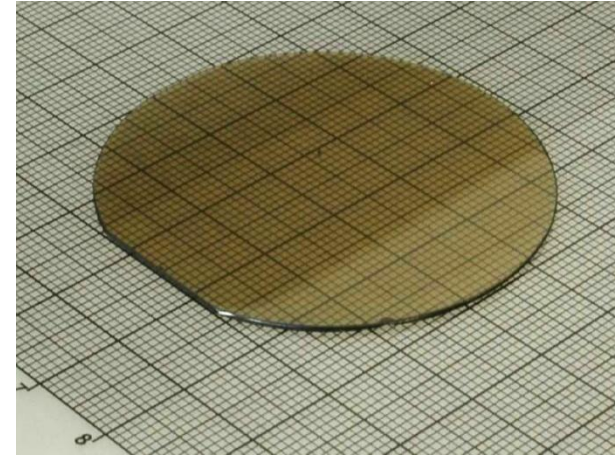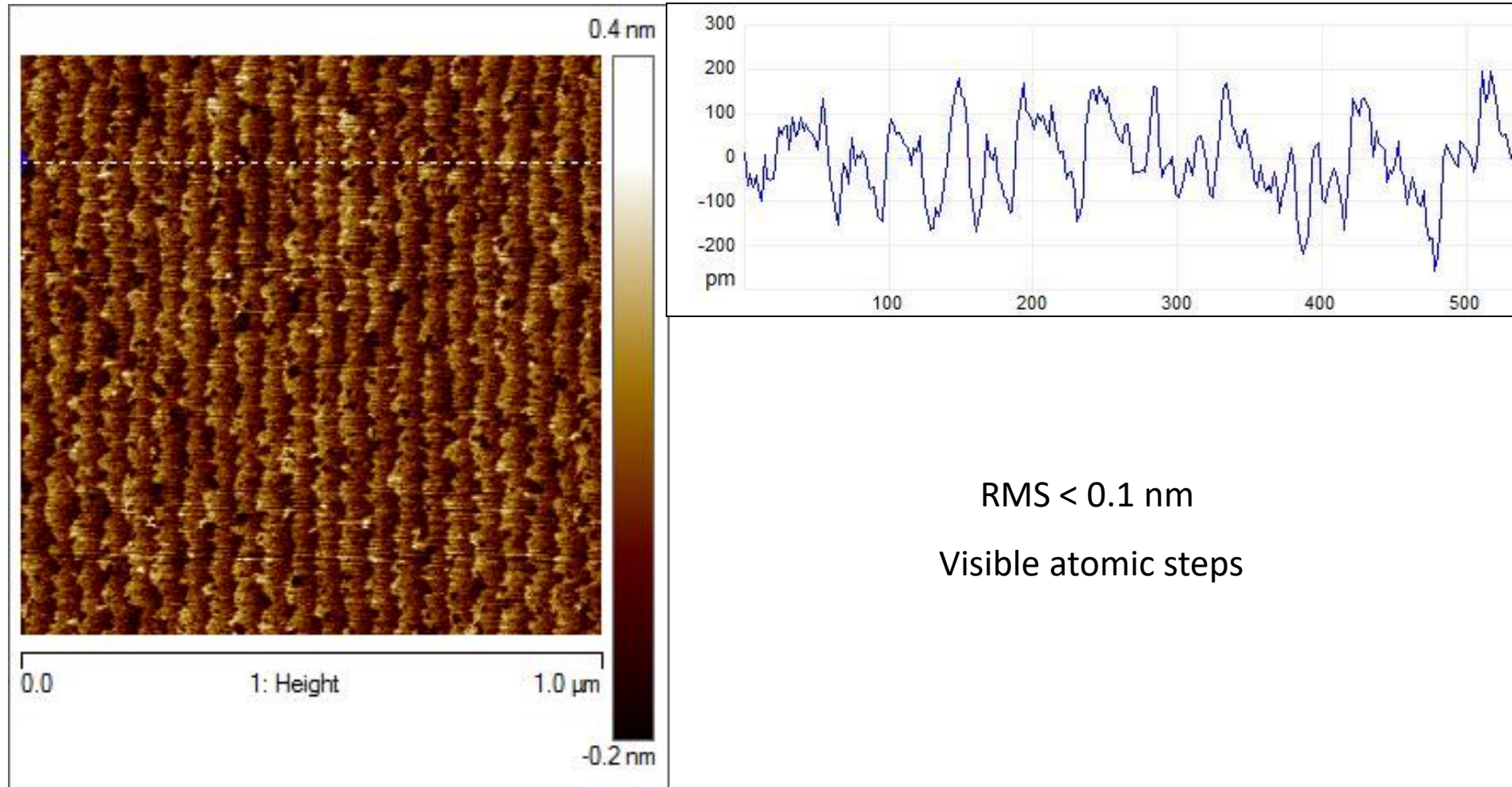
Gallium Nitride (GaN)

After 1-2 h. of growth
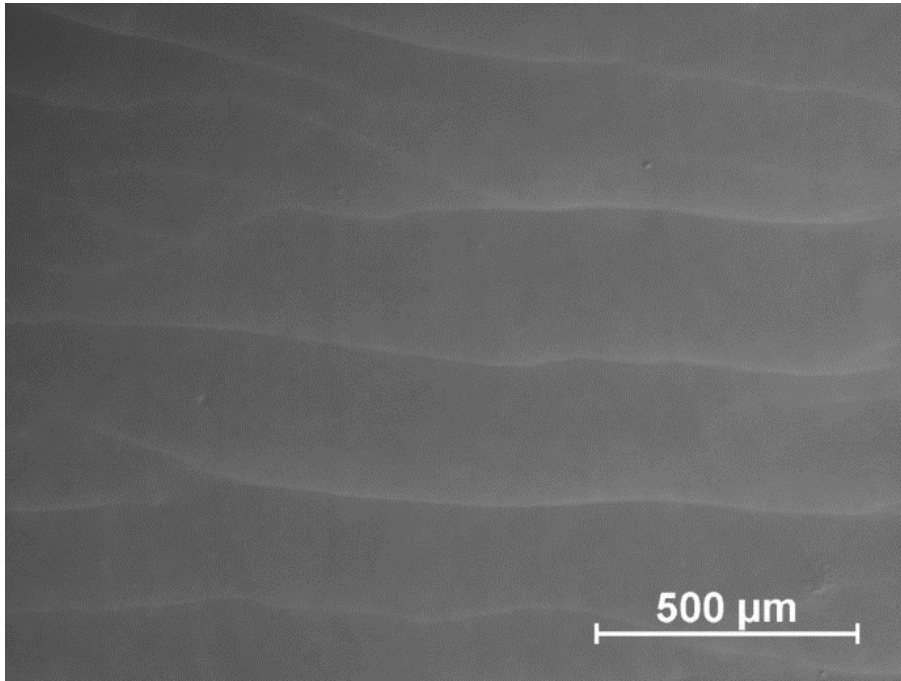
Average growth rate: 60 µm/h
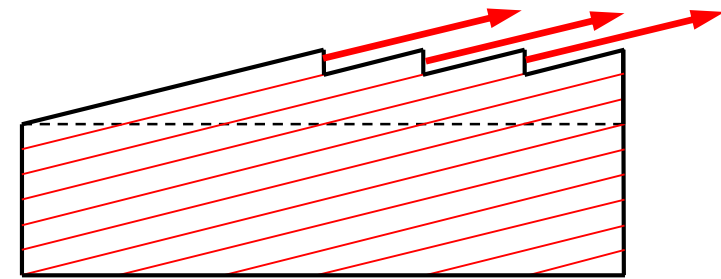
- source of macrosteps disappeares
- c-plane is recovered
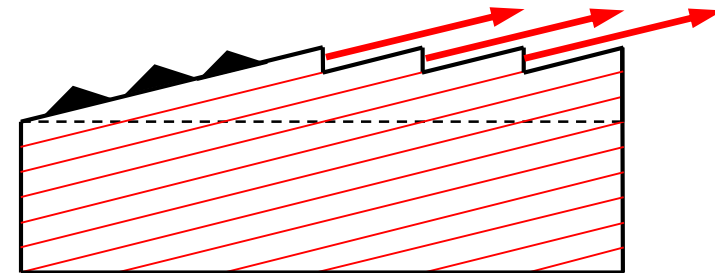
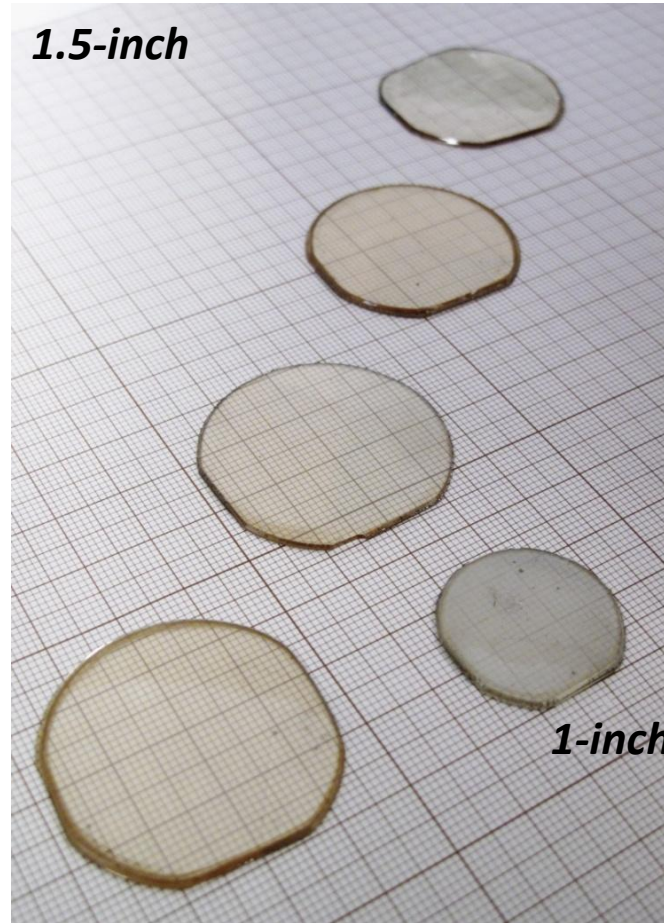# Gallium Nitride (GaN)
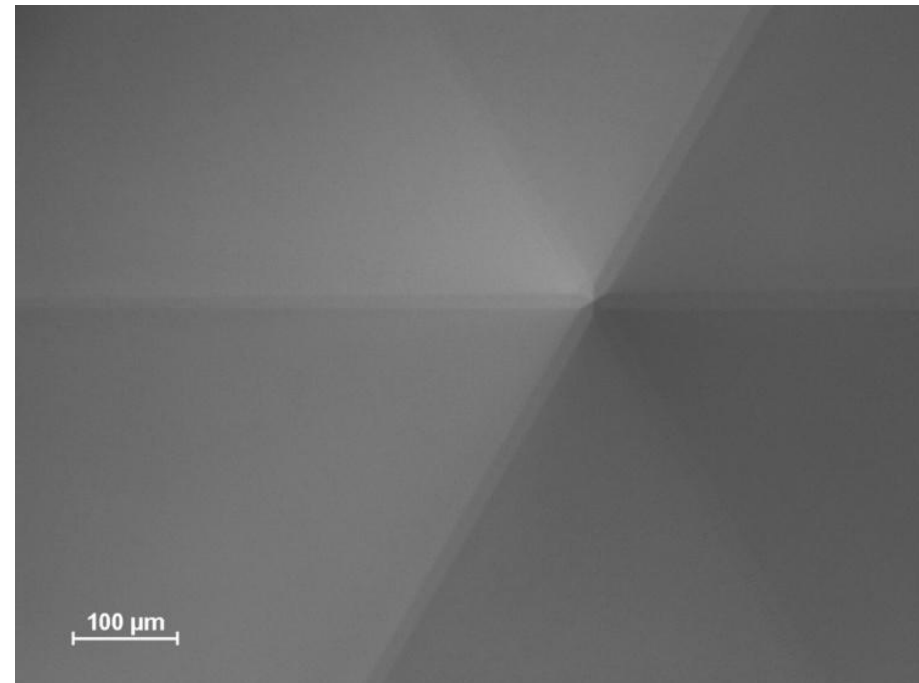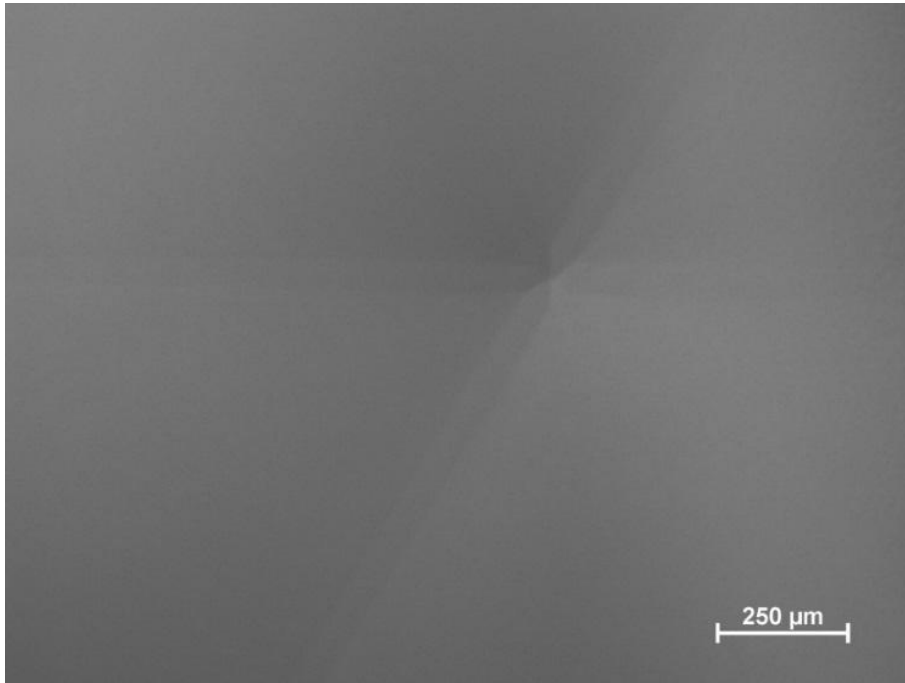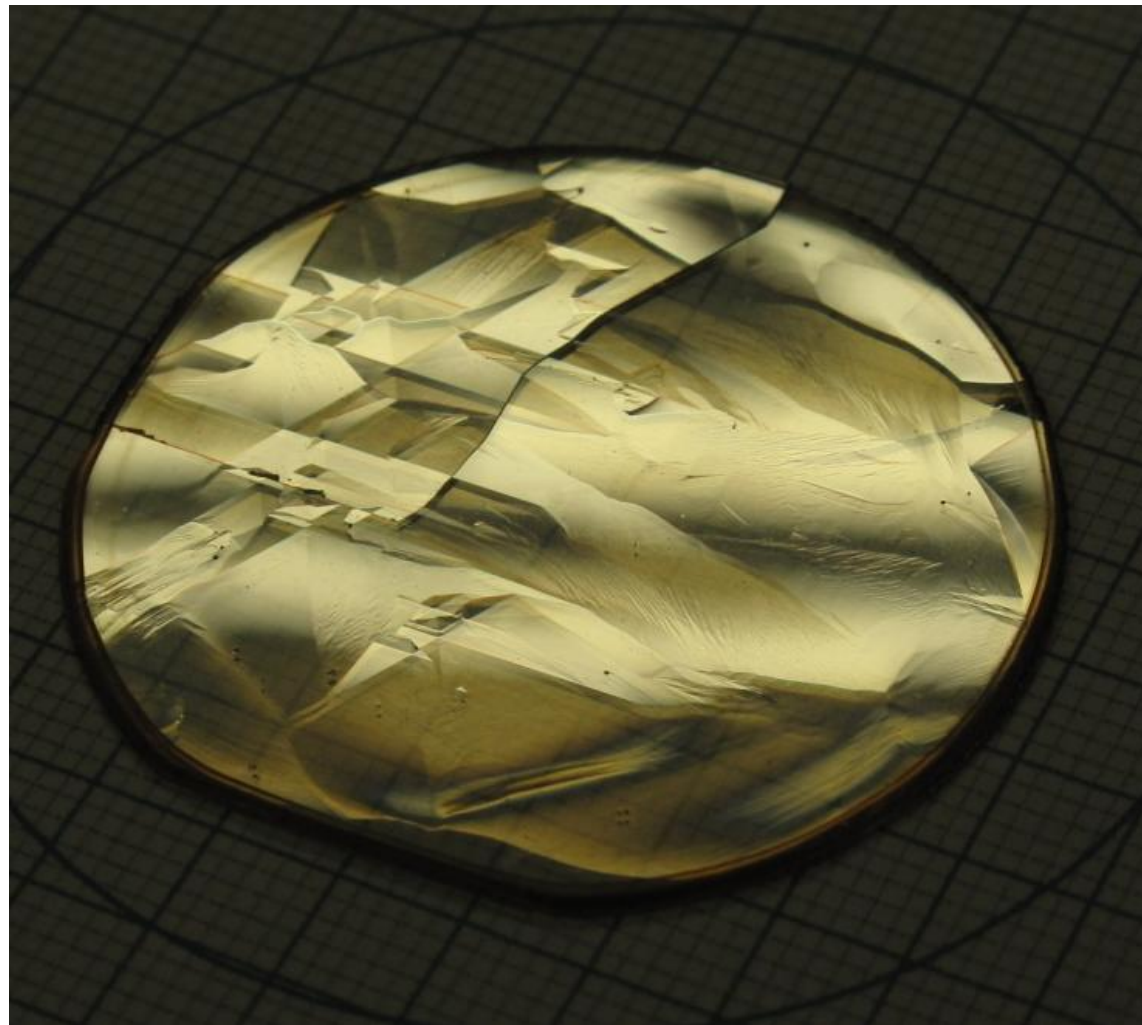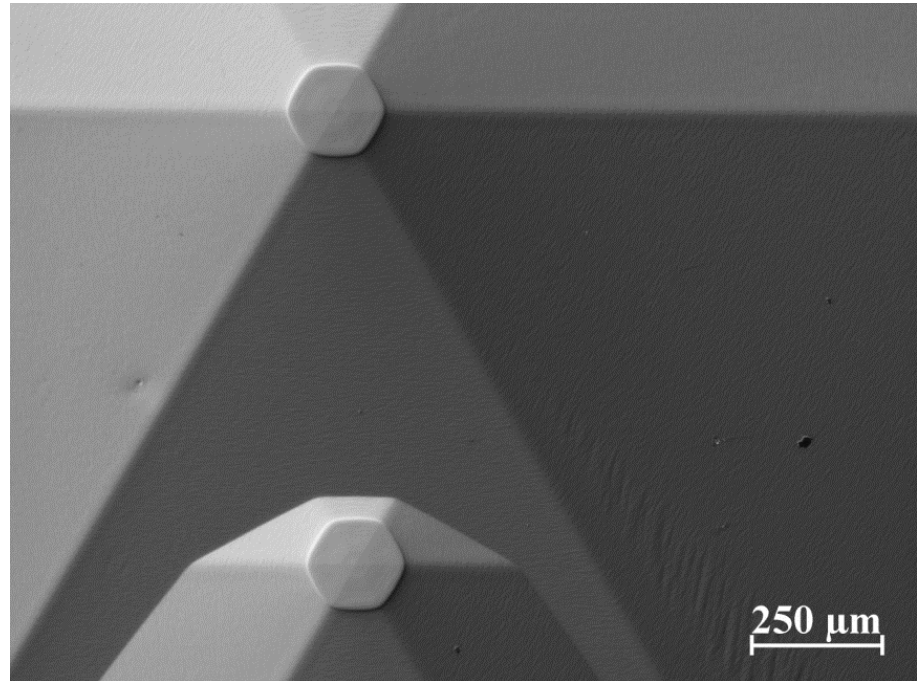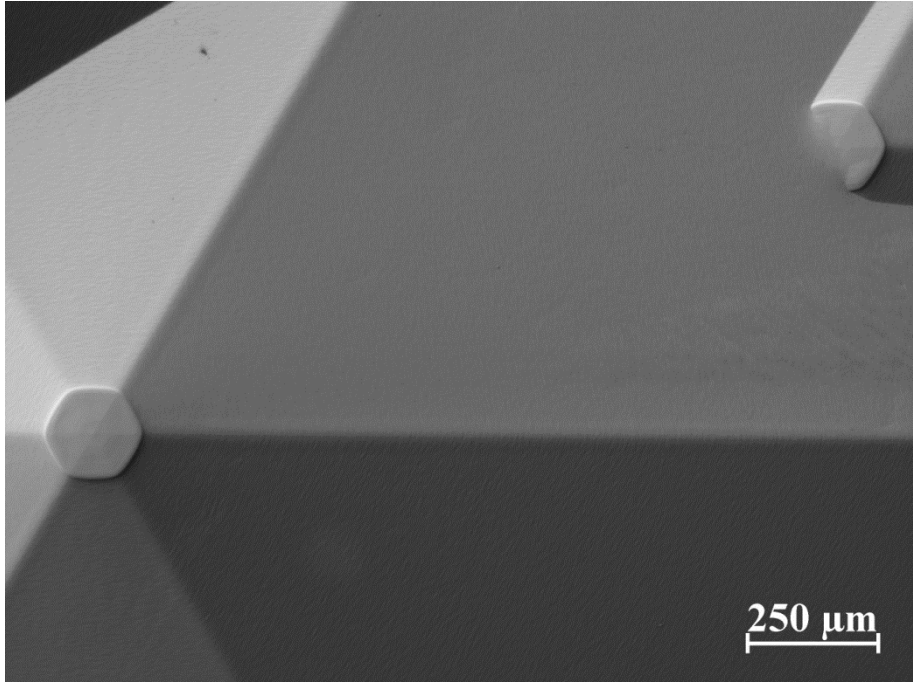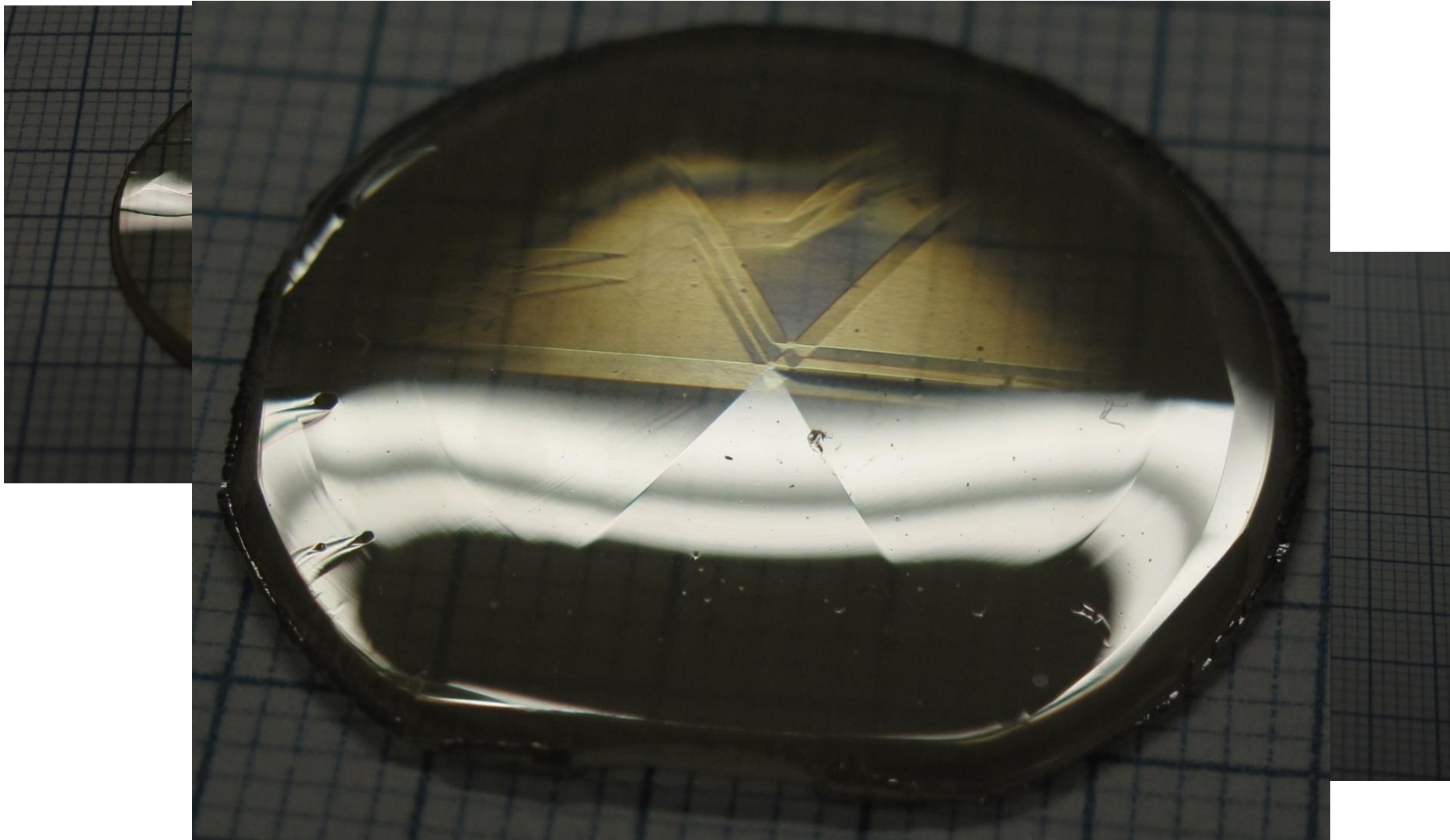
Gallium Nitride (GaN)

Gallium Nitride (GaN)

250 μm

250 μm
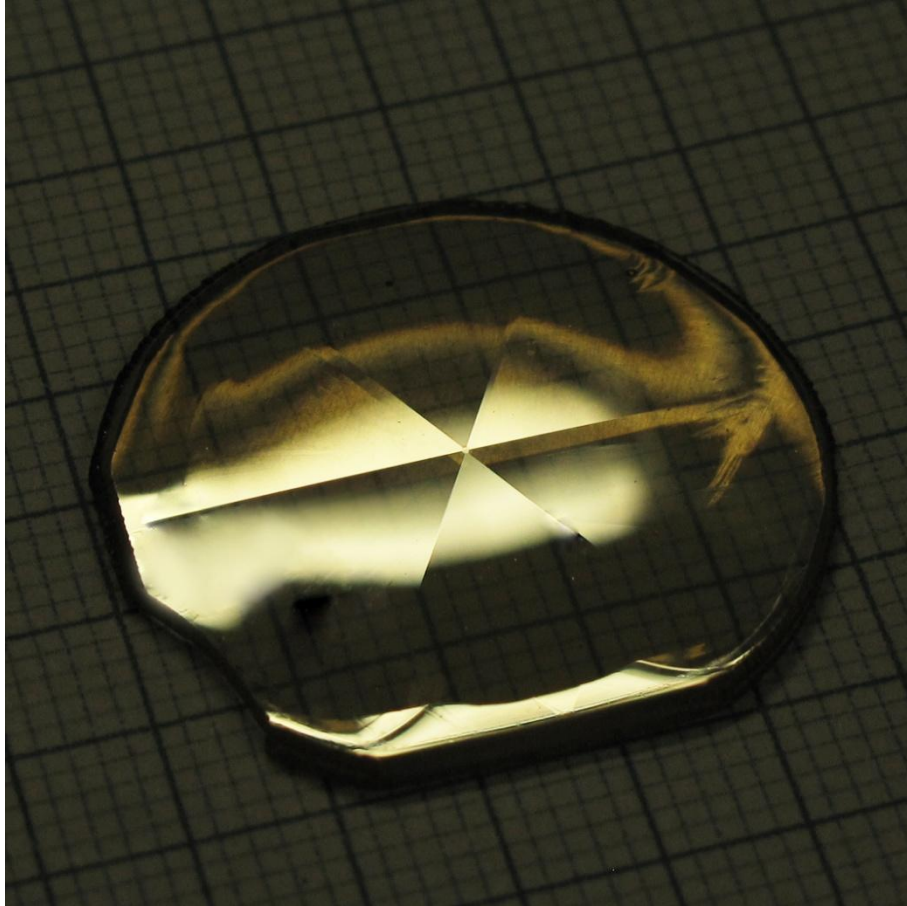
Gallium Nitride (GaN)
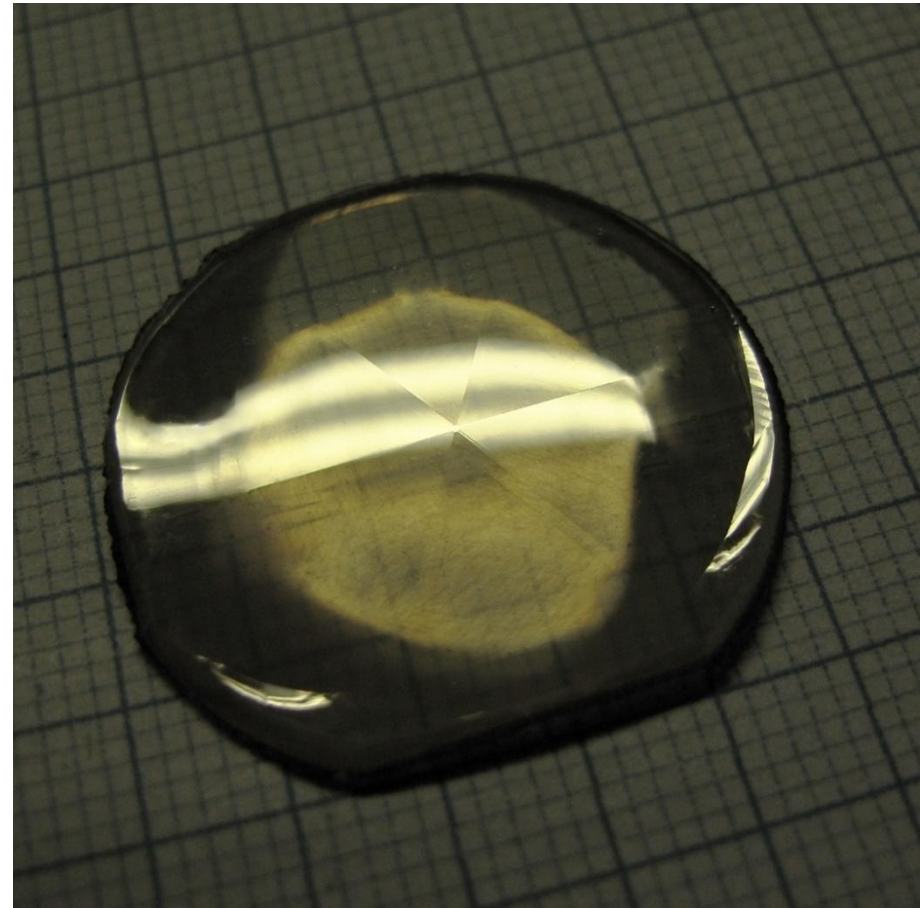
Gallium Nitride (GaN)

Average growth rate: 200-240 µm/h

Gallium Nitride (GaN)

Average growth rate: 200-240 μm/h

G. Nowak, T. Sochacki

Gallium Nitride (GaN)

Average growth rate: 200-240 μm/h

G. Nowak, T. Sochacki

Gallium Nitride (GaN)

G. Nowak, T. Sochacki
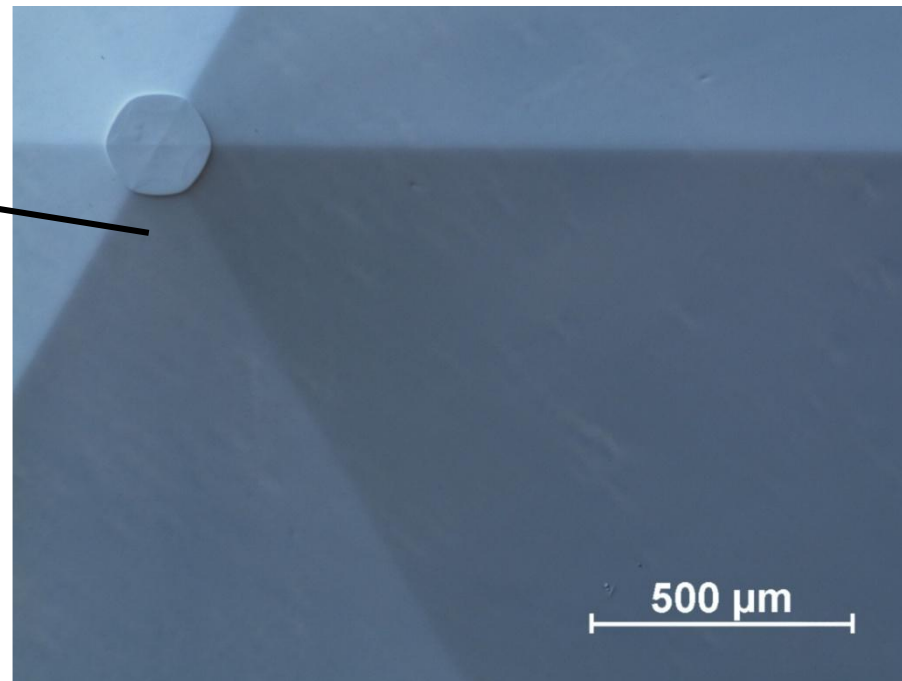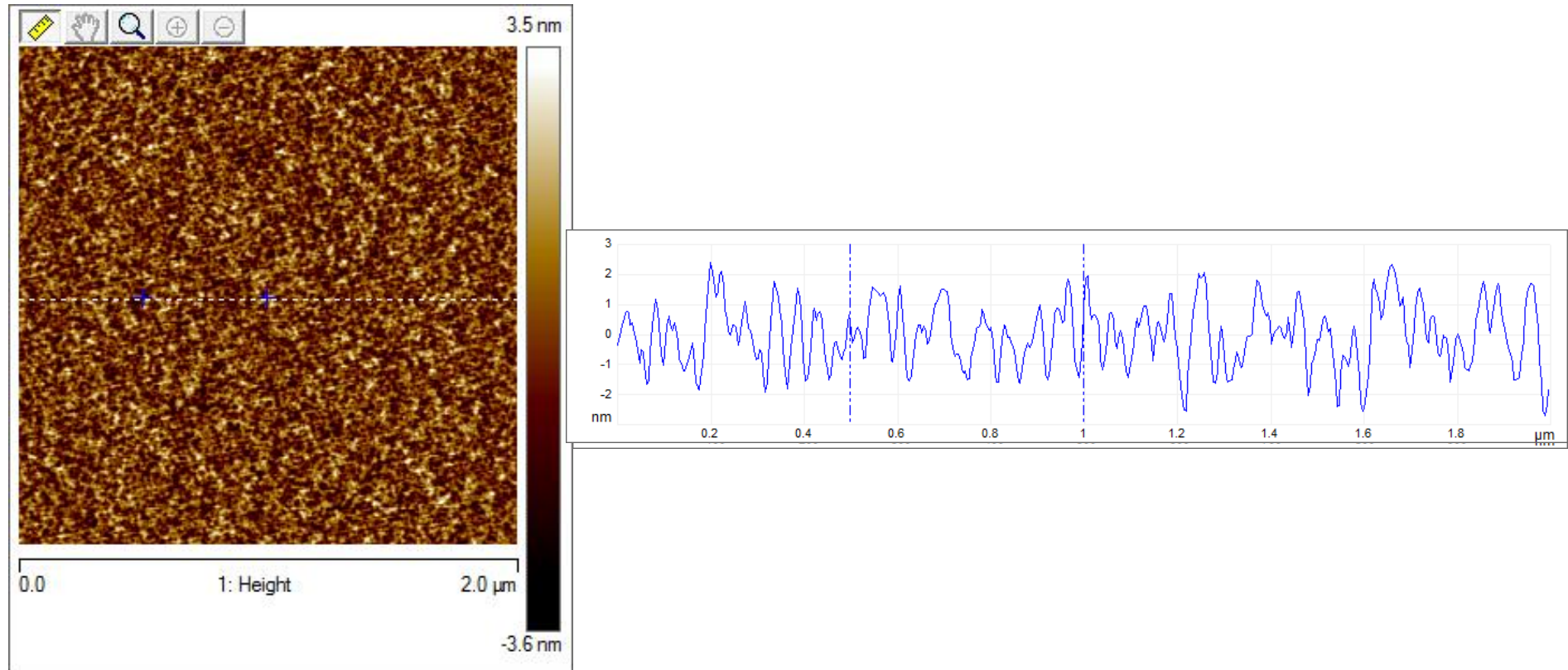
Gallium Nitride (GaN)

Synchrotron white-beam X-ray topography (SWXRT)
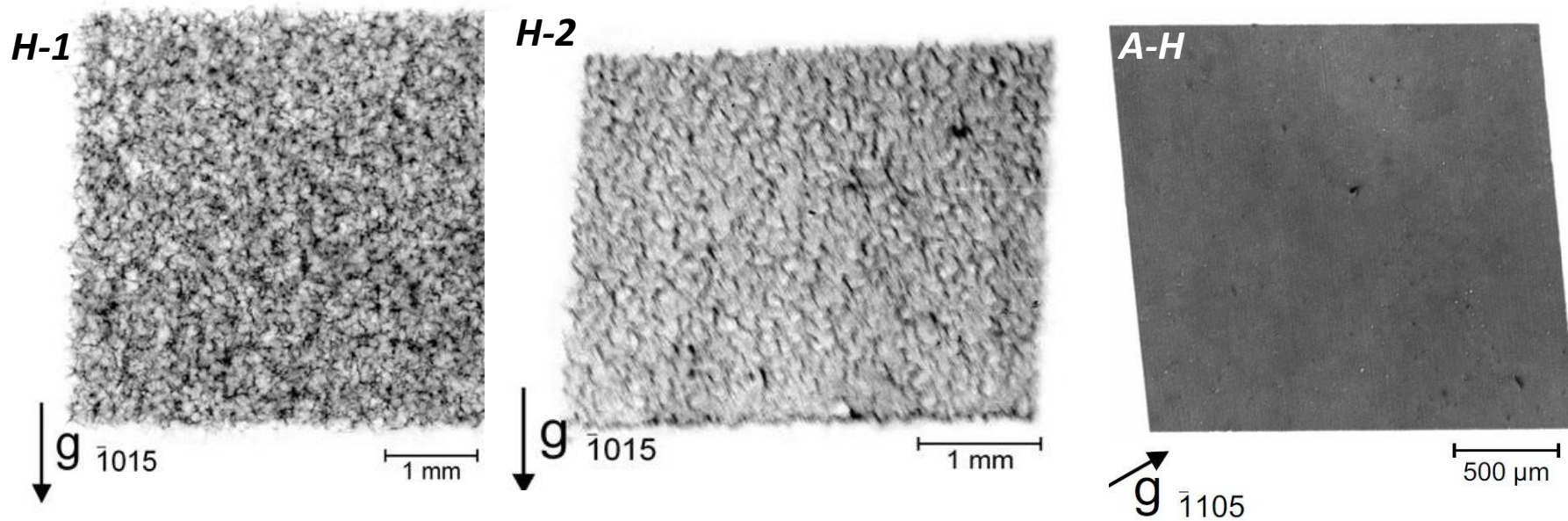
cellular dislocation network

The dislocation rearrangement into cell networks takes place under external or internal stress in the course of plastic relaxation

Uniform gray contrast indicates a high degree of crystalline perfection

L. Kirste ECS Journal of Solid State Science and Technology, 4 (8) P324-P330 (2015)

Gallium Nitride (GaN)

- Omega Rocking curves (ω-scan in double-axis geometry)
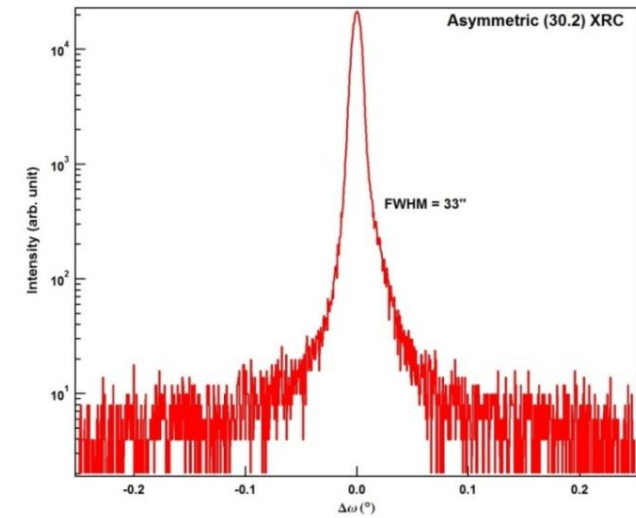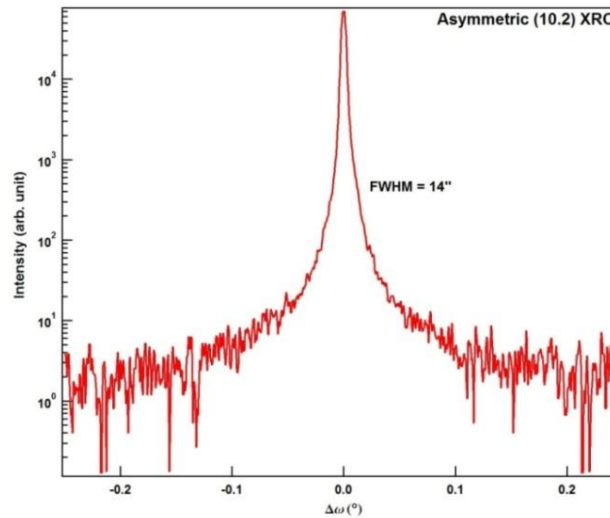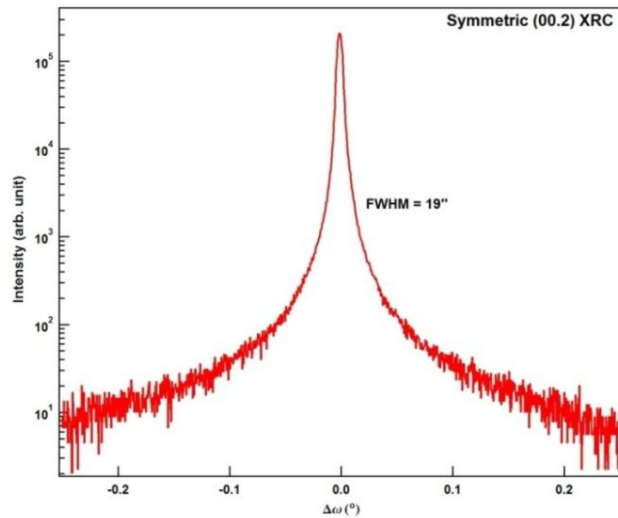
Sample	(00.2)-RC FWHM	(10.2)-RC FWHM	(30.2)-RC FWHM
Sample A	19 arcsec	14 arcsec	33 arcsec

M. Bobea, Z. Bryan, I. Bryan R. Collazo, Z. Sitar

Gallium Nitride (GaN)

Etch pit distribution

molten KOH/NaOH 450°C

EPD = 5×10^4 cm^{-2}

50 μm
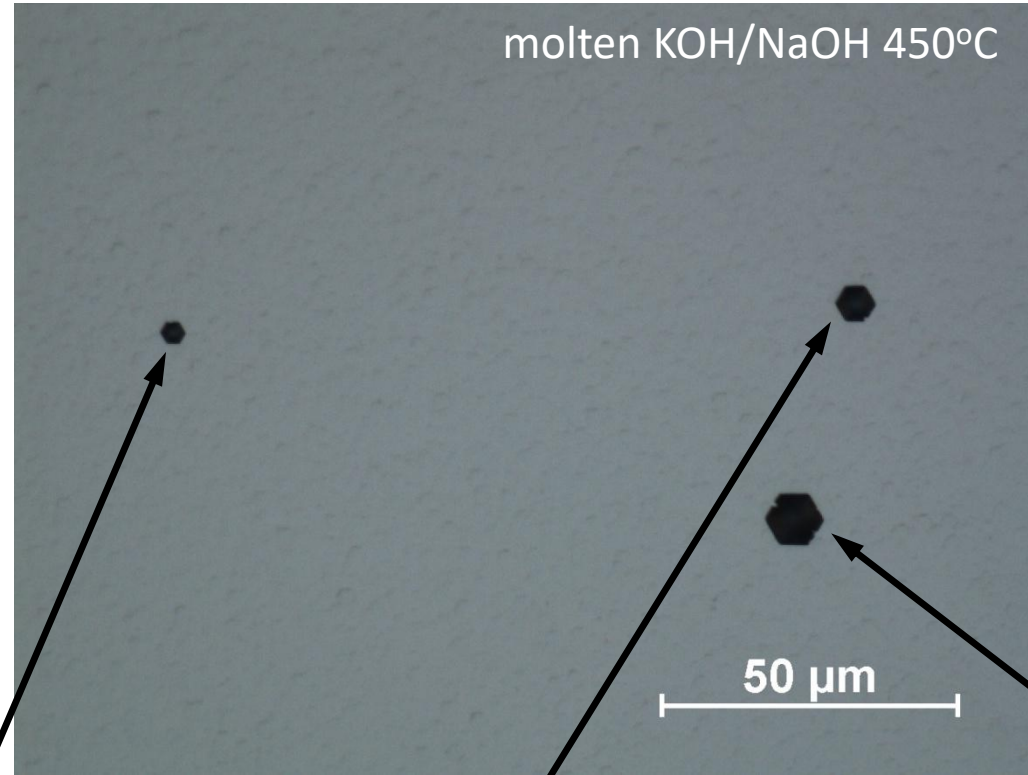
J. Weyher,
T. Sochacki

Edge
dislocation

Mixed
dislocation

Screw
dislocation

J. L. Weyher et al., Journal of Crystal Growth 305 (2007) 384–392

Gallium Nitride (GaN)

Growth rate

$$2Ga_{(l)} + 2HCl_{(g)} = 2GaCl_{(g)} + H_{2(g)}$$
$$GaCl_{(g)} + NH_{3(g)} = GaN_{(s)} + HCl_{(g)} + H_{2(g)}$$

NH$_3$ flow

Constant NH$_3$ flow

HCl flow
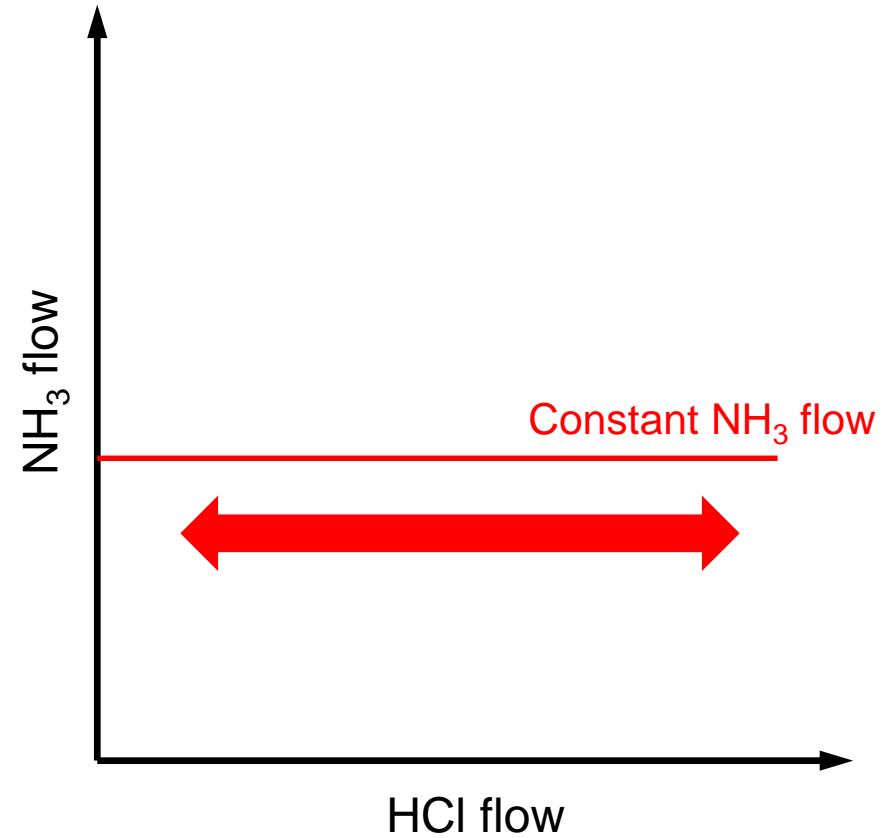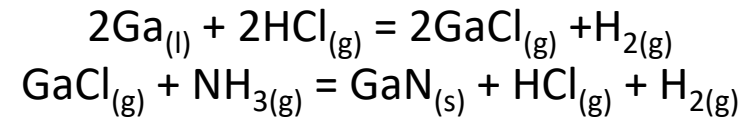
Gallium Nitride (GaN)
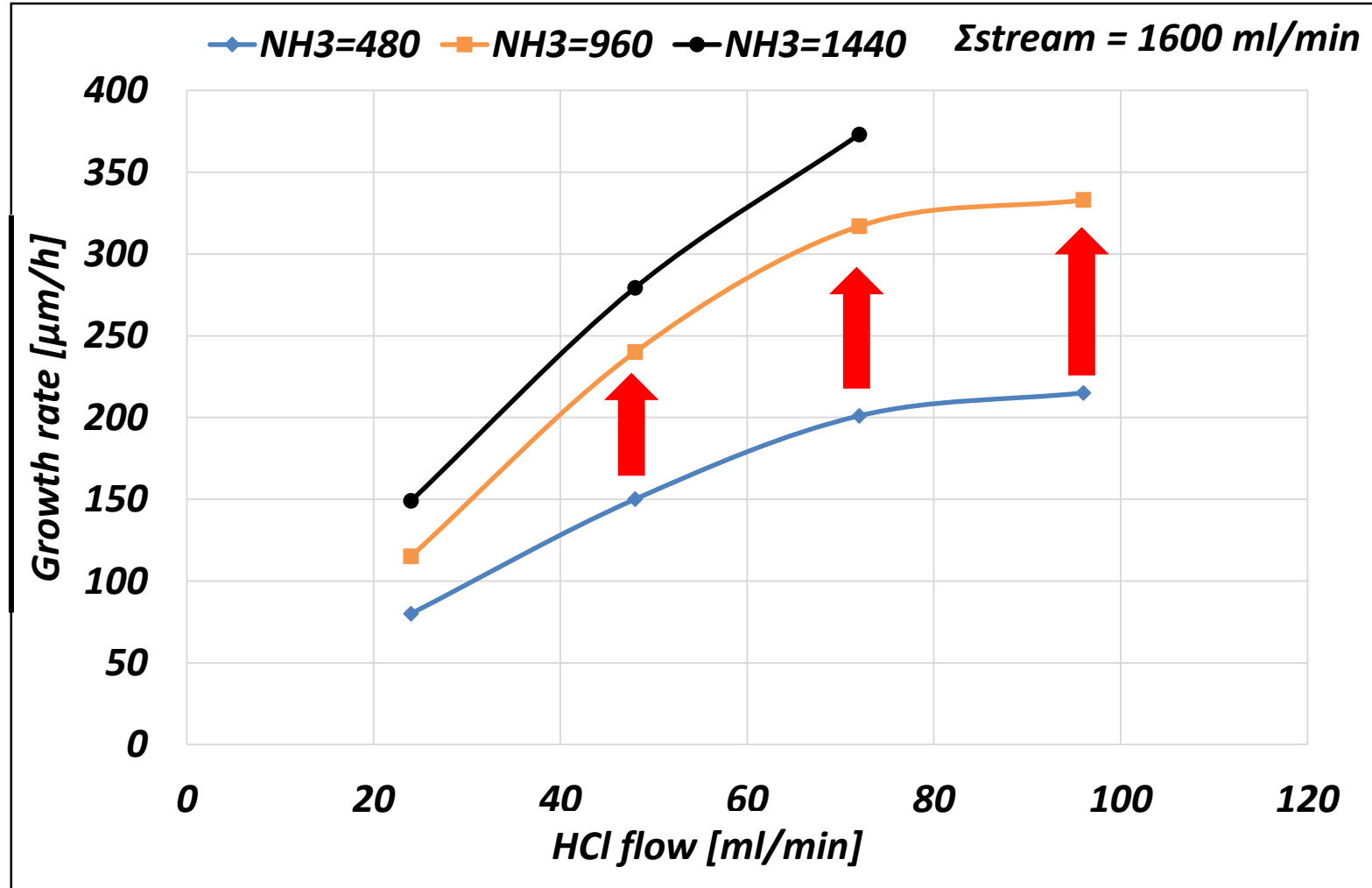
Growth time 8 h.

Gallium Nitride (GaN)
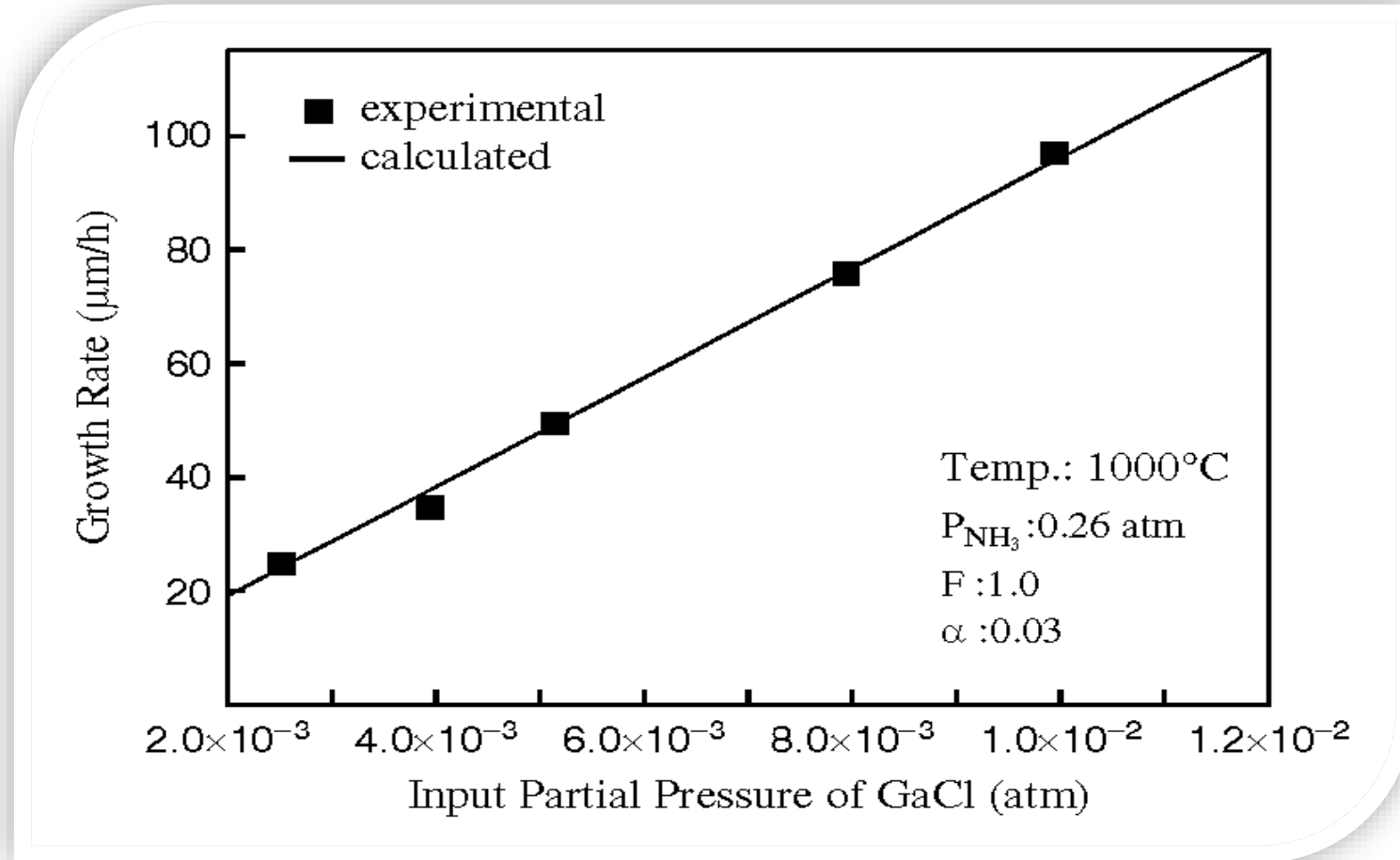
A. Koukitu, Y. Kumagai in Technology of Gallium Nitride Crystal Growth, Springer-Verlag, Heidelberg, 2010, p. 31.
A. Usui et al. Jpn. J. Appl. Phys. 36, L899 (1997)

Gallium Nitride (GaN)
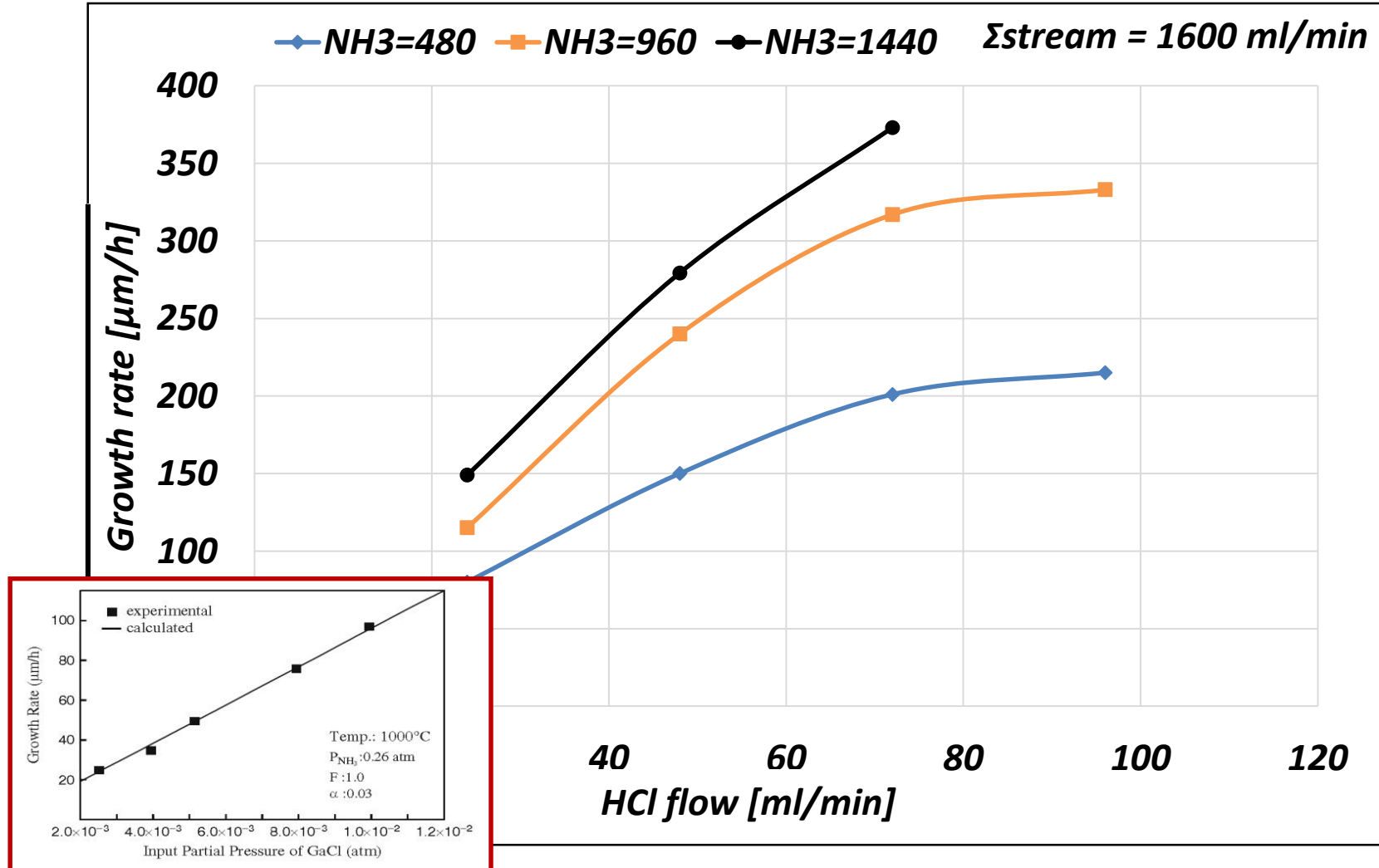
Growth time 8 h.

Gallium Nitride (GaN)

$$2Ga_{(l)} + 2HCl_{(g)} = 2GaCl_{(g)} + H_{2(g)}$$
$$GaCl_{(g)} + NH_{3(g)} = GaN_{(s)} + HCl_{(g)} + H_{2(g)}$$

Gallium Nitride (GaN)

Growth time 8 h.

Gallium Nitride (GaN)

2-inch

1-inch

1.5-inch

1-inch

M. Bockowski et al., Semicond. Sci. Technol. 31 093002 (2016)
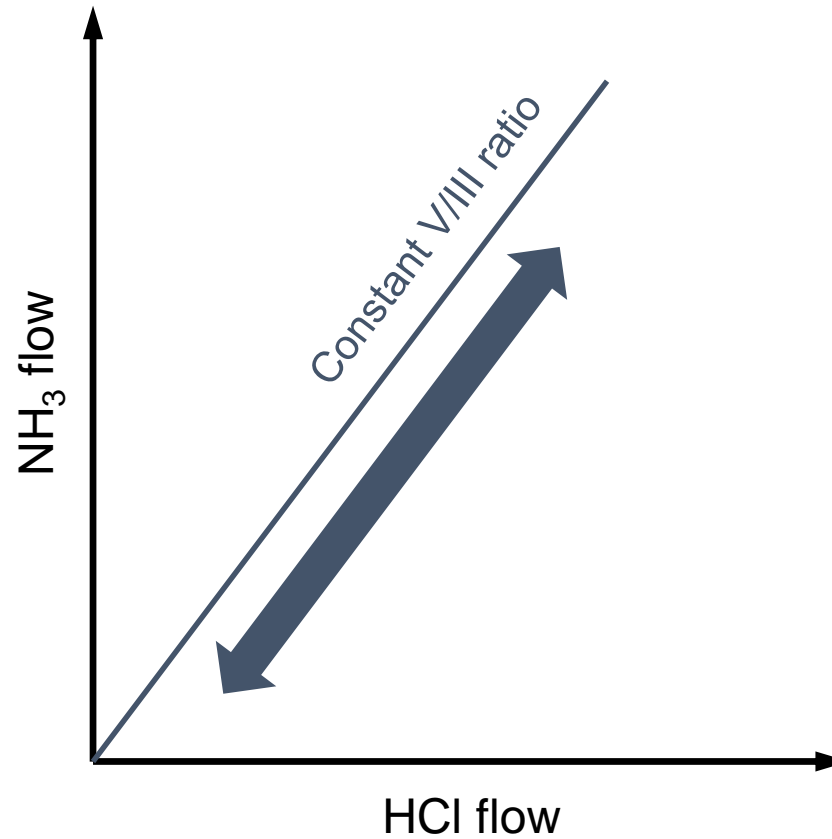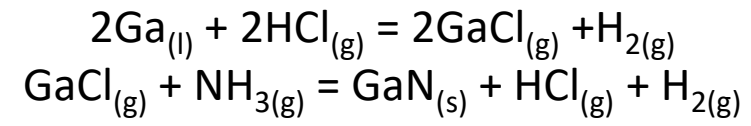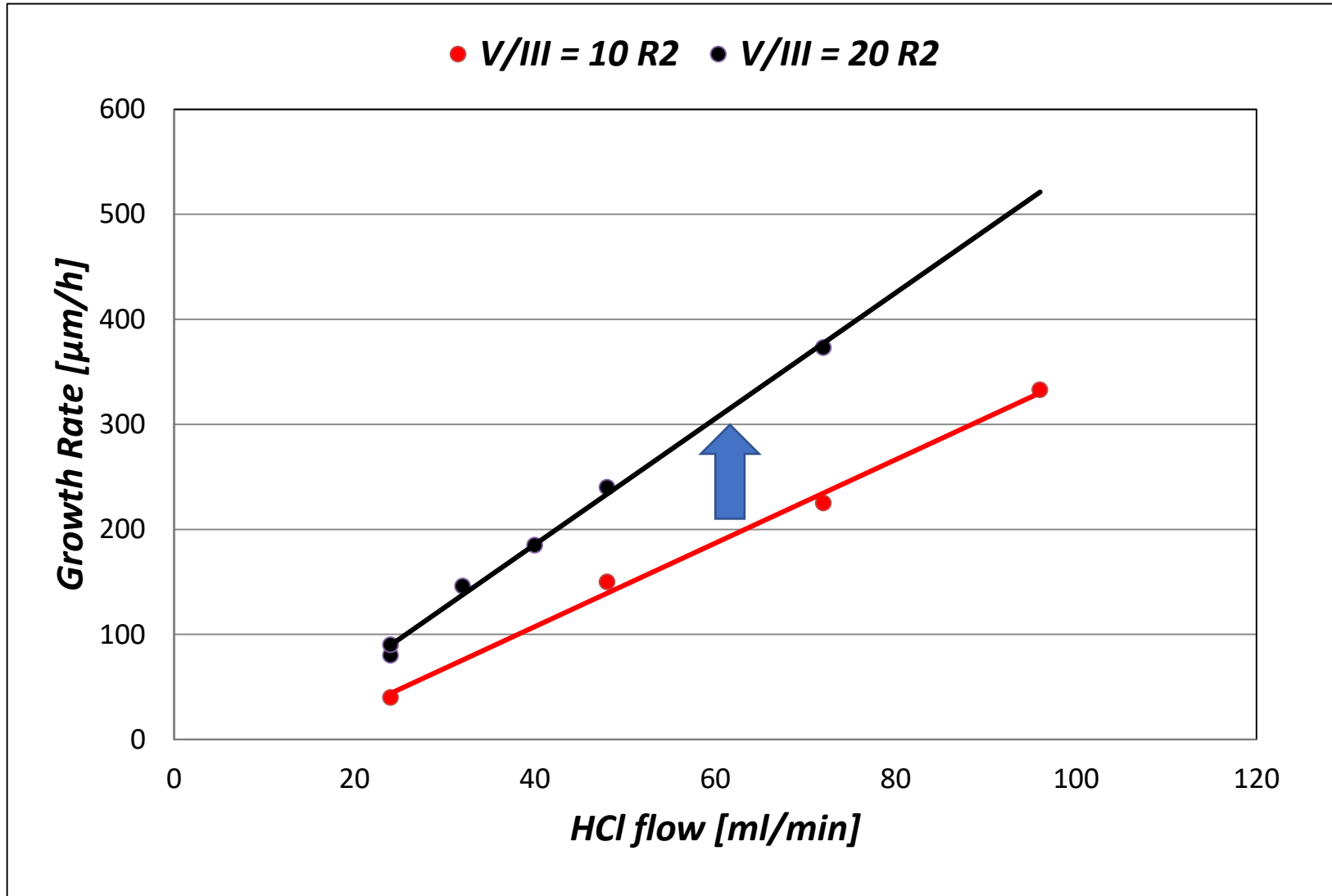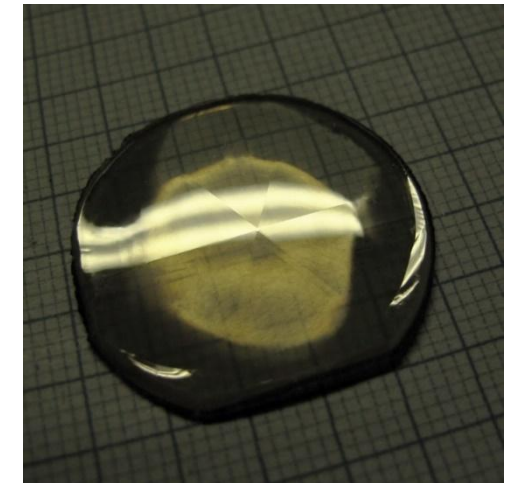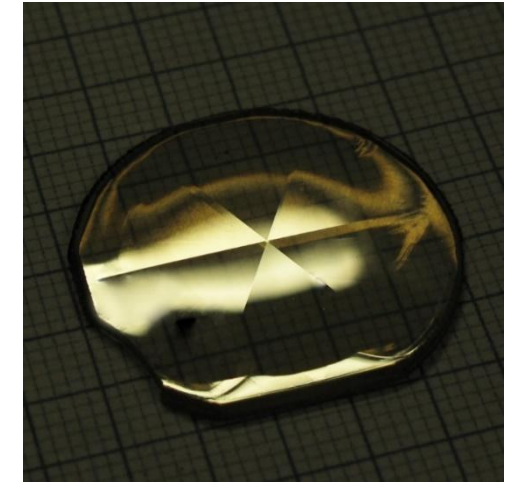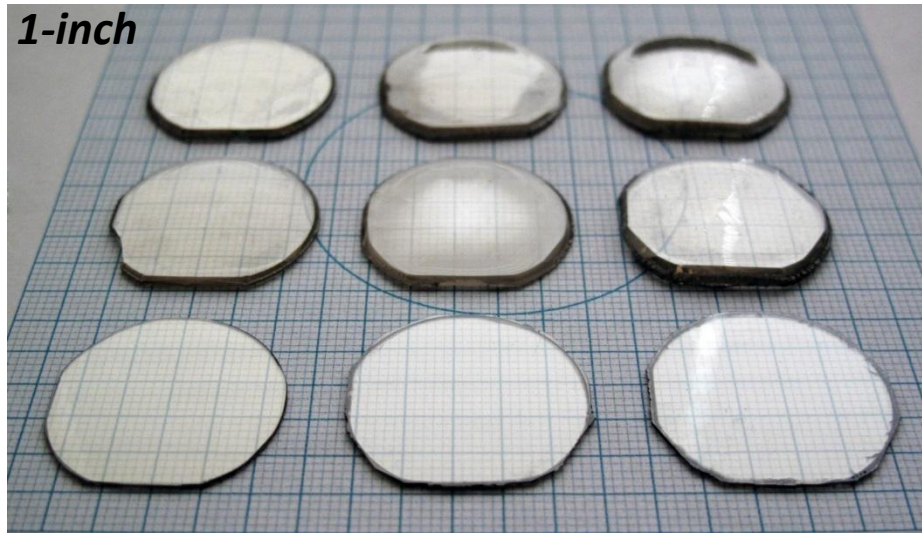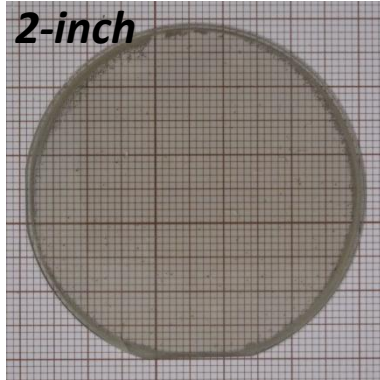
Gallium Nitride (GaN)

No one has demonstrated high-quality bulk GaN crystals yielding several tens of wafers per boule as well as a convenient technology for growing such thick layers.

GaN seed crystal

Bulk GaN growth

Wafer production

seed

slice
polish
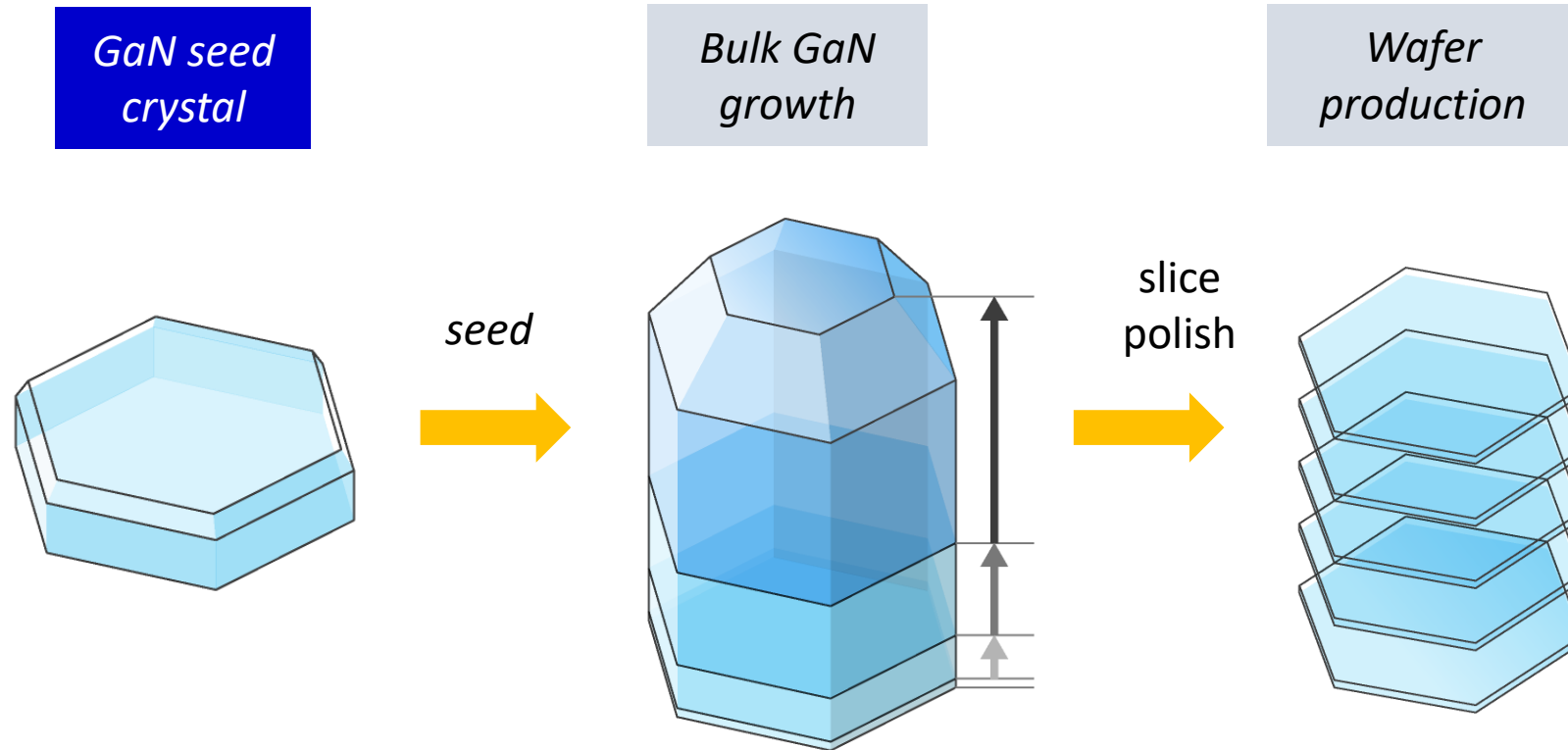
Gallium Nitride (GaN)

Anisotropy of the growth

T. Sochacki et al., Phys. Status Solidi B 252, No. 5 (2015) 1172

Gallium Nitride (GaN)

J. Domagala et al., J. Cryst. Growth, Volume 456, (2016) 80-85
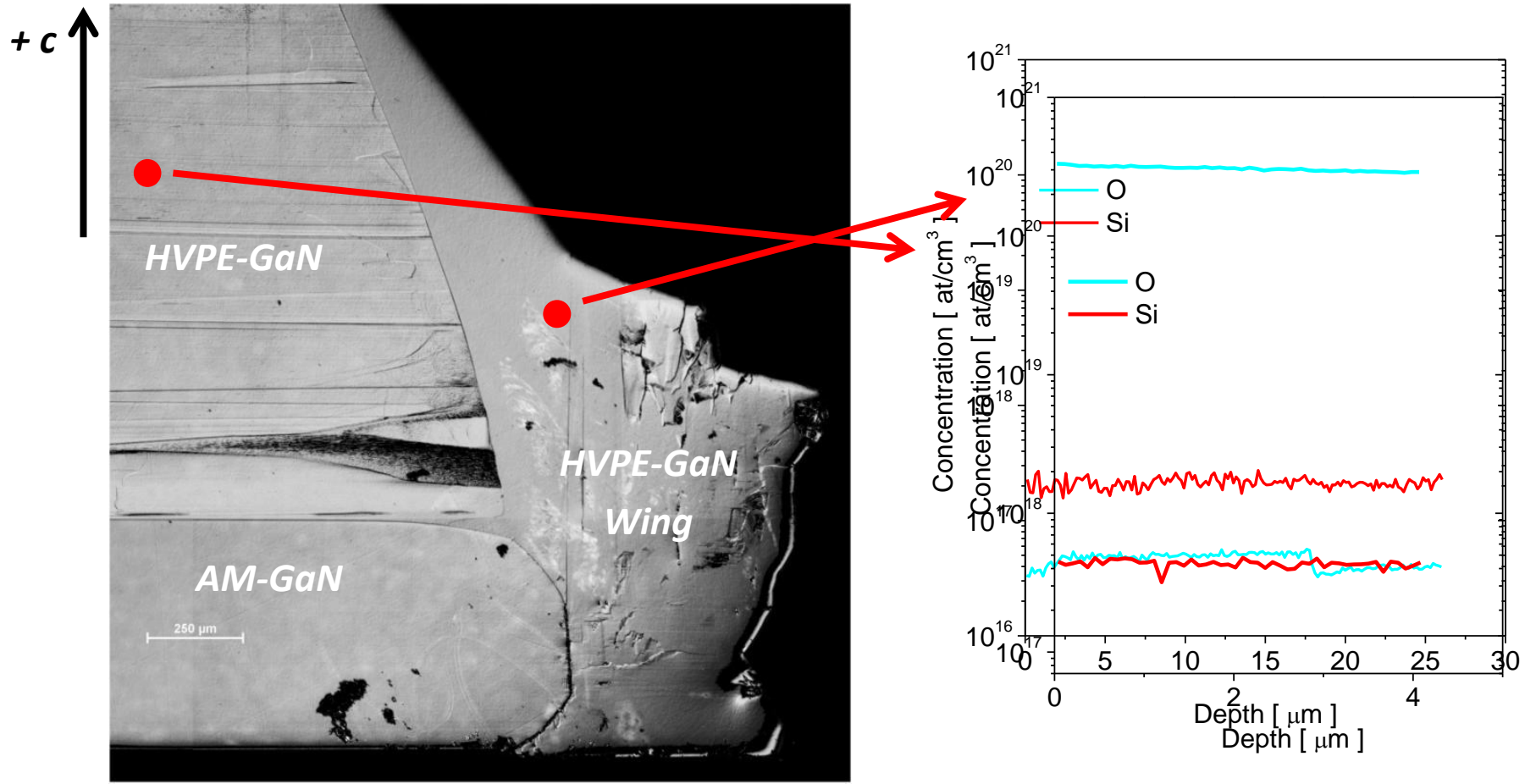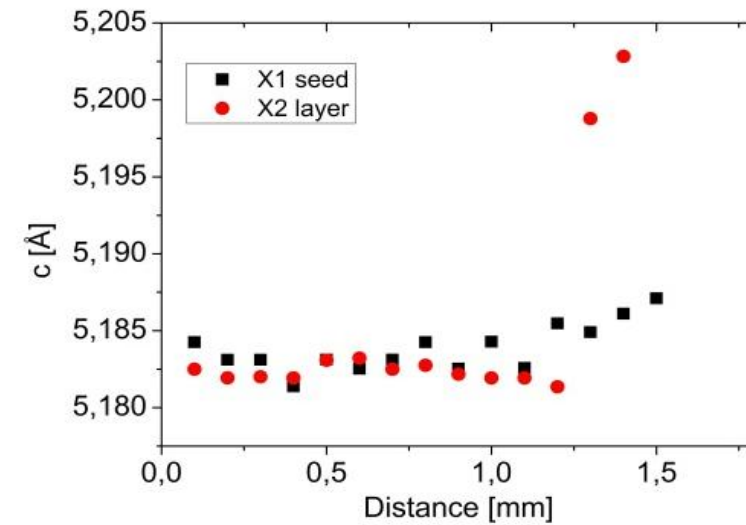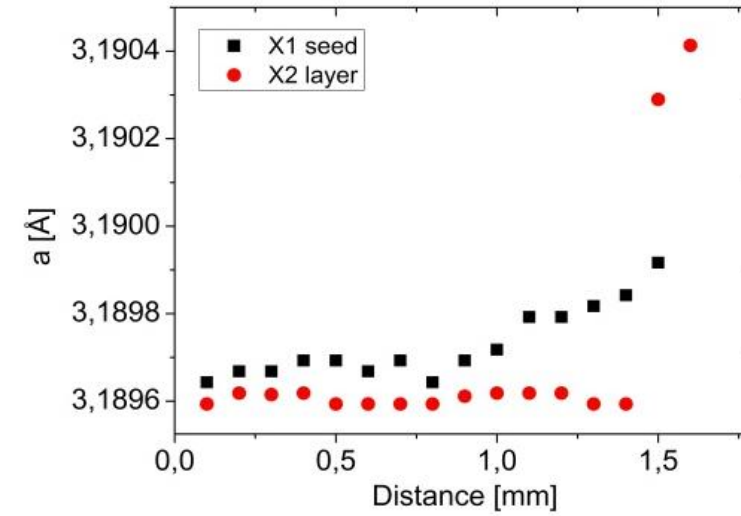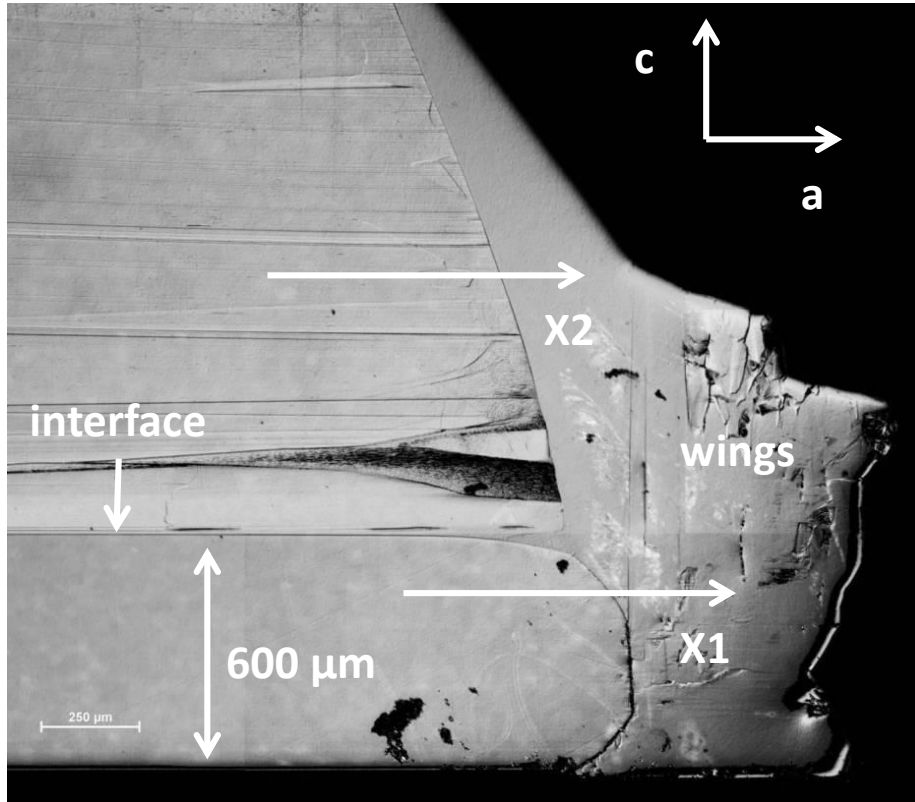
Gallium Nitride (GaN)
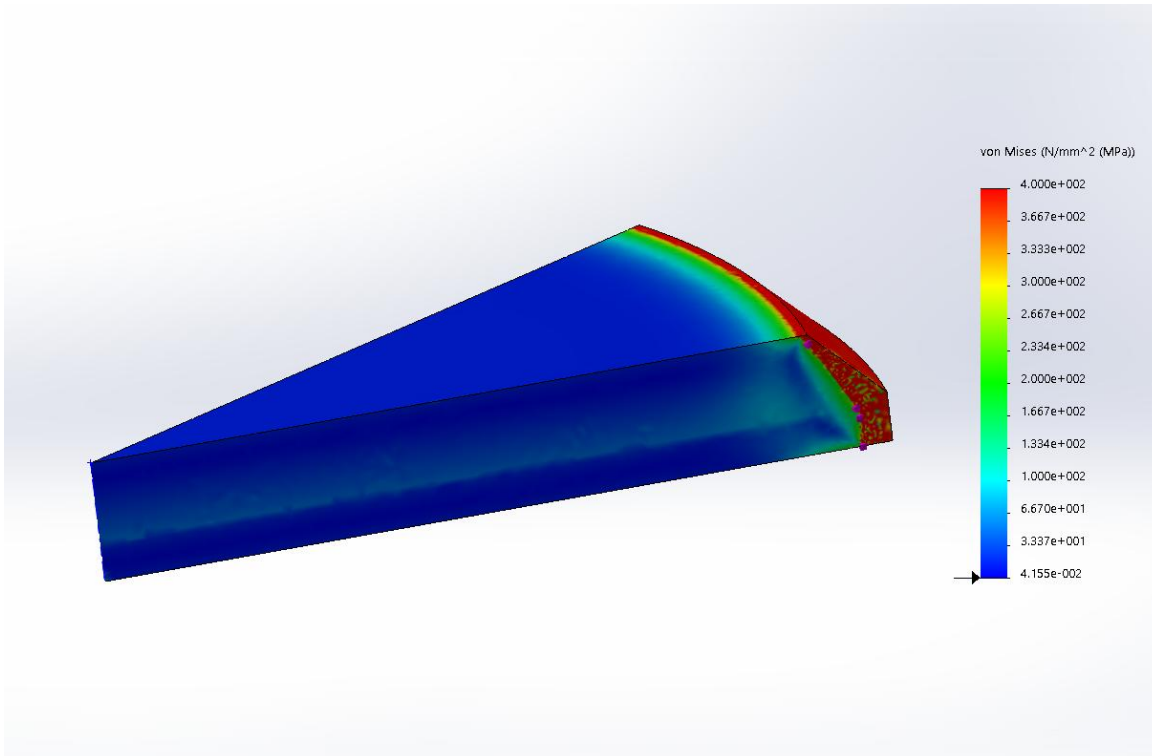
Calculated Von Mises stress distribution in HVPE-GaN deposited on 1-inch Am-GaN seed

Raman map of the stress distribution at the edge of the growing crystal (on 1-inch Am-GaN seed)

M. Amilusik et al., Japanese Journal of Applied Physics 58, SCCB32 (2019)

B. Lucznik et al., Journal of Crystal Growth 456 (2016) 86–90

Gallium Nitride (GaN)

$$\Delta\varepsilon = (a_{seed} - a_{deposited\ layer})/a_{seed}$$

deposited layer

$a > a_{seed}$

$a > a_{seed}$

$a_{seed} > a_{deposited\ layer}$
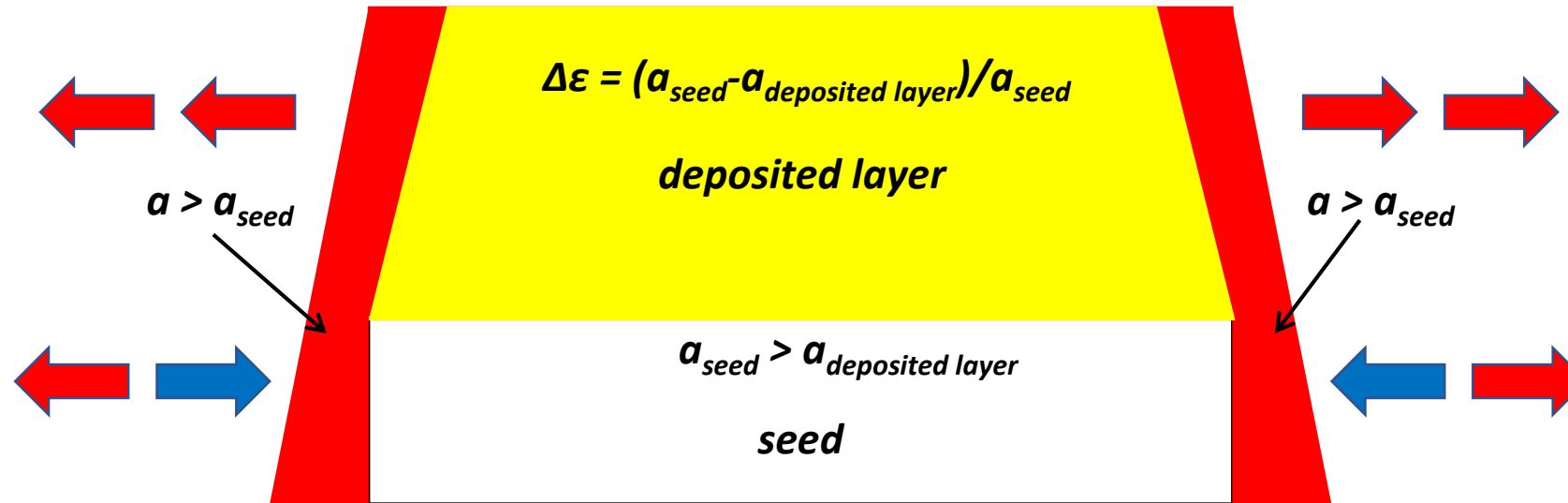
seed

The seed is under tensile and compressive stress;
they can suppress each other; new defects should not be observed in seed.

The deposited layer is under tensile stress derived from two objects;
plastic deformation may occur in the deposited layer.

Gallium Nitride (GaN)
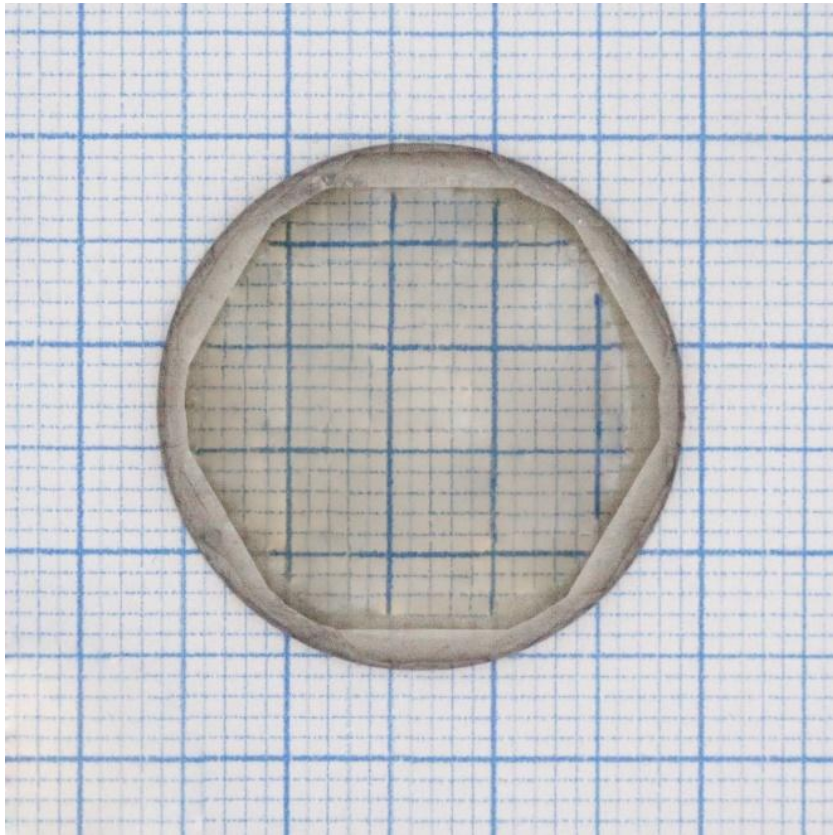
Thickness: 2900 μm
Growth rate: 303 μm/h

R. Kucharski et al., J. Appl. Phys. 128, 050902 (2020)
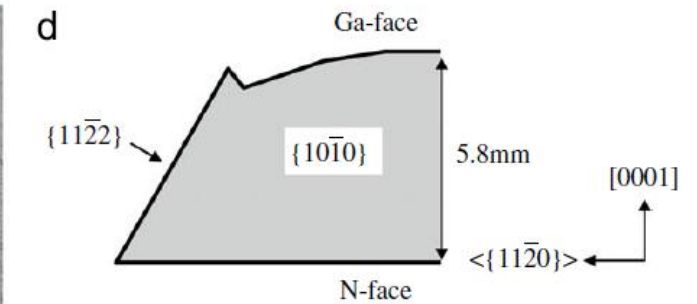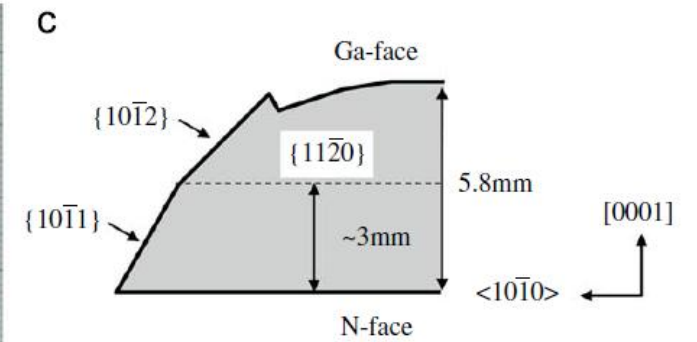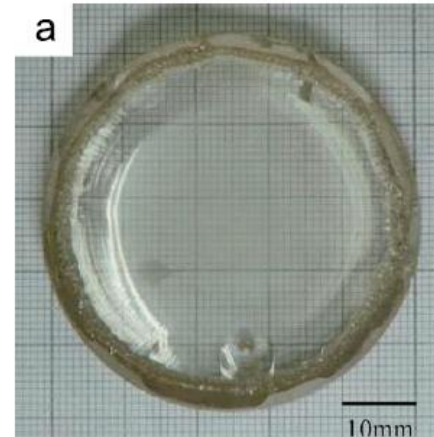
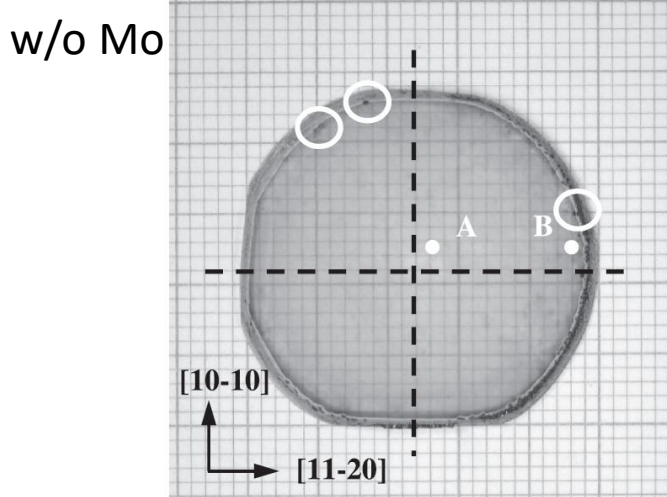K. Fujito et al., J. Cryst Growth 311 (2009) 3011-3014

Gallium Nitride (GaN)

Exercise: growth with and without Mo elements in the growth zone
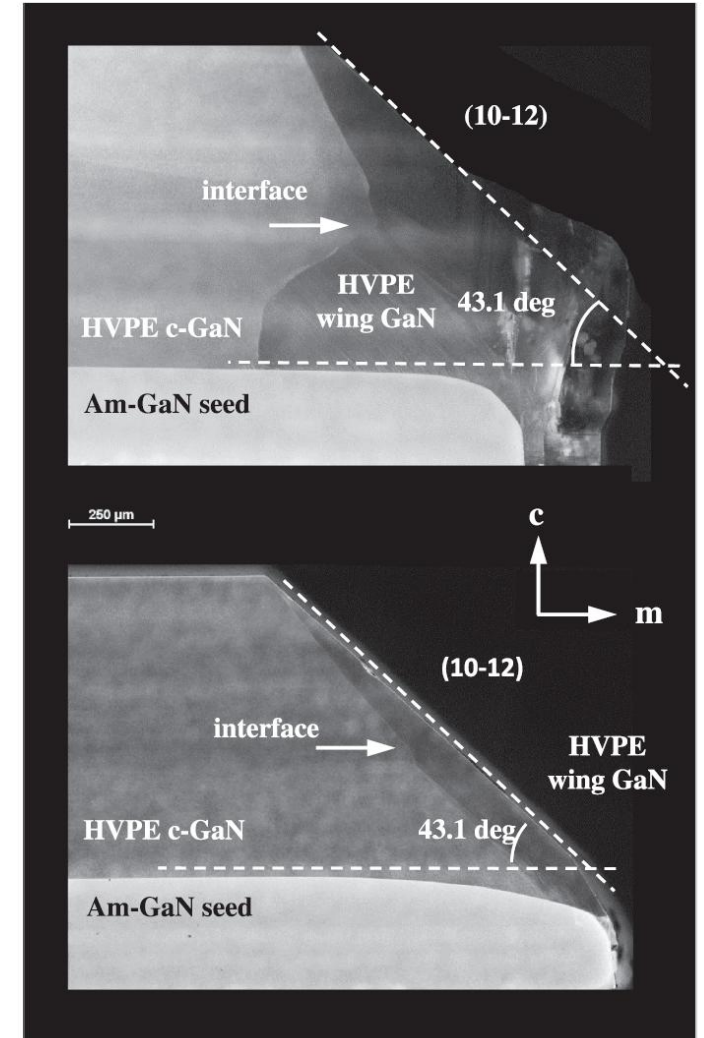

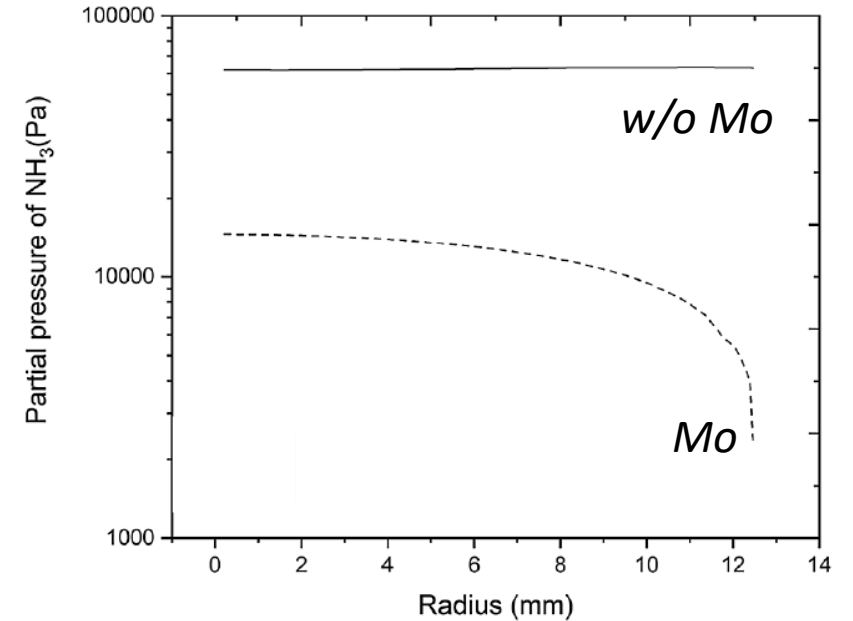T. Sochacki et al., J. Cryst. Growth 556 (2021) 125986
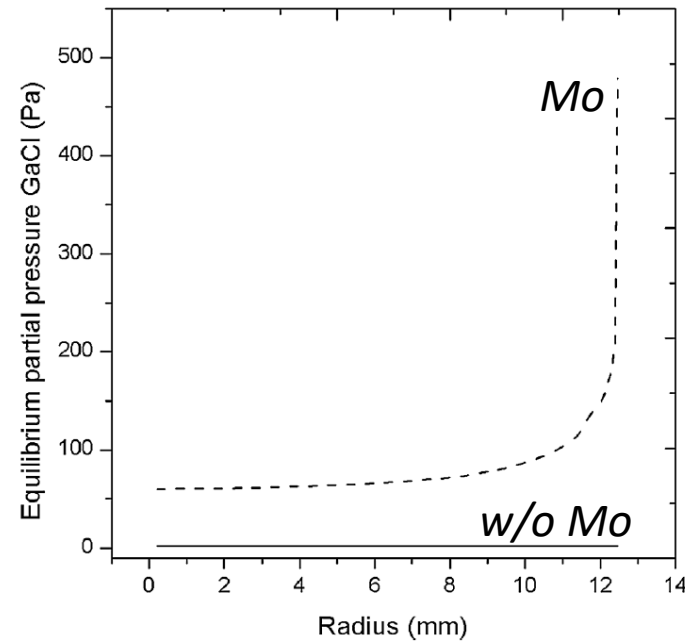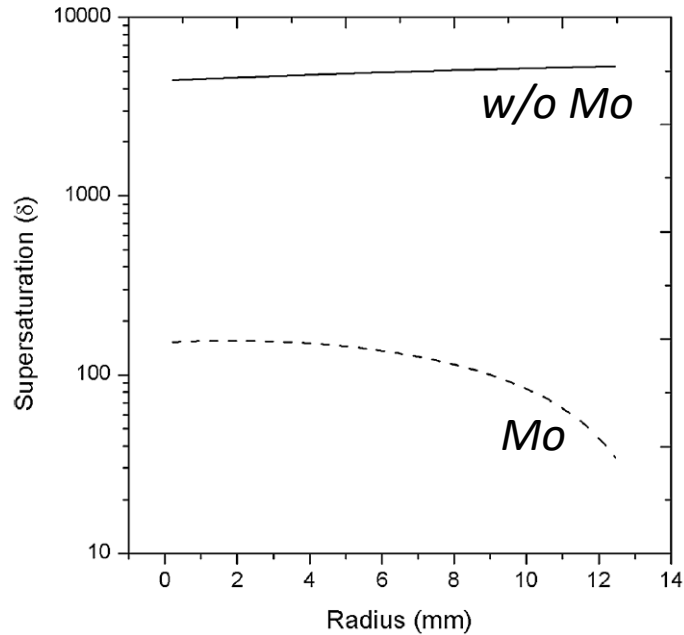
Gallium Nitride (GaN)

w/o Mo

Mo
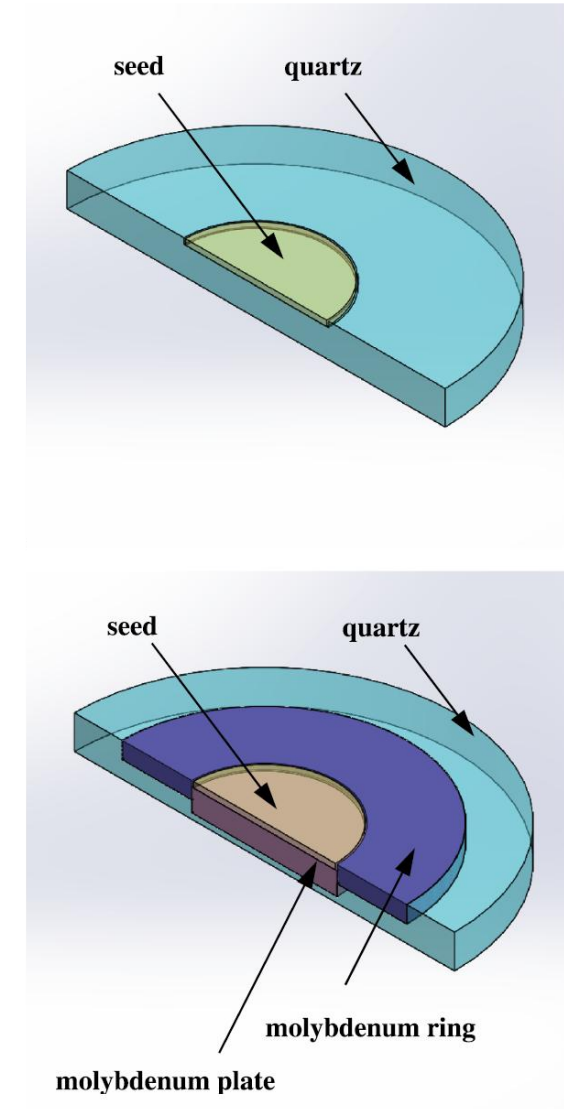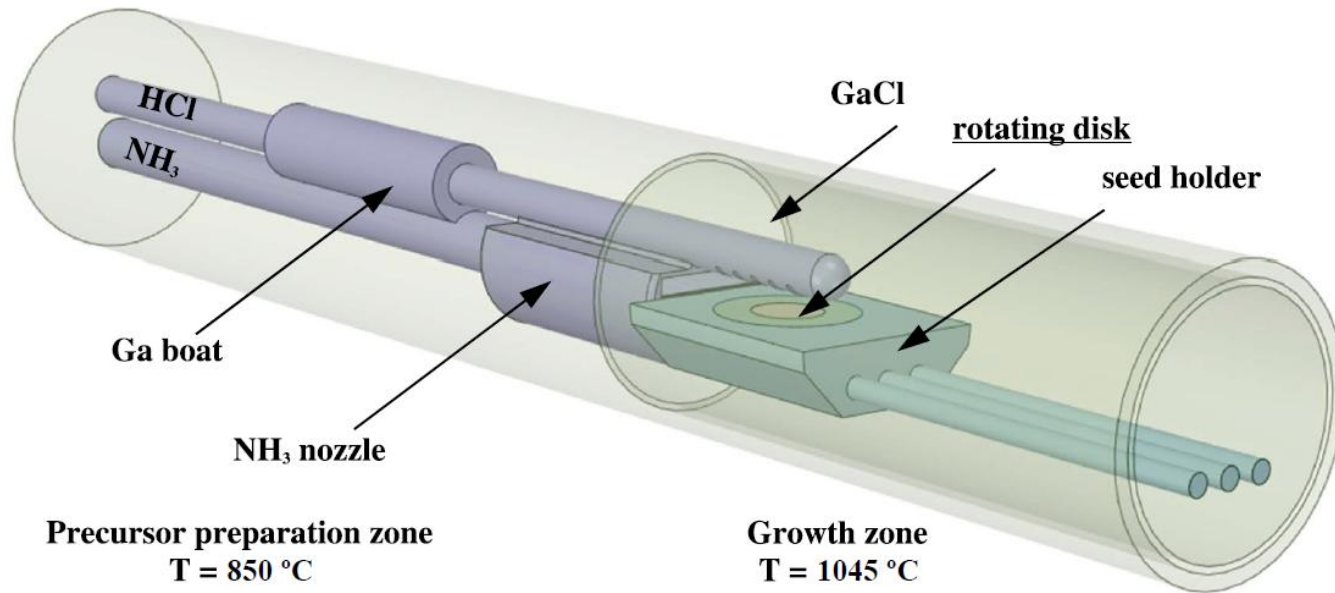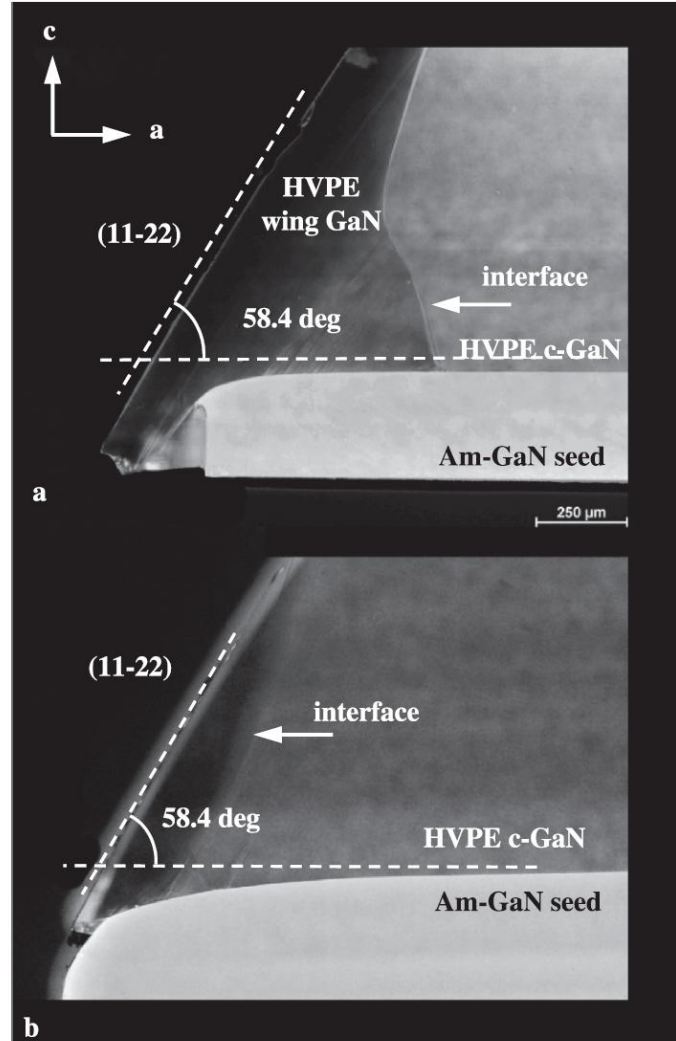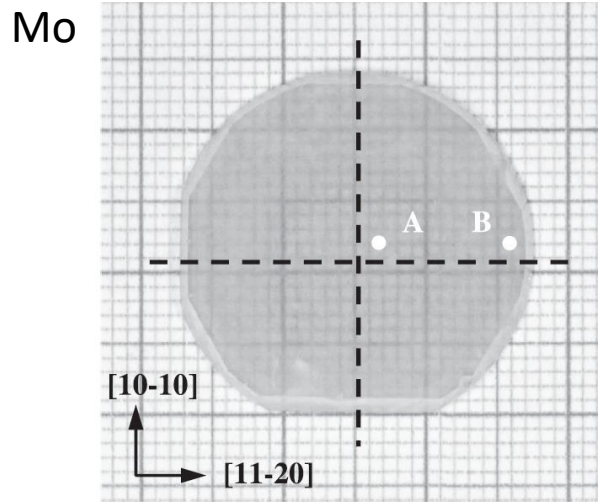
(10-10) cross sections

(11-20) cross sections

T. Sochacki et al., J. Cryst. Growth 556 (2021) 125986

Gallium Nitride (GaN)

Computational Fluid Dynamics simulations

The behavior of supersaturation was a result of an increase in ammonia decomposition which occurred intensively on the molybdenum elements located in the growth zone. This was demonstrated by the much lower molar fraction of ammonia over the surface of the crystal grown in process with Mo in comparison to process performer without it.

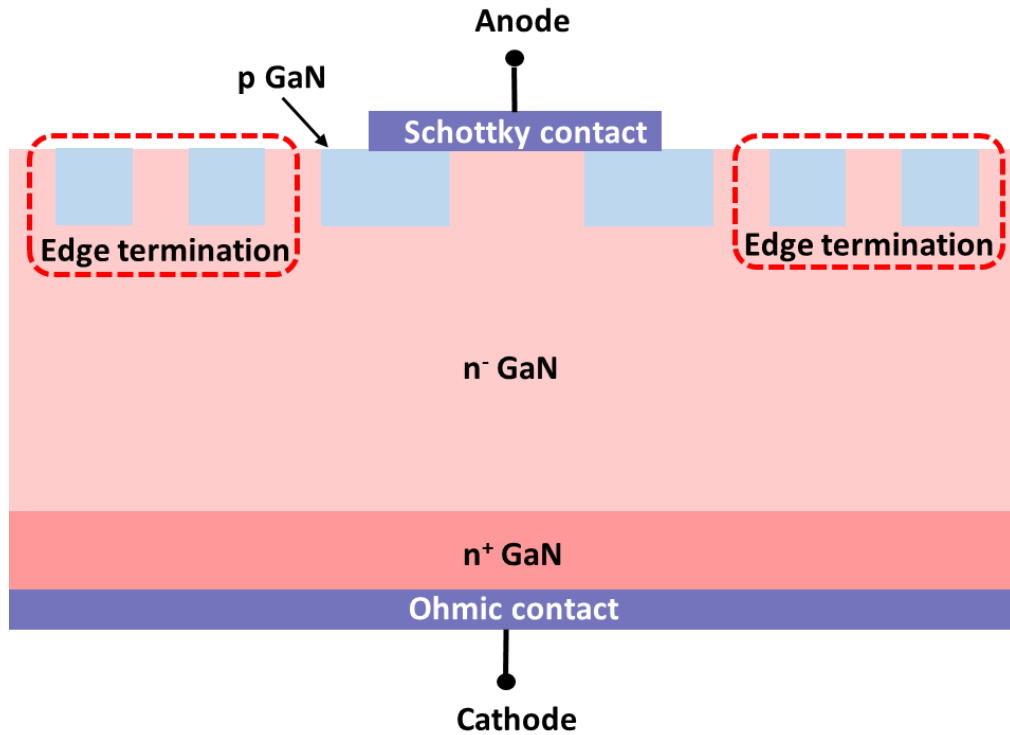# Gallium Nitride (GaN)

- Laser diodes (LDs)
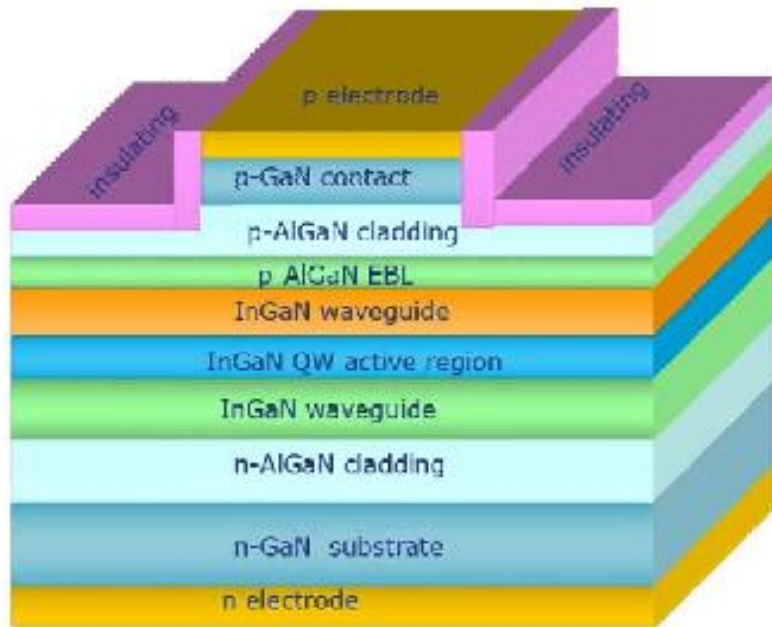
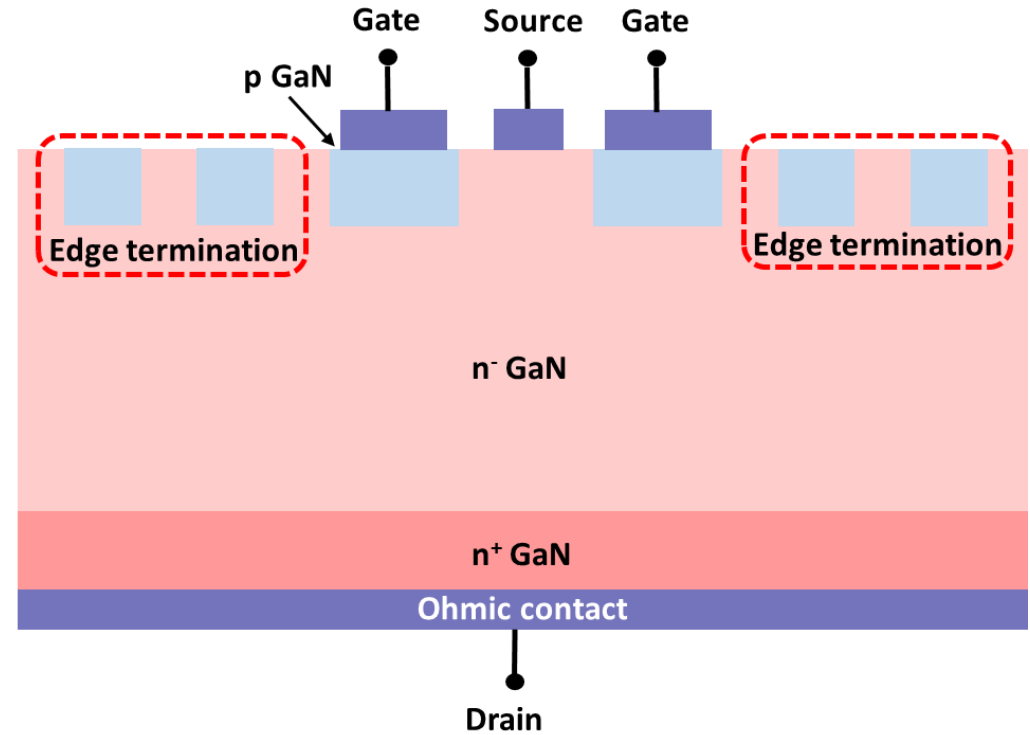- High electron mobility transistor (HEMT)
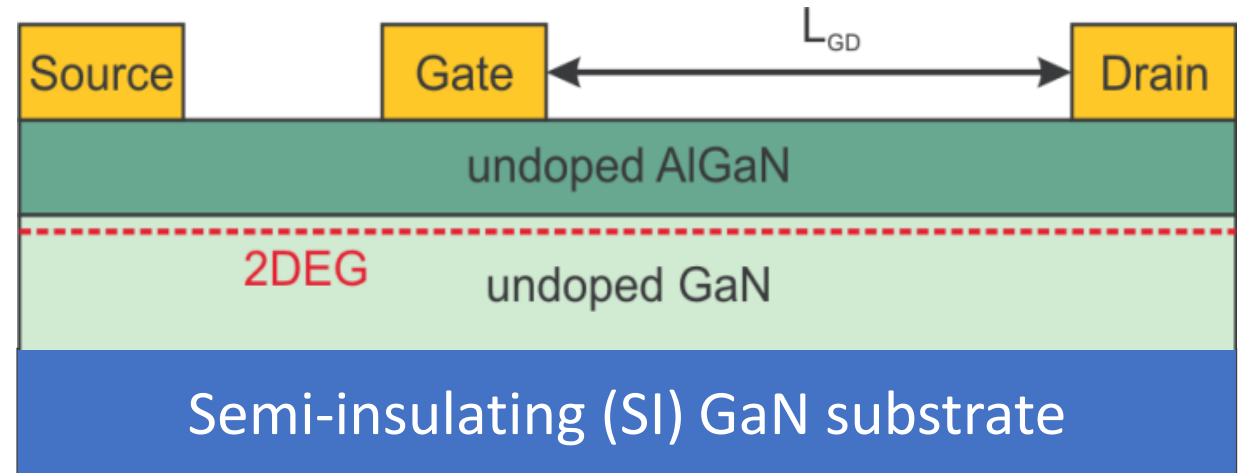
Jianping Liu et al., Materials Science IEEE Photonics Technology Letters

Gallium Nitride (GaN)
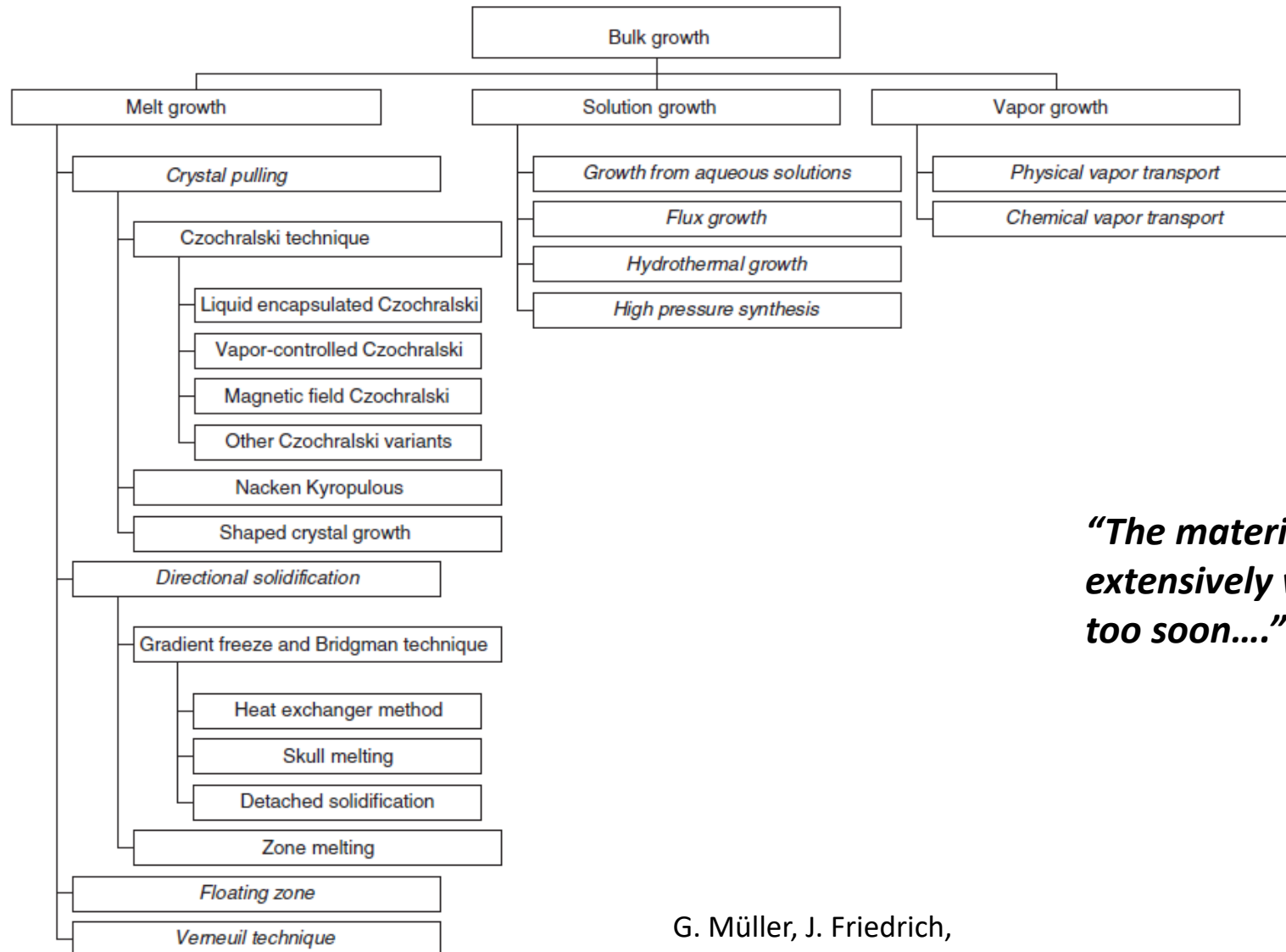
- Junction barrier Schottky diode (JBS)

- Junction field effect transistor (JFET)

HVPE-GaN as substrates
HVPE-GaN as drift layers

Summary

Figure 1   Overview of methods for bulk crystal growth.

"The material problem will have to be extensively worked on." "...one should not give up too soon...." William Shockley 1959

G. Müller, J. Friedrich,
in Encyclopedia of Condensed Matter Physics, 2005